University of Louisville
ThinkIR: The University of Louisville's Institutional Repository

Electronic Theses and Dissertations

7-2019

Feasibility study of intelligent LVAD control for optimal heart failure therapy.

John A. Karlen III
University of Louisville

Follow this and additional works at: https://ir.library.louisville.edu/etd

Part of the Biomedical Engineering and Bioengineering Commons

Recommended Citation
Karlen, John A. III, "Feasibility study of intelligent LVAD control for optimal heart failure therapy." (2019). *Electronic Theses and Dissertations.* Paper 3251.
https://doi.org/10.18297/etd/3251

This Master's Thesis is brought to you for free and open access by ThinkIR: The University of Louisville's Institutional Repository. It has been accepted for inclusion in Electronic Theses and Dissertations by an authorized administrator of ThinkIR: The University of Louisville's Institutional Repository. This title appears here courtesy of the author, who has retained all other copyrights. For more information, please contact thinkir@louisville.edu.

FEASIBILITY STUDY OF INTELLIGENT LVAD CONTROL FOR OPTIMAL HEART FAILURE THERAPY

By

John A Karlen III
B.S., University of Louisville, 2018

A Thesis
Submitted to the Faculty of the University of Louisville
J. B. Speed School of Engineering
As Partial Fulfillment of the Requirements
For the Professional Degree

MASTER OF ENGINEERING

Department of Bioengineering

July 2019

FEASIBILITY STUDY OF INTELLIGENT LVAD CONTROL FOR OPTIMAL HEART FAILURE THERAPY

Submitted by: _____
John A Karlen III

A Thesis Approved On

_____
(Date)

by the Following Reading and Examination Committee:

_____
Steven C. Koenig, Ph.D., Thesis Director

_____
Gretel Monreal, Ph.D.

_____
Thomas Roussel, Ph.D.

_____
Stuart Williams, Ph.D.

ACKNOWLEDGEMENTS

I would like to thank Dr. Steven Koenig for his mentorship throughout my past four years working with the advanced heart failure research (AHFR) team and during this project. Additionally, I would like to thank Dr. Gretel Monreal for her continuous advice and guidance throughout my time with the AHFR team including encouraging to participate in animal surgeries and surgical wet labs hosted by the AHFR team for which I am very grateful. Also, thank you Todd Adams for your help during the study, throughout my trials and errors you were always willing to help with anything I needed and for that I am incredibly grateful. I would like to thank the past and present staff and students of the AHFR team at the Cardiovascular Innovation Institute who either participated in this study or aided during my time spent with the AHFR team: Dr. Mark Slaughter, Mike Sobieski, Cary Woolard, Karen Lott, Laura Lott, Adam Kohl, Landon Thompkins, Chelsea Lancaster, Natalie Ebersold, Abhinav Kanukunta, and Connor Smith. I also would like to express my gratefulness to Dr. Thomas Roussel, and Dr. Stuart Williams for their participation on my thesis committee.

I would like to express my appreciation to Dr. Richard Wampler for developing and providing the intelligent HVAD control system that was used for this study.

Finally, I would like to thank my father and mother for their support throughout my academic career spent at the University of Louisville. Also, thank you to my fiancée for her immense support throughout this project.

ABSTRACT

Background: Left ventricular assist devices (LVAD) are operated at constant speeds (rpm), consequently, pump flow is passively determined by the pressure difference between the LV and aorta. Since the diastolic pressure gradient (~70 mmHg) is much larger than the systolic gradient (~10 mmHg), the majority of pump flow occurs during systole. This limitation results in sub-optimal LV volume unloading, LV washing, and diminished vascular pulsatility that may be associated with increased risk for clinically-significant adverse events, including stroke, bleeding, arteriovenous malformations, and aortic insufficiency. To address these clinical adverse events, an intelligent control strategy using pump speed modulation was developed to provide dynamic LV unloading during the cardiac cycle to produce near-physiologic pulsatile flow delivery similar to that of the native heart.

Materials and Methods: The objective of this study was to integrate a novel algorithm to dynamically control Medtronic HVAD pump speed and demonstrate proof-of-concept by characterizing hemodynamic performance in a mock flow loop primed with a blood analog solution (glycerol-saline, 3 cP) and tuned to simulate class IV heart failure (HF). The intelligent LVAD control was operated a varying pump speeds (Δspeed = 0, 1000, 1500, 2000, 2500 rpm) and systolic durations (30%, 35%, and 40%); systolic duration correlates to the time spent at either the high or low pump speed setting. The intelligent LVAD control strategy modulates pump speed within a cardiac cycle triggered from an R-wave of an EKG waveform set to 80 BPM. This pump speed modulation control strategy allows for pulsatile operation of a continuous flow LVAD within a single cardiac cycle. Hemodynamic waveforms (LV pressure-volume, aortic pressure-flow, and pump flow) and intrinsic pump parameters (speed and current) were recorded and

analyzed for each test condition. We hypothesize that pump speed modulation may be configured for optimal volume unloading (rest), vascular pulsatility (reloading), and/or washing.

Results and Discussion: The intelligent LVAD control system successfully demonstrated the ability to rapidly increase and decrease HVAD pump speed within a single cardiac cycle to provide asynchronous, synchronous co-pulsation, and synchronous counter-pulsation profiles for all systolic durations (30, 35, 40%) and Δrpm tested (Δ1000, Δ1500, Δ2000, Δ2500). Asynchronous support was achieved when pump speed increase (or decrease) was independent of the cardiac cycle, co-pulsation support was achieved when increase in pump speed was timed with beginning of systole corresponding with ventricular contraction (systole), and counter-pulsation support was when increase in pump speed was timed with the end of systole corresponding with ventricular filling (diastole). Ideally, the intelligent control would increase (or decrease) the HVAD pump speed instantaneously upon R-wave detection; however, two distinct time delays were observed: (1) a time delay from detection of the R-wave trigger and increase (or decrease) of pump speed for systolic durations of 35% and 40% (being 45 ± 3.0 ms and 82 ± 3.0 ms respectively and (2) a delay in LVAD flow when pump speed was increased which is hypothesized to be from the blood analog solution's fluid inertia. Left ventricular stroke volume decreased for all LVAD pump speed modulation operating conditions compared to baseline (HF with LVAD off) indicating that the intelligent control strategy was able to reduce LV volume with increasing HVAD support. The highest flow was achieved with the HVAD operated at a fixed speed of 4000 rpm; however, co-pulsation pump speed modulation at the largest pump speed differential (low = 1500, high = 4000, Δrpm = 2500, and systolic duration 30%) resulted in a mean pump

speed 3,300 ± 1,200 rpm. By comparison, the forward flow at fixed pump speed of 4,000 rpm was 4.8 L/min compared to a mean co-pulsation rpm was 4.5 L/min. Additionally, all operating settings for the intelligent control during pulsatile function produced an average forward flow through the aortic valve, while in contrast at higher fixed speeds (3,500 and 4,000 rpm) the mean aortic flow was negative. Pulse pressure (ΔP) decreased with increasing mean pump speed (rpm) for all operating modes (fixed, asynchronous, co-pulsation, counter-pulsation). When operating at the same mean pump speed (rpm) co-pulsation has increased hemodynamic benefit for pulsatility when compared to counter-pulsation and fixed speed at the same mean pump (rpm).

Conclusion: The results of this study show the ability of the intelligent HVAD control strategy to increase and decrease pump speed within a single cardiac cycle. This study showed that asynchronous modulation with phases of co-pulsation can generate near physiologic pulse pressure and vascular pulsatility when compared to counter-pulsation support, while counter-pulsation can generate greater ventricular volume unloading and diastolic augmentation when compared to co-pulsation. Furthermore, the clinical impact of this study is that through speed modulation adverse events of continuous flow LVADs may be reduced such as incidences of bleeding associated with decreased pulsatility and a decrease in the risk of thrombus formation from poor washing around the aortic valve.

TABLE OF CONTENTS

LIST OF TABLES

LIST OF FIGURES

I. BACKGROUND

A. Overview

Heart failure (HF) can be defined as a chronic condition in which the heart is no longer able to adequately pump blood to the body to satisfy the bodies oxygen and nutrient demands. HF accounts for approximately 330,000 adult deaths in the United States annually (Benjamin et al., 2018). HF classification can be divided into four classes based on physical limitations as well as cardiovascular disease severity, with lower level classes (I-II) constituting early stage HF and higher-level classes (III-IV) constituting end stage HF. The classification of HF is used to determine treatment plans for patients depending on the progression and severity of their disease. Early stage HF is often treated with optimal medical management (OMM) that target HF symptoms and improve patient quality of life. End stage HF may also continue to be treated with OMM, heart transplant, and/or mechanical circulatory support, including an implantable left ventricular assist device (LVAD).

LVADs are designed to augment the diseased heart in pumping blood to the body by pulsatile or continuous flow delivery, such as the pulsatile Thoratec HeartMate XVE (Abbott, Chicago, IL) LVAD and a continuous flow HeartWare HVAD (Medtronic, Minneapolis, MN) as shown in Figure 1. LVADs are surgically-implanted through open chest thoracotomy, with the device placed in the chest. The

inflow cannula is implanted into the apex of the left ventricle (LV) and an outflow graft attached to the aorta (Ao) of the HF patient to deliver forward flow from the LV to the Ao. Electrical power and communication to the LVAD is provided through a driveline from the pump to an external controller that is tunneled subcutaneously and exits through the HF patient's skin.

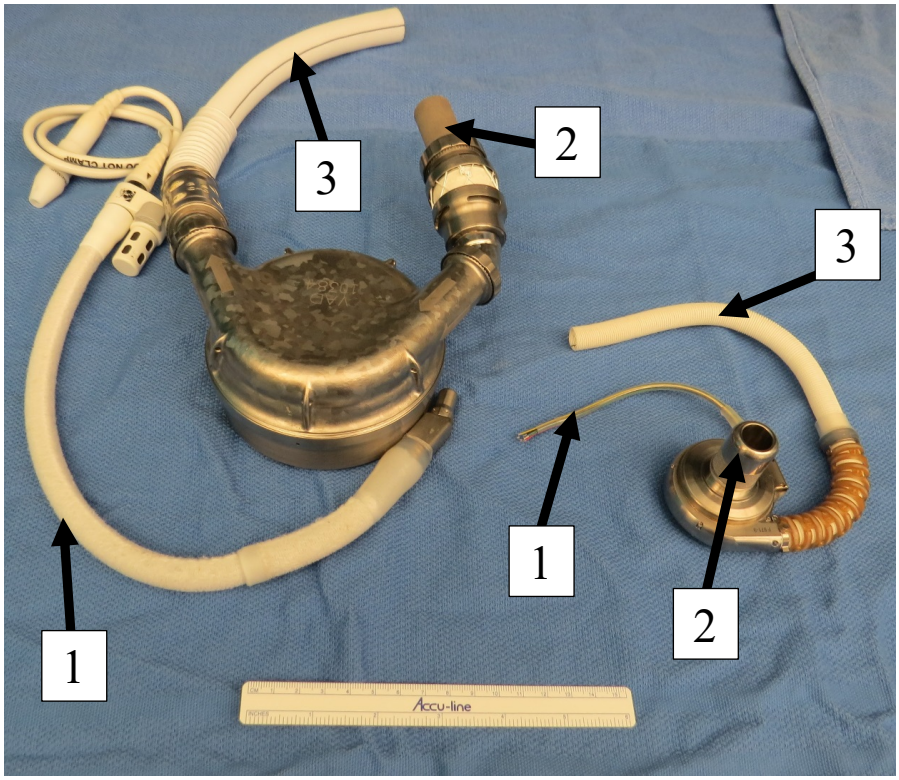

Figure 1. Thoratec HeartMate XVE (pulsatile flow) (left) and Medtronic HVAD (continuous flow) left ventricular assist devices (LVADs). Both LVADs have a driveline (1) that exits the skin to communicate with the device's controller, an inflow cannula (2) that is inserted into the apex of the left ventricle (LV), and an outflow cannula (3) that is sewn to the aorta. The HeartMate XVE propels blood by moving a driver bearing against a pusher plate to eject and fill the device. Blood flow is equal to the amount of volume that the device has and is a fluid displacement pulsatile LVAD. The HeartWare HVAD produces forward blood flow by the rotation of an impeller creating a continuous flow of blood through the device and out of the outflow graft to the aorta to supply blood to the remainder of the body.

LVADs have become a valuable tool in the treatment of advanced HF by helping bridge the gap between the large, growing number of advanced HF population and the limited number of donor hearts available for transplantation each year. LVADs have become more clinically accepted in recent years due to improved survival rates of continuous flow LVADs (CF-LVADs) being approximately 80% and 70% after one and two years of support respectively (Kirklin et al., 2017) comparable to heart transplantation survival rates. Although there are currently approximately, 2,400 LVAD implants a year in the US (Benjamin et al., 2018), adverse events such as bleeding, pump thrombosis (which could lead to stroke if the thrombus detached from the pump), infection, and an increased risk of developing right heart failure are associated with CF-LVAD use (Patel et al., 2014). Infection events are more prominent immediately following LVAD implantation due to the surgical procedure of having an open chest cavity to implant the device (Patel et al., 2014). Pump thrombosis and bleeding are two interconnected adverse events associated with anticoagulation regiments that are administered to LVAD patients. Anticoagulants are administered to patients to reduce the risk of thrombus formation due to the patient's blood being exposed to a foreign body (the LVAD); nevertheless, this therapy may increase the risk of bleeding events by lowering the responsiveness of the body's natural clotting mechanisms. In addition to anticoagulation medications, rotary blood pumps produce high shear stress on blood and platelets, which has been theorized to create molecular changes in clotting factors, including von Willebrand factor (Patel et al., 2014), that may increase the risk of a clinically-significant bleeding event. The adverse events associated with CF-LVADs may also be due, in part, to non-physiologic volume unloading and reduction in pulsatility (Soucy et al., 2013) as a result of operating at fixed pump speeds. Due to the increased

occurrence of these clinical adverse events with rotary blood pumps, which were not as commonly seen in patients with pulsatile flow devices, development of control strategies that enable CF-LVADs to behave more physiologically (dynamic LV volume unloading and pulsatility) has been proposed. Specifically, modulating rotary pump speed (rpm) of CF-LVADs to create a pulse has been proposed as a potential solution to help mitigate the incidence of adverse events. Modulating CF-LVAD pump speed (rpm) is achieved by cyclically increasing and decreasing the current that is supplied to the device. The current is delivered to the pump from the LVAD controller through the driveline and is used to set the operating pump speed (rpm) of the device. Thus, pump speed modulation may be achieved by altering the current supplied to the device within a specified time period as opposed to operating in a continuous flow mode at a fixed pump speed.

This thesis research tests the feasibility of pump speed modulation within a single cardiac cycle using the Medtronic HVAD configured with an intelligent LVAD control strategy in a benchtop mock circulatory loop testing platform. The intelligent control strategy triggers pump speed modulation with detection of an R-wave landmark from an electrocardiogram (EKG) to rapidly increase and decrease pump speed to produce dynamic LV volume unloading and pulsatile flow using a CF-LVAD rotary pump.

B. Heart Failure

1. Epidemiology

HF has been declared a global pandemic affecting approximately 26 million people worldwide and nearly 6.2 million people in the United States (US, Savarese et al., 2017; Benjamin et al., 2019). HF prevalence in the US is expected to increase to over 8 million people by 2030 with an average of approximately 550,000 new cases diagnosed each year

across all age groups, as shown in Figure 2 (Benjamin et al., 2017; Heidenreich et al., 2013).

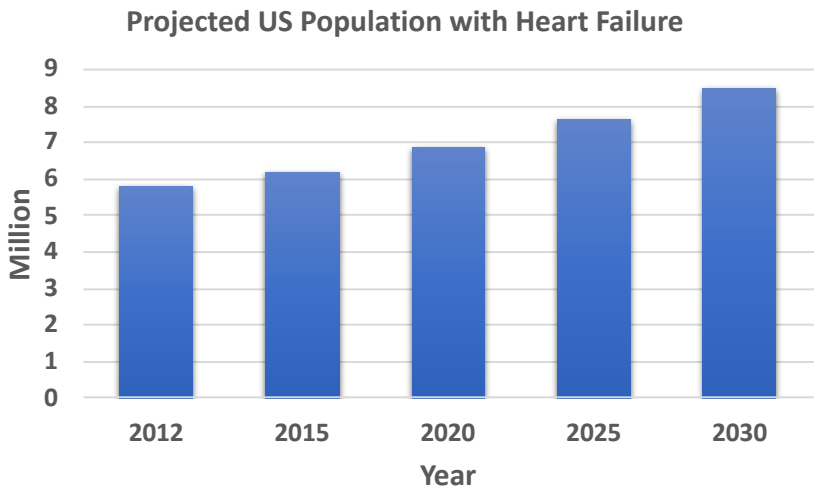

Figure 2: Projected heart failure population in the United States, data in this graph has been modified displayed graphically from Heidenreich et al., 2013.

Currently, HF is the leading cause of adult mortality in the US with nearly 330,000 deaths reported annually (Benjamin et al., 2018). The total medical cost of care for HF patients is estimated at $30.7 billion dollars and is expected to increase 127% to $69.7 billion by 2030 (Heidenreich et al., 2013), which includes medical, surgical, and re-hospitalization expenses associated with HF therapy.

2. Classification

HF may be defined as a chronic condition with the heart losing the ability to adequately deliver enough blood to satisfy the oxygen and nutrient demands of the body. Left ventricular (LV) HF failure may be categorized as systolic and/or diastolic dysfunction. Diastolic dysfunction is characterized by abnormalities in the filling of the

LV and often results in preserved ejection fraction of patients which may result from slowed LV relaxation and increased stiffness of the LV (Abebe et al., 2016; Paulus et al., 2007). Systolic HF may be characterized by the diminished ability of the heart to eject blood within each cardiac cycle resulting in a reduced LV ejection fraction (Chatterjee et al., 2008). HF resulting from myocardial damage is a subset known as ischemic HF that is generally caused by coronary artery disease due to the decreased blood flow through the coronaries to the myocardium. Non-ischemic HF (NI-HF) is a subset of HF that does not result from coronary artery disease, but rather is characterized by myocardial damage leading to ventricular dysfunction. NI-HF has been hypothesized to stem from many potential causes not linked directly to coronary artery disease, which include but are not limited to infection, genetic factors, and immune system abnormalities (Wu et al., 2007).

The New York Heart Association (NYHA) defines HF by four distinct categories (Table I) based on patient symptoms (including dyspnea, fatigue, or peripheral edema) and their inability to perform various exercise tasks (Burgess et al., 2016; Mosterd et al., 2007). Table I lists the functional capacity and objective assessment for each heart failure classification based on the NYHA guidelines (Athilingam et al., 2013). Class III-IV are considered end stage (advanced) HF while classes I-II are considered early stage HF (Friedrich et al., 2007). Depending on the patient's HF classification and the progression of the disease, varying medical treatments such as OMM, heart transplant, and/or mechanical circulatory support (MCS) may be more suited for specific stages of HF.

TABLE I
NEW YORK HEART ASSOCIATION HEART FAILURE CLASSIFICATION

NYHA Heart Failure Classificaton	
Functional Capacity	Objective Assesment
Class I: Patients with cardiac disease but without resulting limitation of physical activity. Ordinary physical activity does not cause under fatigue, palpiation, dyspnea, or anginal pain.	**A.** No objective evidence of cardivascular disease.
Class II: Patients with cardiac disease resulting in slight limitaiton of physical activity. They are comfortable at rest. Ordinary physical activity results in fatigue,palpitaiton, dyspnea, or anginal pain.	**B.** Objective evidence of minimal cardiovascular disease.
Class III: Patients with cardiac disease resulting in marked limitation of physical activity. They are comfortable at rest. Less than ordinary activity causes fatigue, palpitation, dyspnea, or anginal pain.	**C.** Objective Evidence of moderately severe cardiovascular disease.
Class IV: Patients with cardiac disease resulting in inability to carry on any physical activity without discomfort. Symptoms of heart failure or the anginal syndrome may be present even at rest. If any physical activity is undertaken, discomfort is increased.	**D.** Objective evidence of severe cardiovascular disease.

New York Heart Association (NYHA) classification of heart failure. Class I represents the least severe stage of heart failure with its objective assessment described by the NYHA and class IV describes the most severe stage of heart failure and its objective assessment. Classification table was modified and recreated from Athilingam et al., 2013.

3. Etiology

Due to HF having several underlying mechanisms of progression there is not one common cause for all HF patients. HF may be multi-variable leading to varying diseases of the myocardial tissue also known as a cardiomyopathy. Cardiomyopathies may be associated with hypertension, viral myocarditis, valvular disease, genetic predisposition, and coronary artery disease (CAD) (Wexler et al., 2010; Maron et al., 2006). In addition to these cardiomyopathies, other risk factors for the development and progression of HF include diabetes mellitus, aging, smoking, obesity and an excess dietary sodium intake (Frohlich et al., 2014). CAD is considered to be the predominant cause of ischemic HF and is estimated to be the underlying etiology of nearly 70% of patients (Gheorghiade et al., 1998). CAD is defined as the narrowing or blocking of the arteries that supply blood to the heart (coronaries). Reduced blood flow to the heart may result in death of myocardial tissue that may also lead to worsening LV function. With this subsequent myocardial tissue injury or death, a variety of compensatory mechanisms may be activated to try and maintain required cardiac output.

4. Pathophysiology

The basic underlying physiologic mechanisms in the development and progression of chronic HF are an initial insult (i.e. myocardial infarction) followed by ventricular remodeling (Delgado et al., 1999). Ventricular remodeling may be described as the myriad of compensatory mechanisms that subsequently take place temporally and spatially both in response to the dysfunction and as a consequence of the dysfunction. (Monreal et al., 2004)). The initial insult may reduce systolic function of the heart by damaging the surrounding myocardial tissue. This damage can then subsequently

diminish the ability of the myocardium to contract and produce blood flow to the body resulting in reduced cardiac output. The heart attempts to compensate for this condition by increasing heart rate and ventricular remodeling. Ventricular remodeling is initially an adaptive response to the initial insult in order to maintain pump function (Delgado et al. 1999). However, over time the remodeling cascade progresses both temporally and spatially resulting in altered size, shape, and function of the ventricle through scarring, activation of growth factors, and molecular changes of the myocardium (Delgado et al., 1999; Azevedo et al., 2015).

One compensatory response to low cardiac output is known as the Frank-Starling mechanism. The Frank-Starling mechanism describes the hearts ability to alter the force of ventricular contraction in response to venous return. By increasing the venous return of the heart (preload) the LV myocardium stretches allowing for greater force generation and contractility due to increased tension in the myocardium of the failing ventricle, subsequently increasing the stroke volume and cardiac output if the HR remains constant (Kemp et al., 2012; Sequeira et al., 2015). Additional compensation responses target the release of renin from the kidneys in an attempt to maintain normal renal and systemic perfusion by increasing the retention of water and salt; however, if this response is prolonged this can lead to the development of edema and increases the afterload on the diseased heart, furthering the progression of the disease (Delgado et al., 1999). Myocardial damage and worsening LV function leading to decreased contractility of the ventricle increases left ventricular volume, decreases stroke volume, elevates end diastolic pressure and volume, produces a rightward shift in the ventricular pressure-volume (PV) relationship, and decreases aortic pressure, and pulse pressure, as illustrated in Figure 3.

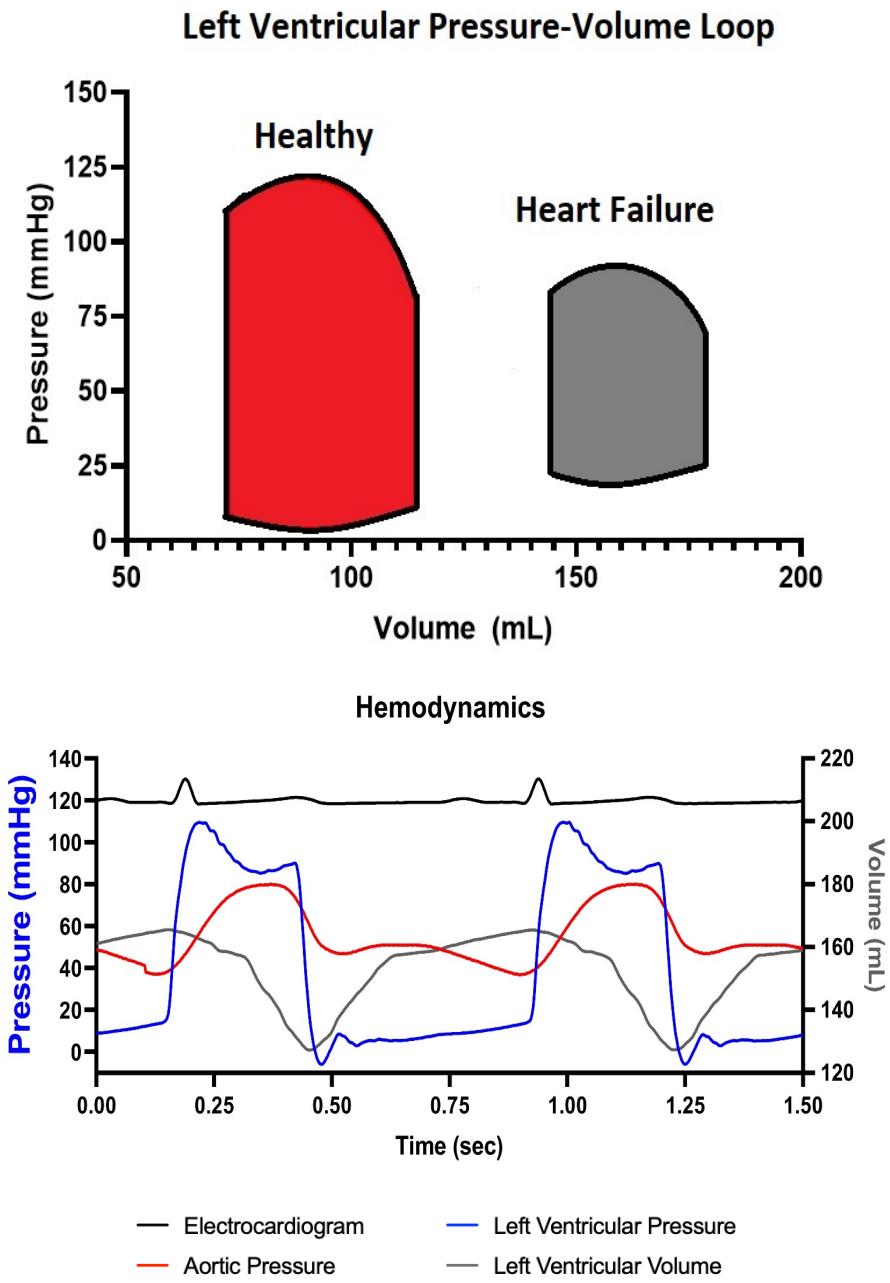

Figure 3. Illustration of pressure volume (PV) loops to visualize differences between an expected healthy PV loop and expected heart failure (HF) PV loop (top). HF failure PV loop has distinct right-ward shift and increased end diastolic pressure as a result of diminished contractile strength and dilation of the left ventricle. Additionally, the HF PV loop has a smaller difference between systolic and diastolic left ventricular pressures represented in the truncation of the loop when compared to the expected PV loop of a healthy adult. Hemodynamic waveforms recorded in a mock circulatory loop to simulate a class IV HF baseline (bottom). Left ventricular end systolic and aortic pressures are reduced from expected healthy adult, while end diastolic pressures are elevated. Stroke volume or the difference between maximum and minimum left ventricular volume is also expected to be reduced when compared to a healthy adult.

5. Deviation from Normal Cardiac Physiology

Significant changes in anatomic features and hemodynamic parameters occur in the transition from a healthy heart to diseased HF heart. Anatomically, the left ventricle becomes dilated and the myocardial walls thin (Inamdar et al., 2016). In advanced HF stages, left atrial pressure (mean) and left ventricular pressures (end-diastolic) increase, aortic and left ventricular pressures (systolic, mean) decrease, cardiac output is reduced, and heart rate increases, as listed in Table II (Yildiran et al., 2010; Melenovsky et al., 2015). As shown earlier in Figure 2, an adult with a healthy heart compared to stages of advanced HF will have a larger stroke volume, lower end diastolic pressure (reduced preload), greater ventricular contractility, and lower end systolic and end diastolic volumes.

TABLE II
HEMODYNAMIC PROGRESSION OF HEART FAILURE FROM NORMAL FUNCTION

Comparison of Hemodynamic Paremters					
Parameter	Healthy	Class I	Class II	Class III	Class IV
Systolic Blood Pressure (mmHg)[1,2]	<120	127 ± 15	123 ± 23	107 ± 15	98 ± 12
Mean Arterial Pressure (mmHg)[1,2]	70-105	98 ± 10	93 ± 15	82 ± 10	77 ± 9
Diastolic Blood Pressure (mmHg)[1,2]	<80	83 ± 9	78 ± 11	70 ± 9	66 ± 8
Aortic Pulse Pressure (mmHg)[1,2]	~30-40	45 ± 10	46 ± 15	37 ± 11	31 ± 9
Ejection Fraction (%)[1,2]	55-75	35 ± 5	35 ± 5	28 ± 5	25 ± 5
Left Atrial Pressure (mmHg)[3,4]	4-12	20 ± 8	20 ± 8	20 ± 8	20 ± 8
Heart Rate (BPM) [1,2]	65-80	81 ± 7	82 ± 14	89 ± 17	92 ± 15

Table II displays the progression from a healthy adult to advanced heart failure. With progression of heart failure, the aortic blood pressure decreases during both systole and diastole, in addition to a decrease in the aortic pulse pressure, due to the inability of the diseased heart to generate as much force when compared to a healthy adult. Also, ejection fraction diminishes with progression of heart failure due to decreased ventricular contractility. Left atrial pressure (preload) is elevated when compared to healthy adults due to volume overload that takes place in heart failure patients. Finally, the heart rate is increased as a mechanism to attempt to increase the cardiac output with the progression of heart failure. Data is represented as mean +/- standard deviation and was created using data modified from Yildiran et al., 2010[1]; Cleveland Clinic, Ejection Fraction[2], Edwards. Normal Hemodynamic Parameters[3], 2014, Melenovsky et al., 2015[4].

C. Treatments

1. Medical Management

The main objective of optimal medical management (OMM) of HF patients is to relieve the symptoms associated with the disease and help to improve their quality of life, functional capacity, and reduce the risk of hospitalization and mortality (Berliner et al., 2017). Some pharmacological therapies for HF patients include the use of angiotensin converting enzyme (ACE) inhibitors (ACEIs), mineralocorticoid receptor antagonists (MRAs), and beta blockers (Berliner et al., 2017; Shah et al., 2017). Beta blockers (adrenergic receptor antagonists) are used to reduce the workload on the heart through the reduction in sympathetic stimulation on the heart and vasculature (Shah et al., 2017). ACEIs act by helping to reduce the workload on the heart by vasodilation decreasing peripheral resistance and to reduce the afterload that the heart has to pump against (Berliner et al., 2017; Shah et al., 2017). Goals of OMM for treating HF patients include alleviating symptoms which may impact quality of life and reducing morbidity and mortality of the disease.

2. Heart Transplant

The gold standard in care for patients diagnosed with advanced HF is a heart transplant. The first successful heart transplant was performed over 50 years ago in 1967. Since 1990, approximately 2,000-2,500 transplants are performed annually in the US (Koomalsingh et al., 2018). Survival rates after heart transplant have steadily improved by approximately 10% for 1-year and 5-year survival rates when compared to the 1980s (Wilhelm et al., 2015), with recent data showing 1-year, 4-year, and 10-year survival rates at 90%, 80%, and 65%, respectively (Lund et al., 2016).

There are many limitations and clinical challenges associated with heart transplantation. Despite a slight increase in the number of transplants over past several years (approximately 500 additional transplants) there continues to be an insufficient supply of donor organs available to meet the current and projected demand estimated to be up to 550,000 HF patients annually (Benjamin et al., 2018). Additionally, comorbidities, such as irreversible pulmonary hypertension, systemic infection, inability to comply with the complex medical regimen, and irreversible dysfunction of the liver or kidneys are known contraindications (Jonge et al., 2008; Taylor et al., 2006). Donor availability, organ rejection, and immunosuppression management are among the most common limitations associated with heart transplant therapy (Sing et al., 2015).

3. Mechanical Circulatory Support

Mechanical circulatory support (MCS) devices have been used to support NYHA Class III-IV patients (Katz et al., 2015). These devices have been approved for use in advanced HF patients as bridge to heart transplantation (BTT), bridge to recovery (BTR), bridge to heart transplant candidacy (BTC), and/or destination therapy (DT) (Puehler et al., 2014). Short-term MCS devices are currently being used as a bridge to decision in patients with refractory cardiogenic shock defined as the condition resulting in tissue hypoxia from a reduced cardiac output (Reyentovich et al., 2016). These patients may then be transitioned to long-term MCS or BTR. Commonly used short-term devices include intra-aortic balloon pumps (IABPs), Impella 2.5 & 5.0, TandemHeart, and extracorporeal membrane oxygenation (ECMO) (den Uil et al., 2017).

IABPs are devices that provide diastolic augmentation using the principle of counter-pulsation defined by augmenting flow during diastole and reducing pressure and

afterload during systole of the native heart. An IABP is placed in the descending aorta. During diastole the balloon rapidly inflates causing blood flow to be displaced equal to the volume of the balloon back toward the ascending aorta to perfuse the coronary arteries and to the descending aorta to improve end-organ perfusion. During systole the balloon rapidly deflates creating a vacuum that decreases the aortic pressure, improves left ventricular unloading, and increases cardiac output (Gilotra et al., 2014).

The Impella system (ABIOMED, Danvers, MA) consists of an axial rotary pump embedded in a catheter that is placed across the aortic valve and can deliver 2.5 to 5.0 L/min blood flow from the LV to the aorta. The Impella 2.5 is implanted by a cardiac catheterization procedure, and the Impella 5.0 is implanted via a femoral cutdown. These devices have a pigtail-tipped catheter that sits inside the left ventricle and pumps blood out the ascending aorta. These devices operate asynchronously (independent of the cardiac cycle) and produce continuous flow to the ascending aorta (Sarkar et al., 2010). The Impella has been shown to be effective in patients with cardiogenic shock and percutaneous coronary intervention (PCI) by increasing cardiac output, reduces ventricular volume, and improving myocardial supply-demand ratio (Kawashima et al., 2011; Mukku et al., 2012).

TandemHeart (CardiacAssist Inc., Pittsburgh, PA) is a percutaneous ventricular assist device (pVAD) that is implanted in a left atrial to femoral artery bypass system. The pVAD consists of a continuous flow centrifugal blood pump and an arterial perfusion catheter. The pVAD draws oxygenated blood from the left atrium that is pumped to the systemic circulation via a femoral artery catheter to bypass the left ventricle of the heart (Gilotra et al., 2014). The hemodynamic benefits of pVAD use

include reduced LV stroke volume and LV preload while increasing cardiac output when compared to an IABP or Impella (Gilotra et al., 2014; Ergle et al., 2016).

Extracorporeal Membrane Oxygenator (ECMO) therapy consists of a centrifugal pump and an external oxygenating system for carbon dioxide and oxygen gas exchange. There are two forms of ECMO based on cannulation site: (1) femoral artery and vein (venoarterial, VA) or (2) internal jugular vein and femoral vein (venovenous, VV). In VA ECMO the patient is provided with both respiratory and hemodynamic support therapy, whereas in VV ECMO the patients have stable hemodynamics, subsequently only respiratory support is required (Makdisi et al., 2015). Advantages of ECMO include the ability to oxygenate blood in hypoxemic states and unload both ventricles simultaneously. Overall the goal of short-term MCS devices is to reduce the afterload and preload on the failing heart while increasing cardiac output to provide better perfusion to the rest of the body (Gilotra et al., 2014).

Ventricular assist devices (VADs) and total artificial hearts (TAHs) are MCS devices designed for long-term support. TAHs are currently approved for use in end-stage biventricular HF as a BT. Currently, the only FDA approved TAH in the United States is the CardioWest TAH (SynCardia Systems, Inc, Tucson, AZ). The CardioWest consists of two polyurethane ventricles with stroke volumes of 70 mL. To implant the CardioWest TAH, (1) the ventricles are excised, (2) quick connects of the TAH are sutured to the valve annulus, mitral valve annulus for the left side of the heart, and the tricuspid valve annulus for the right side of the heart, and (3) the aortic and pulmonary artery grafts are then connected (Cook et al., 2015).

LVADs may be classified as pulsatile flow VADs (PF-VADs) and CF-LVADs, which are both able to be implanted into the left or right ventricle by surgically grafting

the inflow cannula into the apex of the ventricle and the outflow graft to either the aorta (LVAD) or pulmonary artery (right ventricular assist device). VADs augment the heart by volume unloading the ventricle (reduce workload) and restoring cardiac output to adequately perfuse end-organs. These devices may be placed completely inside the chest, extracorporeally, or percutaneously. With devices placed percutaneously inflow and outflow cannulas are tunneled into the chest in instances of larger devices not having adequate room to be implanted inside the chest. The first-generation devices were PF-VADs that were large in size and weight, had many moving parts, and limited durability (Soucy et al., 2013). PF-VADs were actuated using a pneumatic driver to rapidly inflate and deflate an artificial membrane, such as the Thoratec PVAD (Pleasanton CA), or electro-mechanically using a pusher-plate mechanism, such as the Thoratec XVE (Pleasanton CA) to produce near-physiologic pulsatility and dynamic volume unloading. These devices have been replaced by second generation CF-VADs, including the HeartMate II (Abbott, Chicago, IL) and HeartWare HVAD (Medtronic, Framingham, MA), that continuously unload ventricular volume and deliver blood flow through the aorta by the constant fixed speed rotation of high-speed impeller (4,000-10,000 rpm) using axial or centrifugal design configurations. CF-VADs are smaller in size and weight, require fewer moving parts and no valve, and have demonstrated significantly improved durability (Soucy et al., 2013). Despite the improvement in MCS device technology, concern with clinically-significant adverse events, including bleeding, pump thrombus, and stroke, may be associated (and have been hypothesized) with the non-physiologic conditions (small fixed volumes, diminished pulsatility) of rotary blood pumps operated at fixed impeller speeds.

D. Challenges of VAD Support

As MCS devices have gained widespread clinical use, common clinical complications and significant adverse events associated with CF-LVADs have been reported, including bleeding, pump thrombosis (stroke), infection, and the risk of developing right heart failure (Patel et al., 2014). Bleeding has been reported in up to 20% of HF patients supported by LVADs (Eckman et al., 2012). Acquired von Willebrand syndrome has been hypothesized as a potential cause of the reported high incidence of bleeding due to high shear stress on the blood generated by rotary blood pumps (Eckman et al., 2012; Nascimbene et al., 2016). Despite use of anticoagulation during chronic CF-LVAD support, thrombosis is another clinically-significant adverse event due to the risk of stroke (Eckman et al., 2012). LVAD infections are one of the most common adverse events with a reported incidence rate ranging from 14-28% (Rose et al., 2001), and which predominantly occur in the driveline for up to 19% of reported infections (Goldstein et al., 2012; Hernandez et al., 2017). Depending on the severity of the infection, clinicians may prescribe two potential treat options: (1) broad-spectrum oral antibiotics (Toda et al., 2015; Maniar et al., 2011) or (2) surgical intervention by either driveline debridement or device replacement (Hernandez et al., 2017).

Right ventricular (RV) failure has also been reported following LVAD implantation with a reported incidence of 9-40% (Fida et al., 2015), which is considered a major risk factor in the morbidity and mortality of HF patients supported by CF-LVAD (Argiriou et al., 2014). RV failure may occur when the output of the right ventricle cannot achieve balance (or keep up with the left ventricle) resulting in high RV preload. There may also be a leftward shift of the intraventricular septum due to LVAD unloading, especially at higher pump speeds, that may also contribute to impaired RV contractility (Argiriou et

al., 2014). Treatment options for patients with RV failure include (1) OMM and/or (2) surgical intervention. OMM is aimed at keeping the central venous pressure less than 15 mmHg to maintain lower RV workload using inotropes and vasodilators; additionally, the LVAD may be set at a pump speed that provides sufficient cardiac output without producing a septal shift toward the LV to help prevent detrimental RV anatomical changes (Fida et al., 2015; Slaughter et al., 2010). Surgical intervention consists of implanting a right ventricular assist device (RVAD) to support the failing right ventricle. Approximately 6-10% of patients with an LVAD will also receive an RVAD, resulting in bi-ventricular support (Bi-VAD) (Boulate et al., 2014).

E. Pump Speed Modulation

Due to the adverse events associated with continuous flow LVADs, pump speed modulation has been proposed to produce physiologic ventricular volume unloading and pulsatility. LVAD pump speed modulation is the concept of varying (increasing and decreasing magnitude over a defined time period or frequency) pump speed (rpm) rather than operating at a constant or fixed pump speed. Pump speed modulation may produce better (more physiologic) hemodynamics compared to continuous mode operation. Pump speed manipulation may also enable other operation modalities, such as timing of pump speed manipulation within the cardiac cycle (frequency), pump speed range with defined high and low settings (magnitude), time spent at each operating rpm (period), and feedback control using external trigger signal(s) to define pump speed modulation algorithms.

1. Pump Speed Modulation: Hemodynamics

Hemodynamic responses with pump speed modulation may vary as a function of LVAD operating modality, as previously shown in a mock circulatory loop (MCL) model. The hemodynamics for a simulated class IV HF (no LVAD), continuous flow using the HVAD (4000 rpm), and pulsatile flow using the HVAD (mean pump speed 3,300 rpm) produced varying hemodynamic responses during this experiment based on the operating modality of the LVAD (Figure 4). Continuous flow produces decreased aortic pulse pressure, decreased LV stroke volume, and pulsatility when compared to pulsatile LVAD operation and class IV HF patients with no LVAD (Soucy et al., 2013). As shown in Table III, there are several benefits and limitations associated with LVAD pump speed modulation, including the benefits of decreasing LV workload and increasing pulse pressure when compared to fixed speed, but at the cost of increased power requirements and the risk for hemolysis with the rapid change in pump speed (Soucy et al., 2015).

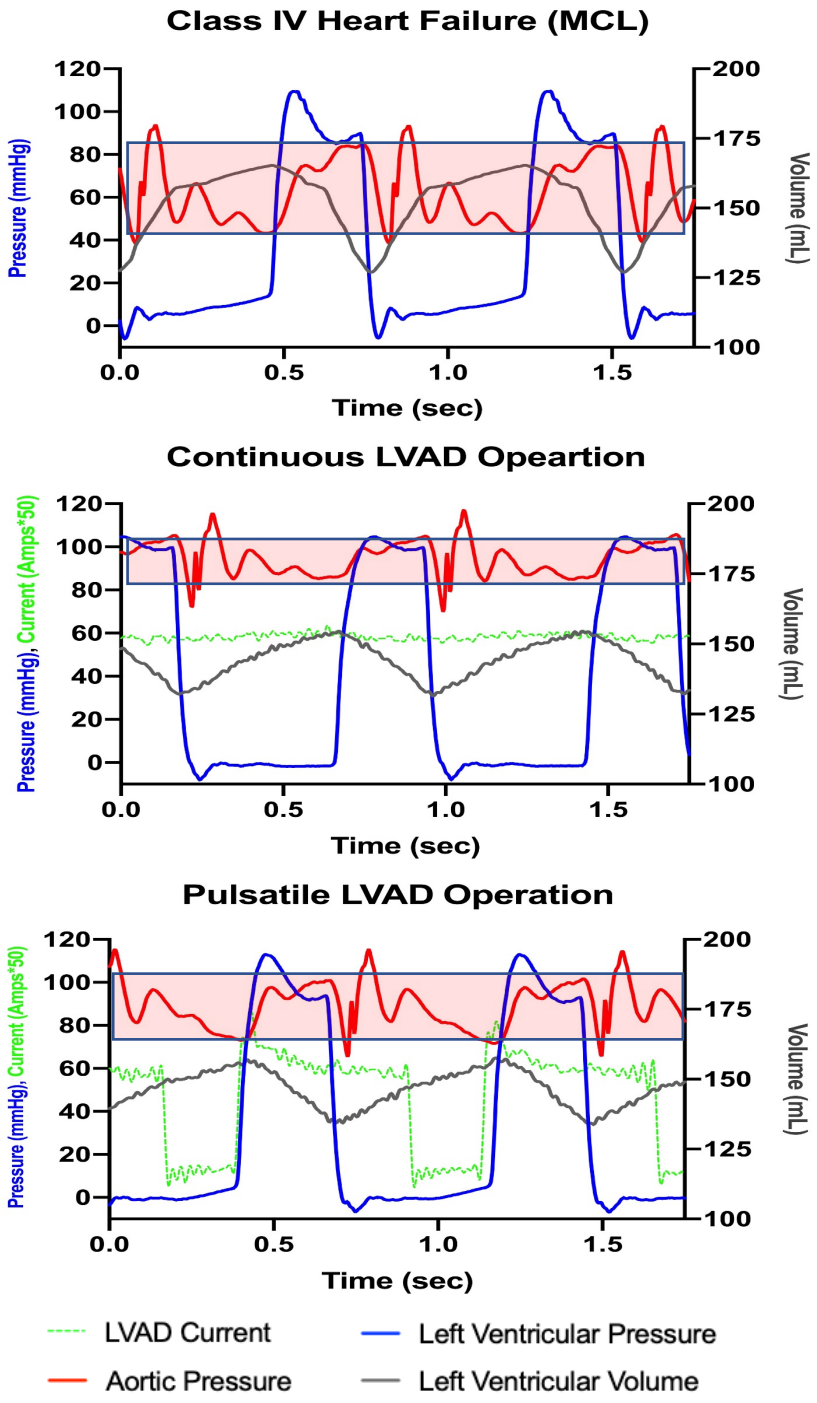

Figure 4. Comparison of hemodynamic waveforms for class IV heart failure (HF) baseline recordings taken in mock circulatory loop and then left ventricular assist device (LVAD) operation in a continuous flow and pulsatile flow manner. Of note is decreased pulse pressure in both operating settings of LVAD but pulsatile operation creates pulse pressure (red-hue area) that is closer to baseline. Left ventricular volume: LVV, Left ventricular pressure: LVP, aortic pressure AoP, current supplied to LVAD: current (controls pump speed).

TABLE III
BENEFITS & LIMITATIONS OF FIXED SPEED AND PULSATILE LEFT VENTRICULAR ASSIST DEVICE OPEARTION

	Benefits	**Limitations**
Fixed Speed	LV work = ↓ Power = ↓ Hemolysis = ↔ Sensor-less control	Aortic Valve Opening = ↓ ΔP = ↓ Adverse events ΔV = ↓
Pulsatile Operation	LV work = ↓↓ ΔV = ↑↑ ΔP = ↑↑ Aortic Valve Opening = ↑ Washing = ↑ Myocardial perfusion = ↑	• Power = ↑ • Hemolysis = ↑
↑ = increases; ↓ = decreases; ↔ = clinically insignificant amounts		

Table III. Benefits and limitations associated with both fixed (continuous) speed operation and pulsatile operation of left ventricular assist devices (LVADs). Pulsatile operation may have the benefits of improved pulsatility, aortic valve opening, and pump washing when compared to fixed speed operation while having the drawback of requiring more power to operate LVADs in a pulsatile fashion. Relationships in this table have been determined from Soucy et al., 2015.

2. Pump Speed Modulation: Triggering

Pump speed modulation of CF-LVADs may be accomplished using time-dependent variation (increase or decrease) in pump speed and triggering from an external source such as detection of specific landmarks within aortic pressure or EKG waveforms. Current examples of how pump speed modulation may be achieved, include time-based pump speed modulation algorithms used with Thoratec HeartMate 3 (Burlington, MA), Lavare cycle using the HVAD, and the Jarvik 2000 (Jarvik Heart, New York, NY) intermittent low speed controller. Each of these clinically approved LVADs use pump speed modulation to increase (or decrease) pump speed based on a set time interval of operation. The HeartMate 3 modulates pump speed every two seconds while the Lavare cycle and Jarvik 2000 modulate pump speed once per minute independent of external trigger or time during cardiac cycle. An additional way to trigger pump speed modulation

is to use an external trigger, such as a pressure waveform or EKG. This technique is employed when using the IABP that is either triggered by the patient's EKG or aortic pressure waveform to provide counter-pulsation support. Triggering from an EKG R-wave detection algorithm is the technique employed in this study using a simulated EKG from a patient simulator. The intelligent control algorithm detects the R-wave on the EKG corresponding to ventricular contraction to increase (or decrease) pump speed. This technique is different from current clinically used pump speed modulation algorithms due to the feedback that the controller has to time the increase in pump speed from an internal trigger source and the specific time points in the cardiac cycle to provide support in asynchronous, co-pulsation, and counter-pulsation modes. The R-wave threshold detection for triggering pump speed modulation with the intelligent control algorithm used in this study is shown in Figure 5. This threshold is set at a high enough amplitude for reliable R-wave detection (true positive) to avoid detection of the P or T-waves (false positive) and low amplitude ensure cardiac beats are not missed (false negative).

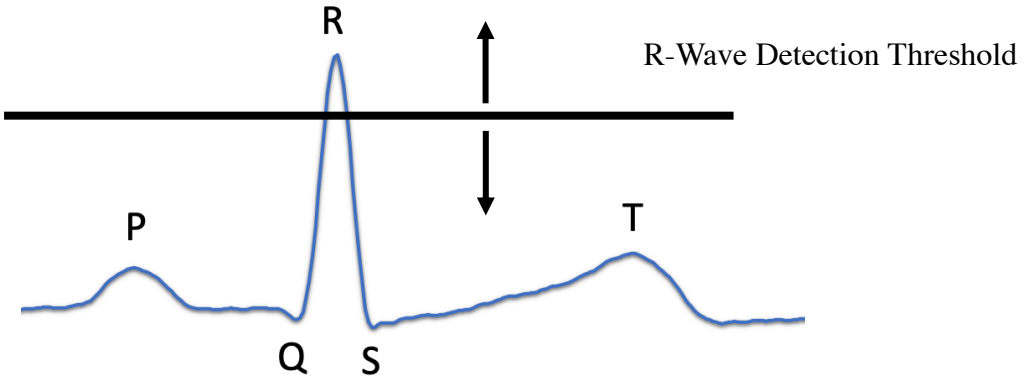

Figure 5. Illustration of electrocardiogram (EKG) cartoon with R-wave detection algorithm threshold. Ability in intelligent left ventricular assist device (LVAD) control strategy to increase or decrease threshold to trigger solely from R-wave without interference from P or T-wave. The R-wave of the QRS complex is targeted for pump speed modulation triggering because it corresponds to ventricular contraction (depolarization) and has a distinct peak and separation from the P and T wave. The P-wave corresponds to atrial contraction (depolarization) in the cardiac cycle while the T-wave corresponds to ventricular filling (repolarization).

3. Pump Speed Modulation: Modalities

Pump speed modulation techniques currently in clinical use focus on increasing (or decreasing) pump speed using an internal timing interval within the LVAD controller independent of the cardiac cycle. These techniques are employed in the HeartMate 3, in the Lavare cycle using the HVAD, and via the intermittent low speed of the Jarvik 2000 as seen in Figure 6. The HeartMate 3 is a centrifugal flow device that is implanted inside the chest and provides an artificial pulse by lowering operating rpm of the pump by 2000 rpm for 0.15 seconds and then subsequently increasing operating rpm by 4000 rpm for 0.20 seconds before returning to the original fixed speed (Castagna et al., 2017). The Lavare cycle is a control strategy integrated into the HVAD to provide intermittent pump washing to reduce the risk of pump thrombosis. The Lavare cycle is an algorithm that decreases operating rpm by 200 for a period of two seconds and then increases the operating rpm by 400 for one second and then returns to the operating rpm of the initial fixed speed (Kumar et al., 2019). The Jarvik 2000 is an axial flow device and was the first LVAD to utilize cyclic speed rotation (one cycle per minute) to minimize the risk of thrombus formation by promoting periodic aortic valve opening allowing washing of the aortic valve.

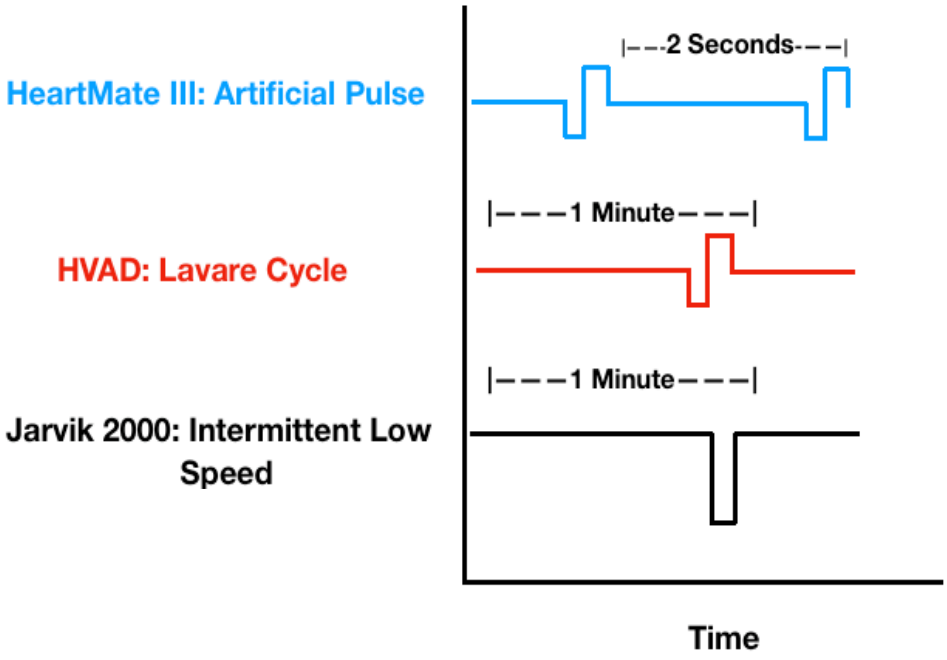

Figure 6. Graphical representation of pump speed modulation used by the HeartMate 3, Lavare cycle (HVAD), and Jarvik 2000 intermittent low speed controller. All techniques modulate pump speed on an internal time interval independent of cardiac cycle. HeartMate 3 modulates pump speed every two second while the Lavare cycle and Jarvik 2000 modulate pump speed once per minute.

By triggering pump speed modulation from external sources, such as the EKG or aortic pressure waveforms, pump speed modulation can be timed to increase (or decrease) pump speed at specific points in the cardiac cycle. Pump speed can be triggered during specific points in the cardiac cycle to produce co-pulsation (ventricular contraction), counter-pulsation (ventricular filling), and asynchronous (independent of cardiac cycle) support, as shown in Figure 6. Pump speed modulation may be timed using the R-wave EKG trigger (dotted line) for co-pulsation and counter-pulsation to give support during specific points during the cardiac cycle, while asynchronous pump speed modulation is increasing (or decreasing) pump speed independent of the cardiac cycle, as shown in Figure 7.

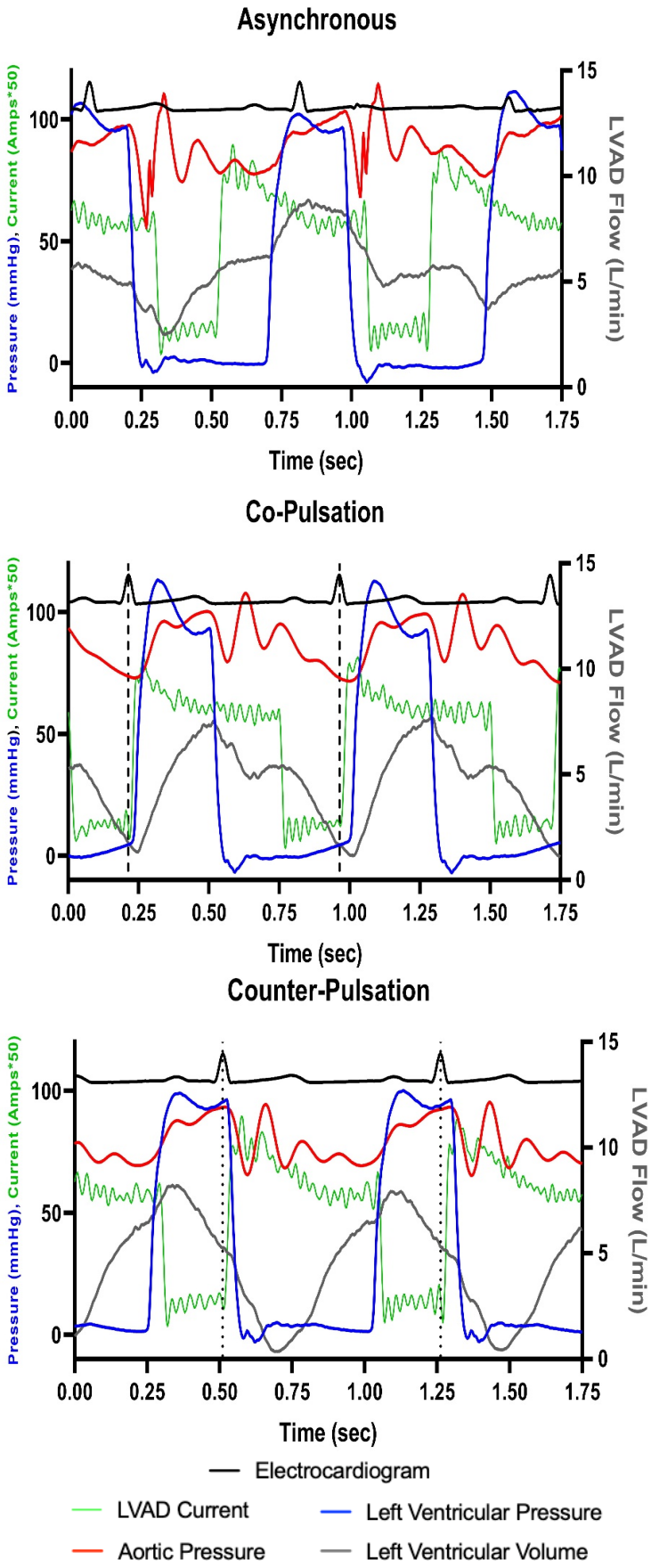

Figure 7. Pump speed modulation based on timing increase (or decrease) in pump speed with consideration to the cardiac cycle recorded in a mock circulatory loop simulating class IV heart failure (HF). Asynchronous modulation increases (or decreases) pump speed independently of the cardiac cycle. Co-pulsation increases (or decrease) pump speed in response to R-wave trigger (dotted line) at the beginning of systole and has higher pump speed during ventricular contraction. Counter-pulsation increases (or decreases) pump speed in response to R-wave trigger (dotted line) at the end of systole and has higher pump speed during ventricular filling. EKG: electrocardiogram, LVP: left ventricular pressure, AoP: distal aortic pressure, LVAD flow: left ventricular assist device (LVAD) flow, Current: current supplied to LVAD (controls pump speed).

In addition to timing pump speed modulation with respect to the cardiac cycle, pump speed modulation can also be achieved independent of timing (asynchronous). As shown in Figure 8, pump speed modulation can be controlled by increasing the Δrpm around a fixed mean rpm (black). This strategy increases the rpm above and below a mean rpm that is consistent between each operating setting. Low pump speed may be set while the higher operating pump speed is increased, thus changing the Δrpm between operating settings (orange). This would also in turn alter the mean pump speed, due to mean pump speed being a function of both high and low pump speed settings in addition to the time spent at each of these settings. High and low pump speed settings may also be set independent of mean pump speed and/or fixed high or low setting (blue).

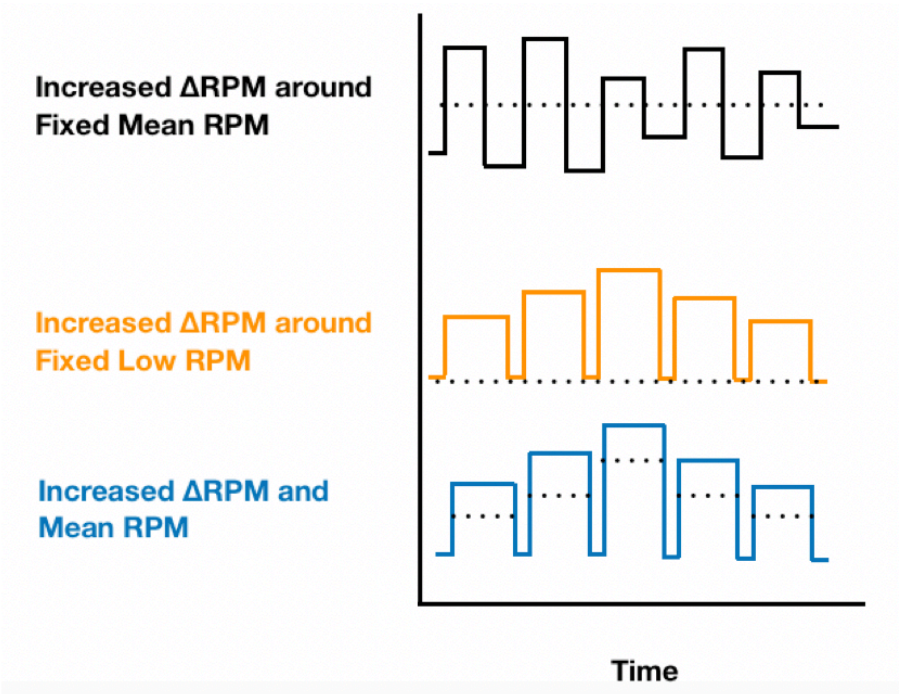

Figure 8. Pump speed modulation based on varying pump speed (rpm) settings around a fixed mean rpm (black), set low speed while altering high pump speed setting (orange), and changing pump speed settings independent of target mean rpm or fixed high or low pump speed (blue).

F. Intelligent LVAD Control

In this thesis project, a Medtronic HVAD was operated using a novel pump speed modulation algorithm to produce varying degrees of phasic ventricular volume unloading and pulsatile flow during asynchronous, co-pulsation, and counter-pulsation hemodynamic support in a MCL model. The HVAD was chosen because it is a clinical grade rotary blood pump and met the design criteria with required slew rate (defined as rate of change in pump speed per unit time, i.e. 1000 rpm/ms) for rapidly modulating (increasing, decreasing) pump speed using the supplied controller current. The intelligent LVAD control strategy is designed to rapidly increase (or decrease) pump speed with timing triggered to EKG (R-wave threshold detection) and user-defined duration (period). An EKG simulator was used to produce an EKG to trigger the intelligent controls pump speed modulation of the HVAD. The R-wave was selected as the trigger due to it corresponding to ventricular contraction. The percent time spent at high and low speed as well as the difference between high and low pump speed (rpm) were the operating controls varied throughout this experiment, as shown in Figure 9.

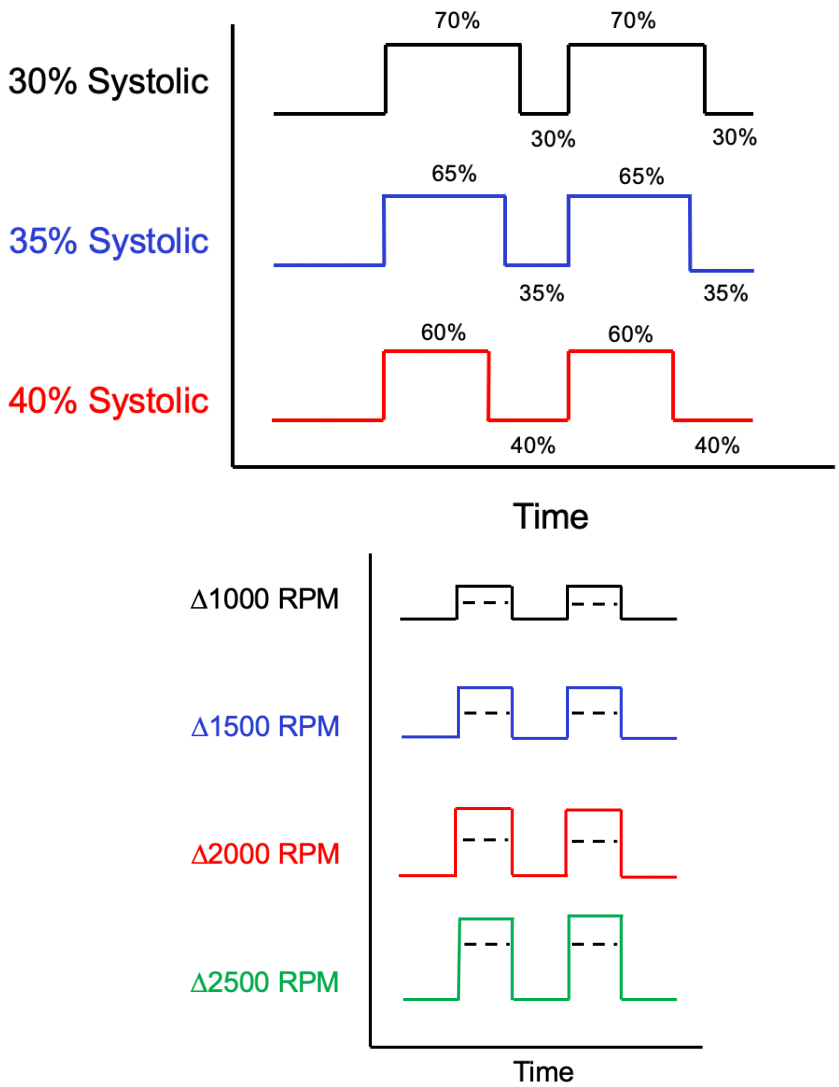

Figure 9. Illustration of intelligent left ventricular assist device (LVAD) control pump speed modulation controls. Pump speed has two controls the first being the time spent at the lower pump speed represented by 30, 35, and 40%. Also, the difference between high and low pump speed represented as Δrpm. For this study the low rpm was set and the Δrpm indicates the difference between the low setting and high setting, with the horizontal dotted line indicating the mean rpm of each setting. Mean rpm increased with increasing Δrpm in this study due to the fact that the low setting was set, and the high pump speed was increasing thorough out this study.

We hypothesized that (1) co-pulsation would provide the greatest increase in forward flow and pulse pressure compared to fixed pump speed due to the HVAD operating at higher speed during ventricular contraction (systole) and pumping at the lowest pressure

gradient, while (2) counter-pulsation would provide the greatest decrease in ventricular volume and workload compared to fixed pump speed due to the HVAD operating at the highest pump speed during ventricular filing (diastole). We also hypothesized that the greater the variation in high and low pump speed (Δrpm) and the longer the systolic (or diastolic) duration the greater the hemodynamic benefit that may be achieved. These hypotheses were tested in a single-sided, mock flow loop model constructed to simulate hemodynamic values equivalent to clinical NYHA Class IV HF.

II. METHODS

A. Study Overview

The objective of this study was to test the feasibility a novel intelligent control algorithm designed to rapidly increase and decrease pump speed of a LVAD (Medtronic HVAD, Minneapolis MN) within each cardiac cycle using a mock circulatory loop (MCL) model. The MCL was configured and tuned to simulate the systemic hemodynamics equivalent to NYHA class IV HF state in an adult. The MCL was primed with a blood analog solution (glycerol-saline) with a viscosity of 3 centipoise (cP) representing a hematocrit of 38% (Cheng et al., 2008). The goals of this study were 1) to demonstrate the ability to rapidly increase and decrease HVAD pump speed (rpm) within each cardiac cycle using R-wave trigger detection and quantifying the slew rate and trigger response time; 2) to identify HVAD intelligent control operating parameters the provide the highest degree of dynamic ventricular volume unloading, cardiac output, and/or vascular pulsatility; and 3) to characterize hemodynamic responses as a function of (a) fixed speed, synchronous systolic (co-pulsation), and diastolic (counter-pulsation) timing, (b) systolic or diastolic duration (30%, 35%, 40%), and (c) modulated differential pump speed (Δspeed = 0, 1000, 1500, 2000, 2500 rpm). We hypothesized that pump speed modulation will provide better volume unloading (rest), pulsatility (reloading),

and/or washing (pump, valves, ventricle) than with the LVAD operated at fixed pump speeds.

B. Study Design

1. Intelligent LVAD Control System

The intelligent LVAD control system consists of a controller (hardware) and programmed algorithms (software). The intelligent HVAD control system uses a HF patient's EKG waveform data to identify the R-wave landmark in real-time for every cardiac cycle using a threshold detection algorithm. The trigger time point (R-wave detection) is then used to rapidly increase or decrease user-defined pump speeds and the start and end time-points within the native heart cardiac cycle. The controller software enables the end-user to define the lower and upper pump speed settings (for a derived Δrpm), time delay from R-wave time point, and duration of modulated pump speed cycle (% systole or % diastole). In this study, the intelligent control system was tested using a clinical grade LVAD (HVAD, Medtronic, Minneapolis, MN). The HVAD is a continuous flow centrifugal blood pump with a therapeutic window of 1,800 – 4,000 rpm as specified by Medtronic's instructions for use (IFU).

The control algorithm used to modulate HVAD pump speed was developed by Dr. Richard Wampler (Oregon Health Sciences University, Portland OR), which is currently protected by provisional patent (proprietary), and was implemented using LabVIEW (National Instruments, Austin, TX). A high-fidelity EKG waveform (1kHz) from a Patient Simulator (Fluke Biomedical, Everett, WA, medSim 300B) and R-wave detection algorithm were used to trigger an increase (or decrease) in HVAD pump speed by increasing (or decreasing) the current supplied to the HVAD. The software program provided the following user-defined input parameters via a graphical user interface

(GUI): (1) R-wave detection threshold (V), (2) low and high pump speeds (rpm), (3) time delay after successful R-wave detection to initiation of pump speed modulation sequence (ms), and (4) systolic duration (%). In addition, the GUI continuously displays in real-time the EKG waveform, R-wave trigger landmark, and pump speed. The key components of the intelligent LVAD control system are shown in Figures 10 and 11.

Figure 10: Medtronic HVAD centrifugal blood pump (Medtronic, Minneapolis MN). The HVAD is a continuous flow LVAD that operates at a clinical therapeutic window of 1,800-3,200 RPM as stated by HeartWare IFU (TOP). Intelligent controller (hardware) that has connections for the HVAD, a current measurement, and EKG input. (BOTTOM) The controller interfaces with the HVAD and intelligent control algorithm to allow the algorithm to visualize the EKG and detect the R-wave trigger. The algorithm then interfaces with the controller to increase (or decrease) pump speed based on R-wave detection with an additional output connection to measure the current being delivered to the HVAD (pump speed increase (or decrease)).

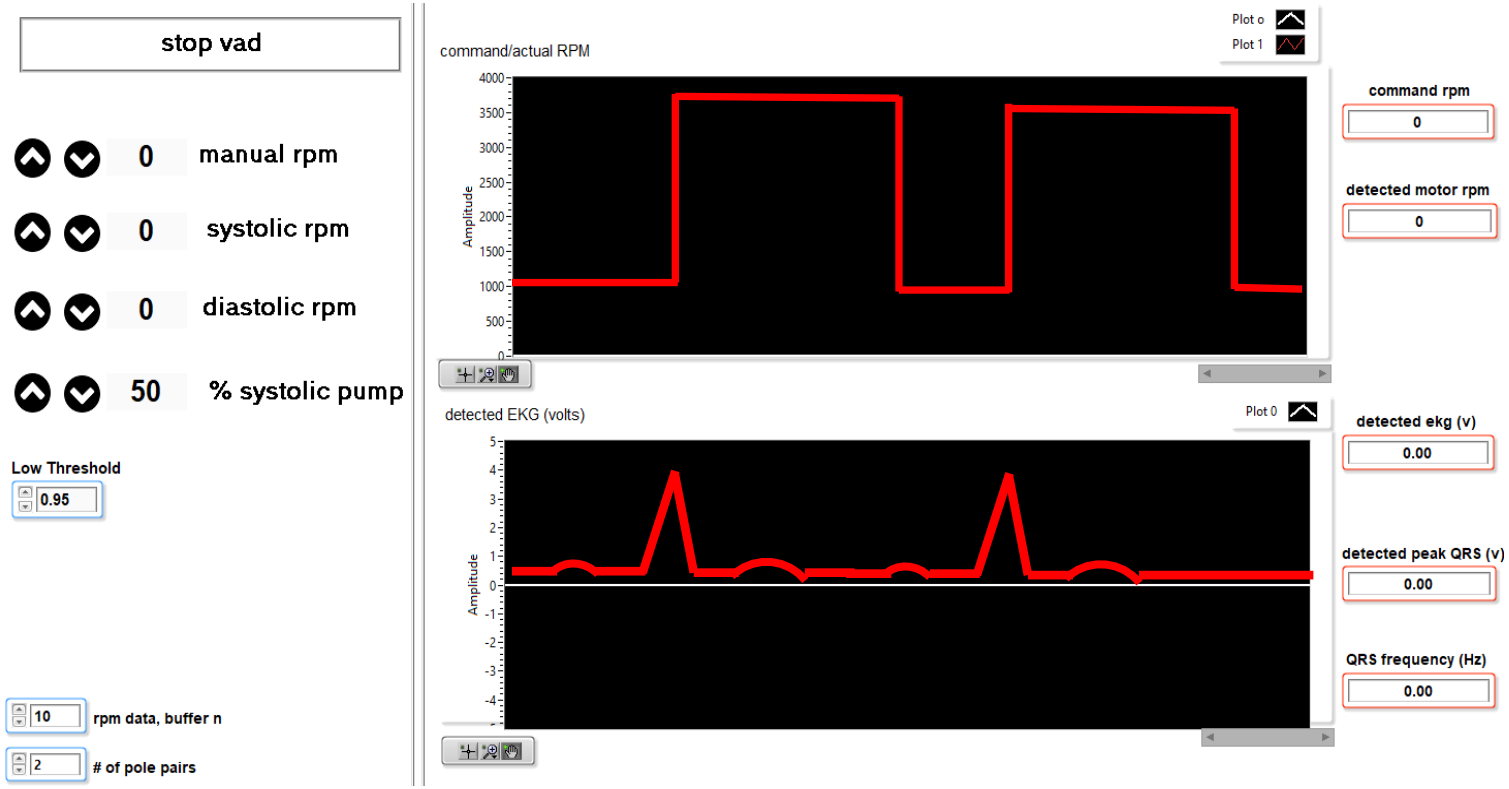

Figure 11: Front panel display of Graphical User Interface (GUI) of intelligent control software, including two waveform graphs that plot commanded RPM (top) for the HVAD to operate at and EKG waveform (bottom). The command RPM waveform has two indicators (1) command RPM to be sent and (2) the detected RPM of the HVAD. The EKG waveform has three indicators one for the detected EKG in volts, another for detected QRS peak in volts, and finally detected QRS frequency in hertz to determine beat rate of signal. The GUI has five controls for operating the HVAD (1) a stop VAD command to stop the HVAD, (2) a manual RPM if the HVAD was to be run in a fixed speed, (3) systolic RPM to operate the HVAD, (4) diastolic RPM to operate the HVAD, and (5) percent systole that determines how long the HVAD should operate at the systolic RPM. A threshold control is set to lower (or increase) the peak detection voltage to allow only the R-wave to trigger increase (or decrease) pump speed while in operating in a pulsatile manner.

2. Intelligent LVAD Control Operation

The intelligent control strategy was tested using an HVAD with left ventricular apical inflow and aortic outflow cannulation in the MCL model during a simulated HF test condition. Baseline hemodynamics were recorded with the HVAD off and outflow graft clamped before and after data epoch to confirm minimal (non-significant) changes in the HF test condition. Hemodynamic data were recorded with HVAD operated at fixed pump speeds (1500, 2000, 2500, 3000, 3500, 4000 rpm) and with pump speed modulation, each operating setting tested during this experiment is listed in Table IV. During pump speed modulation, the intelligent controller was set to a low pump speed (1500 rpm), high pump speeds (2500, 3000, 3500, 4000 rpm), and systolic (or diastolic) durations (30%, 35%, 40%), as illustrated in Figure 9. The operating range of high and low pump speeds was determined by using the therapeutic window (1,800-4,000 rpm) specified by the HVAD IFU. The pump speed modulation (Δrpm) was defined as the difference between low and high pump speed settings (i.e. low = 1500 rpm, high = 4000 rpm, Δrpm =2500rpm). The intelligent LVAD control strategy was triggered from an EKG simulator at a constant beat rate of 80 BPM, while the MCL artificial ventricle was set at a beat rate of 78 BPM. This slight offset allowed for asynchronous operation of the intelligent LVAD control strategy, which gave multiple phases of purely asynchronous support, phases of co-pulsation support, and phases of counter-pulsation support over a four-minute test run (single data file). A single four-minute epoch (n=1) was recorded once for each pump setting. The order of data acquisition was fixed speed, 30% systolic duration, 35% systolic duration, and 40% systolic duration operating settings (note: order was not randomized).

TABLE IV: EXPERIMENTAL DESIGN OF INTELLIGENT LVAD CONTROL STRATEGY EXPERIMENT

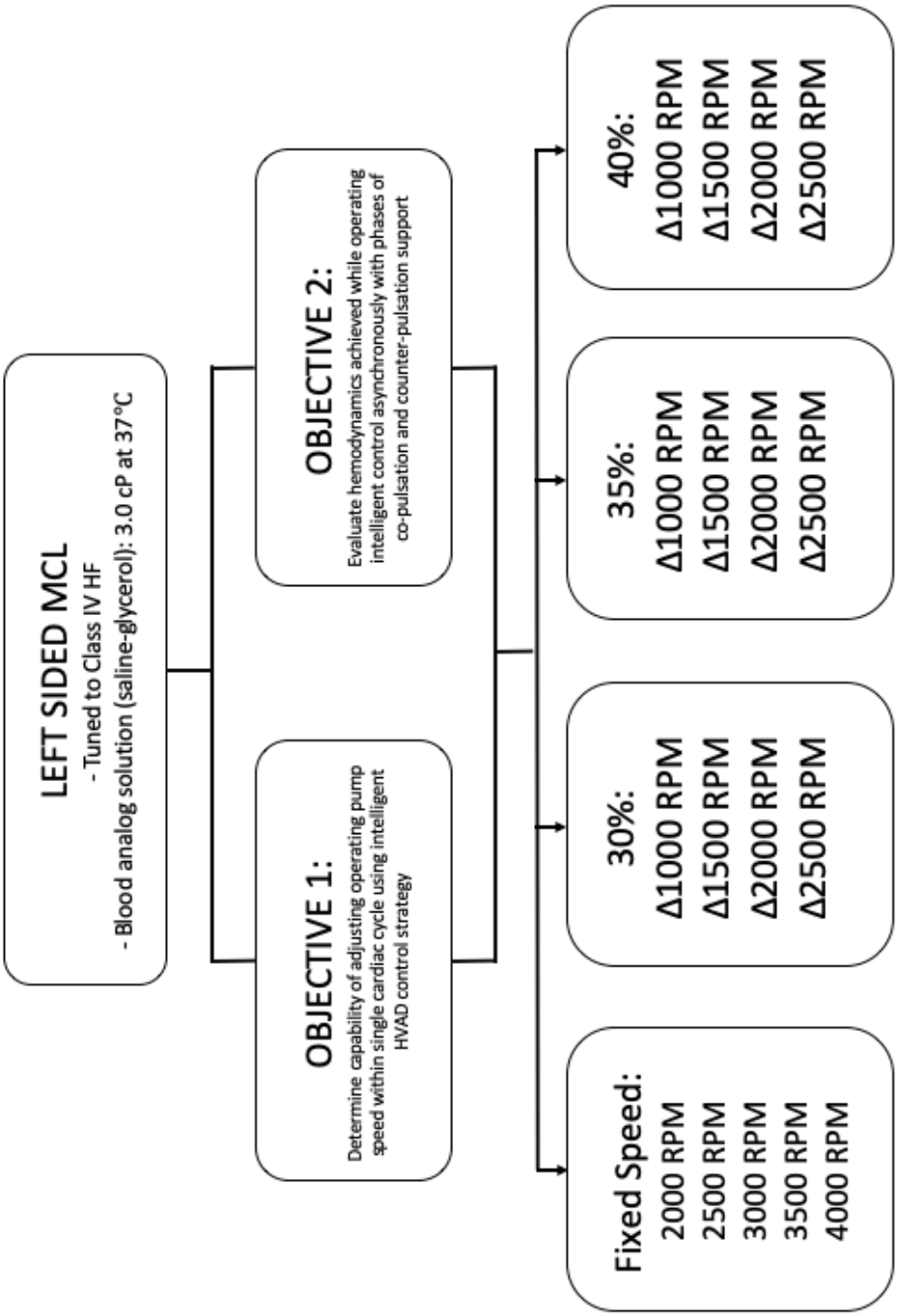

Table IV. Study design of intelligent LVAD control strategy experiment. A mock circulatory loop (MCL) tuned to simulate class IV heart failure (HF) to (1) determine the capability of pump speed modulation within a single cardiac cycle, and (2) evaluate the hemodynamics achieved while operating the intelligent LVAD control strategy asynchronously with phases of co-pulsation and counter-pulsation. To accomplish these two objectives the intelligent LVAD control strategy operated a HeartWare HVAD at fixed speed and then at various Δrpm and systolic durations (30%, 35%, and 40%). Systolic duration corresponded to the amount of time spent at the lower operating pump speed (1,500 rpm) during each cardiac cycle while the Δrpm represents the difference between high and low pump speed. Each operating condition was recorded once with a four-minute data file (n=1).

3. Mock Loop Model

A MCL was developed to simulate the hemodynamics of a NYHA class IV HF patient. The MCL was primed with a blood analog solution of glycerol (Fisher Scientific, G33-4, Lot 180512)-saline to simulate a viscosity range of 3.0±0.2 cP to represent a hematocrit of approximately 38%. Saline was created at a concentration of 0.9% using distilled water and sodium chloride (Fisher Scientific, L-11635). A hematocrit of approximately 38% was chosen to mimic the hemodilution that occurs in patients diagnosed with HF resulting from an increased plasma volume (Androne et al., 2003; Guglin et al., 2012). The viscosity of the solution was tested before the first test condition and repeated after completion of last test condition to validate that the viscosity did not change significantly over the entire time-course of the study. A viscometer ("Q" Glass Company, Inc., Towaco, NJ) and water bath (Thermo Scientific, Marietta, OH) were used to test the viscosity of the solution at 37°C by recording the transit-time of the solution through the viscometer. The viscosity of the solution was derived from the relationship between the viscosity constant, transit time, and density of the solution, as defined in Equation 1.

$$Viscosity = 0.00743 * transit\ time\ (seconds) * density \quad (1)$$

The MCL was configured to simulate an adult single-sided systemic (high pressure) circulation with the following major components: (1) volume reservoir to simulate venous return, (2) inflatable balloon to simulate the compliance of the left atrium, (3) arterial compliance chamber, (4) pneumatically-actuated silicone sac to simulate the left ventricle, and (5) silicone tubing (1/8" to 3/4" inner diameter) to

simulate the aorta (Figure 12). A Sarns cardiopulmonary bypass machine (Terumo, Somerset, NJ) and a Sarns heater-cooler were used to maintain a physiologic temperature of 37°C of the blood analog solution. The construction of the MCL is representative of a lumped parameter model, and thereby assumes minimal losses compared to a distributed (network) model or human anatomic structure.

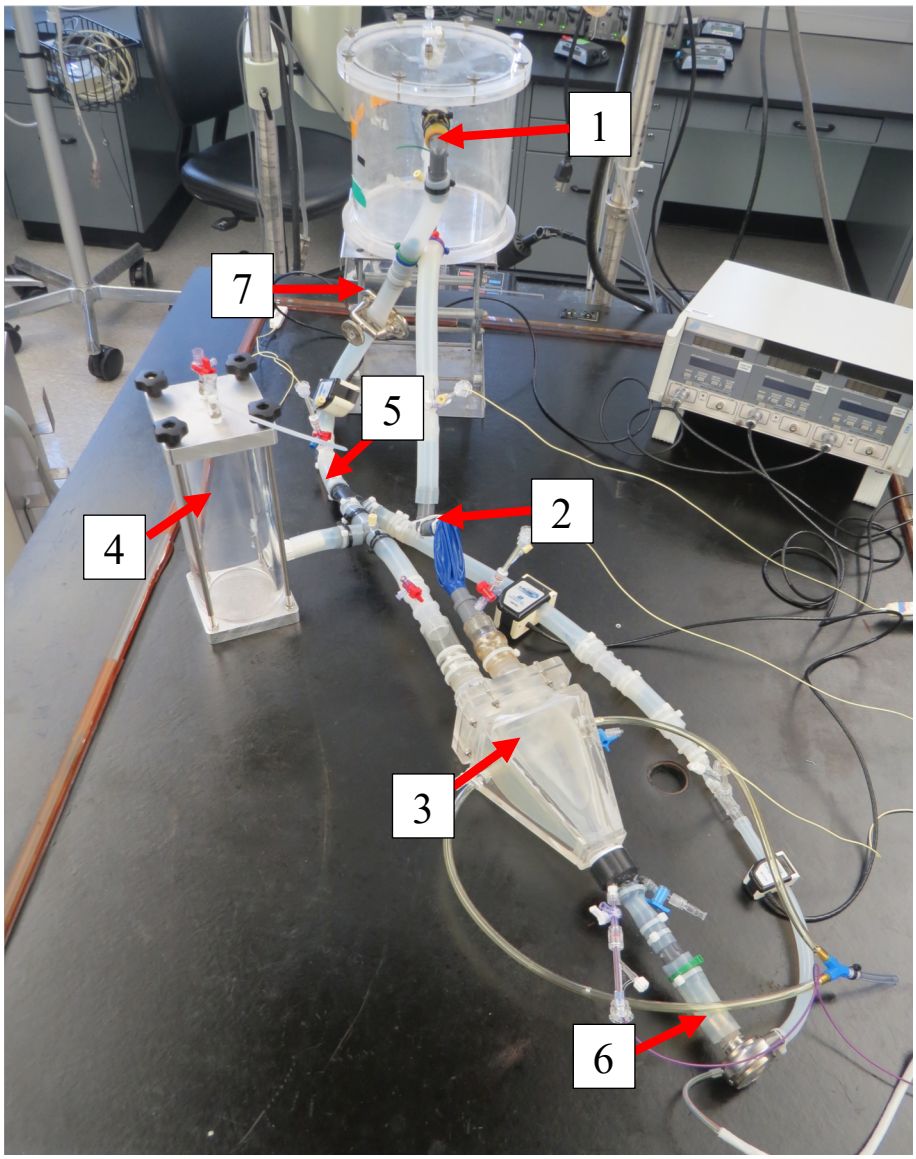

Figure 12. The mock circulatory loop (MCL) used to test the intelligent HVAD control system consisted of a (1) volume reservoir, (2) artificial left atrium, (3) artificial ventricle, (4) arterial compliance chamber, (5) 1/8" to ¾" silicone tubing to simulate aorta, (6) HVAD insert into apex of artificial ventricle, (7) and peripheral resistor clamp to adjust afterload.

4. Hemodynamic Measurements & Data Acquisition

Data acquisition (DAQ) and LabChart (AD Instruments, Version 8, Colorado Springs, CO) were used for signal conditioning (Koenig et al., 2004), real-time A/D conversion (400 Hz sampling rate, 100 Hz low pass filter), visual display, and recording of 11 hemodynamic parameters, as shown in Figure 13. Signal conditioning of the left ventricular pressure (LVP) and aortic pressure (AoP) distal waveforms was performed using a 10 Hz low pass filter (LabChart, finite impulse response (FIR)) to reduce the signal noise recorded produced by the mechanical valve used in the mock loop model to simulate the aortic valve. Similarly, a low pass filter of 40 Hz was applied to the current waveform to reduce the electrical noise. The EKG waveform was amplified to an R-wave peak of ~2.5 volts to enable reliable threshold detection by the programmed intelligent control algorithm. A medSim 300B patient simulator was used to produce an EKG at a heart rate of 80 BPM to test the intelligent HVAD control system R-wave detection and pump speed modulation algorithms. Each intelligent LVAD control strategy pump operating setting was recorded using four-minute epochs to allow for phases of asynchronous, co-pulsation, and counter-pulsation support.

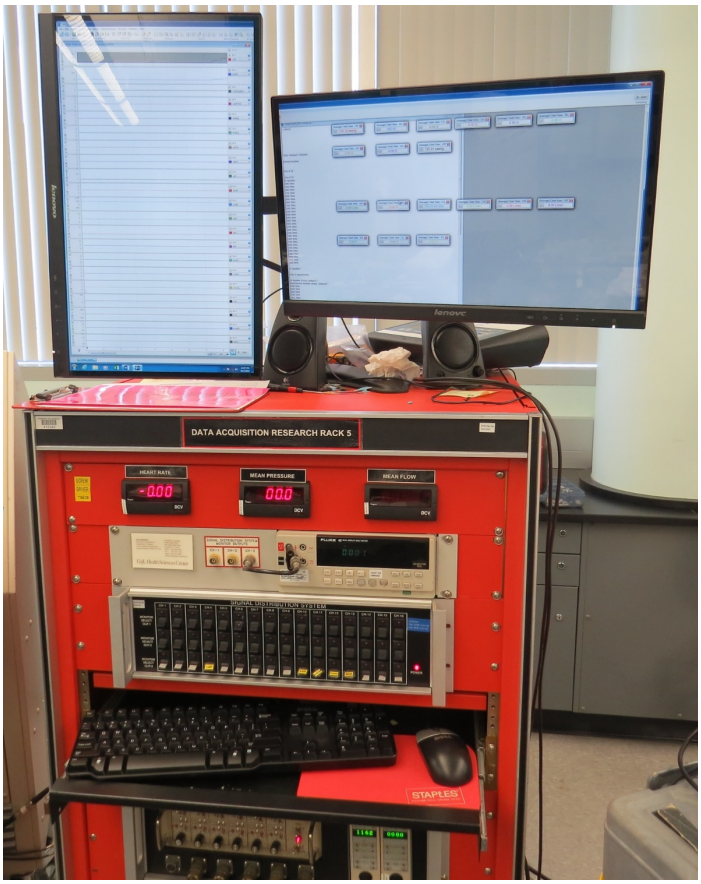

Figure 13. Data acquisition system (DAQ) with LabChart software used throughout the experiment to record hemodynamic waveforms.

Left atrial pressure (LAP) was measured using a low-fidelity (20 Hz) fluid-filled catheter (ARGON, Frisco, TX) and cardiac care patient monitor (Agilent, Santa Clara, CA). Left ventricular (LV), distal aortic pressure (AoP), and LVAD pressures were measured using single-tip, high-fidelity (5kHz) catheters (Millar, Houston, TX). Aortic root flow (AoF), total flow (TF), and VAD flow (VADF) were measured using high-fidelity (100Hz) transit-time flow probes (Transonic Systems, Ithaca, NY). Left ventricular pressure-volume loops were measured using a pressure-volume admittance catheter (Transonic Systems, 5F, 4 segments, 10mm spacing).

Fluid-filled catheters were open to atmosphere and zeroed using the cardiac care patient monitor and calibrated using a TruCal Simulator/Tester (Baxter, Tulsa, OK) over a clinically-relevant range of pressures (-5 to 150 mmHg). Millar pressure catheters were pre- and post-calibrated using a digital manometer (Meriam, Cleveland, OH) and pressure chamber over a clinically-relevant range of pressures (-5 to 150 mmHg). Flow probes were pre-calibrated electronically using a flow module calibration step (0 volt to 1-volt (full-scale)) and factory calibration settings based upon flow probe size, mock loop tubing diameter, and style (in-line, clamp-on). Sample pressure and flow sensor calibration sequences are illustrated in Figure 14.

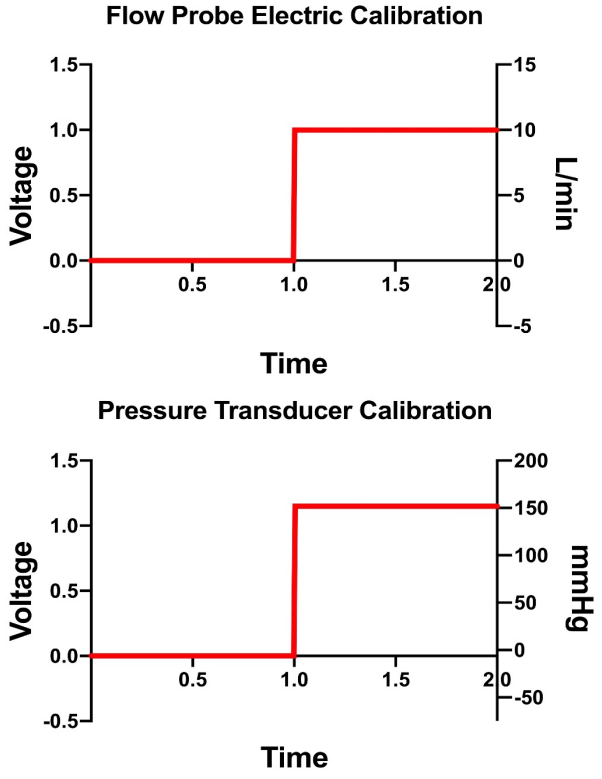

Figure 14. Illustration showing flow probe and pressure transducer electrical calibration. Flow probes were electrically calibrated using built in electrical calibration from flow module based on flow probe size and tubing diameter. Pressure transducers were calibrated by creating a known pressure in a pressure chamber (-5 to 150 mmHg) and then correlating each electrical signal with its corresponding pressure.

The pressure-volume admittance catheter was calibrated using internal electronic calibration settings programmed into the ADVantage PV system (Transonic, ADV500; 0 to 400 mL, phase 0 to 20°, and mag 0 to 50 mS). The stroke volume input was set prior to the baseline HF recording for each set of data recordings (Table V) and was calculated by dividing the measured cardiac output by the beat rate of the artificial ventricle. Pre- and post-calibrations were completed for all sensors and signal conditioners to verify gain and offset were consistent (i.e. no significant drift). Intrinsic pump parameters that were recorded directly and/or derived during post-processing, included current, pump speed (rpm), and power. The hemodynamic parameters recorded throughout the intelligent LVAD control strategy experiment and the instrumentation used to acquire each parameter in this study are listed in Table V. The placement of each sensor within the MCL model for recording each of the eleven hemodynamic parameters is illustrated in Figure 15.

TABLE V
HEMODYNAMIC PARAMETERS RECORDED DURING
INTELLIGENT LVAD CONTROL EXPERIMENT

Parameter	Abbreviation	Instrument	Range	Unit
Electrocardiogram	EKG	Patient Simulator	-0.2-3	Volts
Left Ventricular Pressure	LVP	Millar Catheter	-5-150	mmHg
Left Atrial Pressure	LAP	Fluid Filled Transducer	0-30	mmHg
VAD Pressure	VADP	Millar Catheter	0-150	mmHg
Aortic Root Flow	AoF	Transonic Flow Probe	0-4	L/min
Left Ventricular Assist Device Flow	LVAD Flow	Transonic Flow Probe	-1-10	L/min
Aortic Pressure Distal	AoP Distal	Millar Catheter	0-150	mmHg
Total Flow	TF	Transonic Flow Probe	0-6	L/min
Current	A	Intelligent Controller	0-2	Amps
Left Ventricular Volume	LVV	Transonic PV Catheter	0-400	mL
Pump Speed	RPM	Intelligent Controller	0-4000	RPM

Table V. Hemodynamic parameters recorded during intelligent LVAD control strategy experiment. The abbreviation, instrument used to record each parameter, range, and unit of each parameter recorded is listed above.

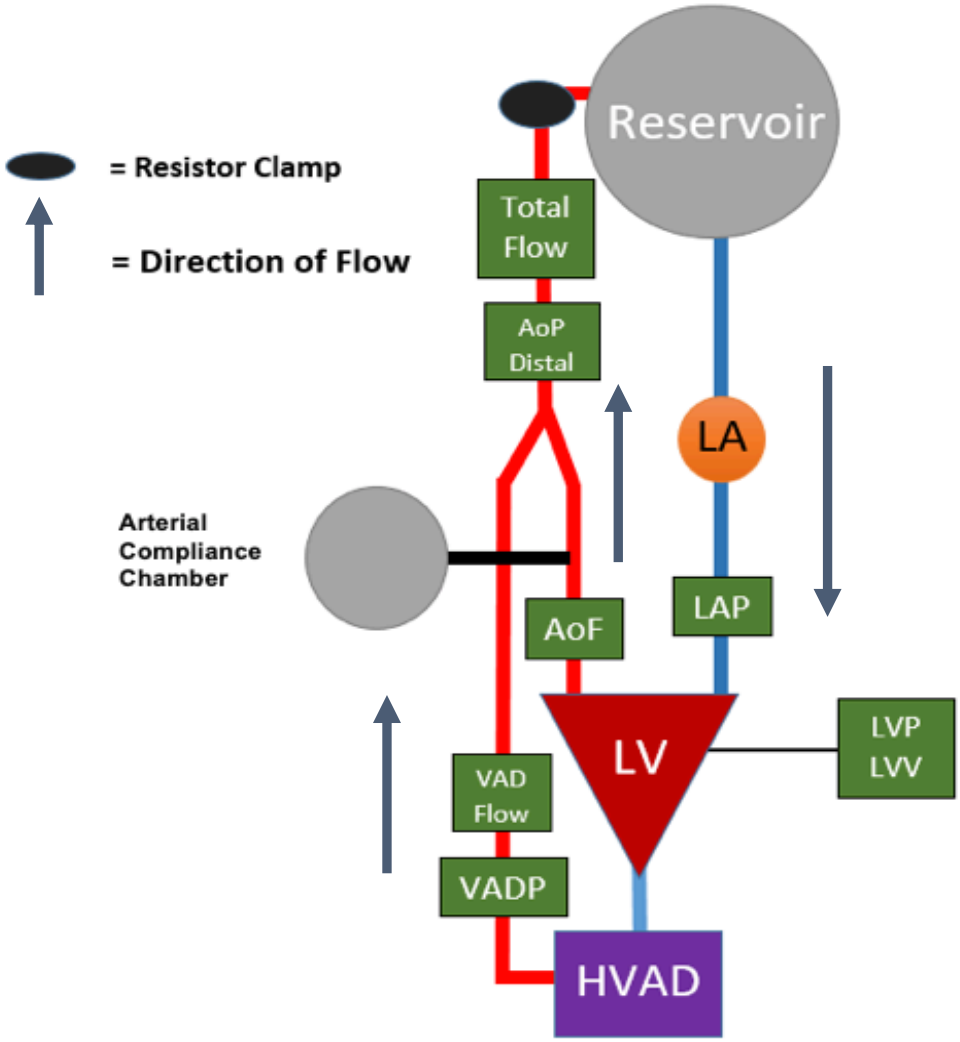

LA: Left Atrium
LAP: Left Atrial Pressure
LV: Left Ventricle
LVP: Left Ventricular Pressure
LVV: Left Ventricular Volume
VADP: LVAD Pressure
VAD Flow: LVAD Flow
AoF: Aortic Flow
AoP Distal: Distal Aortic Pressure

Figure 15. Schematic of mock circulatory loop (MCL) with location of each hemodynamic parameter recorded during the intelligent LVAD control strategy experiment.

The MCL was constructed and tuned to simulate hemodynamics of NYHA class IV HF (Yildiran et al., 2010; Melenovsky et al., 2015) with the mock LV heart rate set at 80 bpm, systolic duration of 35%, and cardiac output of 3 L/min representative of the

values seen in class IV HF patients with body mass index (ratio of weight to height: (kg/m^2)) and cardiac index (assessment of cardiac output with respect to patients size) (Carlsson et al., 2012). The MCL was tuned by adjusting the preload (atrium), source (ventricle), and afterload (vasculature). The preload of the MCL was set by adjusting the height of the venous reservoir, as well as increasing the total volume of the reservoir until the LA pressure was within the target clinical range. The silicone mock LV pneumatic drive (positive) and vacuum (negative) pressures, percent systole, and beat rate were set using a clinical-grade pneumatic driver (P/N 500099-0006-005E Thoratec, Pleasanton CA). Afterload of the MCL was set by increasing (or decreasing) the peripheral resistance of the MCL by the closing (or opening) the turn-screw clamp (resistor) placed on the aorta and before the venous reservoir.

5. Data Analysis

Data were analyzed on a beat-to-beat basis with the recorded time period to quantify the hemodynamic performance of operating the intelligent LVAD control at fixed speed or in a pulsatile manner and test the proposed hypothesis that pump speed modulation provides improved hemodynamic support compared to HF baseline (pump off) and fixed pump speed. Data recorded using the intelligent control strategy to induce pump speed modulation were parsed into co-pulsation and counter-pulsation segments for each recorded four-minute asynchronous data file and each operating condition (i.e. 30% systolic duration at a Δ1000 rpm, n=1), as listed in Table IV. By operating the artificial ventricle at a beat rate of 78 BPM and triggering pump speed modulation using the intelligent LVAD control strategy at a beat rate of 80 BPM, phases of asynchronous, co-pulsation, and counter-pulsation support were achieved in a single data file (as opposed to

recording three separate data files for each phase of support). To determine co-pulsation and counter-pulsation beat segments, the increase (or decrease) in pump current was aligned with the corresponding landmark of the LVP waveform. For the co-pulsation beat segment, a beat with an increase (or decrease) in LVAD current aligned with the beginning of systole, and the beats before and after were selected to create a three-beat co-pulsation segment. For counter-pulsation beat segments, a beat with an increase (or decrease) in LVAD current aligned with the end of systole, and the beats before and after were selected to create a three-beat counter-pulsation segment. These segments were then analyzed to quantify the hemodynamic performance during fixed speed, co-pulsation, and counter-pulsation to investigate their effect on ventricular volume unloading, cardiac output, and pulsatility. The hemodynamic waveforms were also graphed to evaluate the ability of the intelligent control strategy to modulate pump speed within a cardiac cycle.

Data were normalized by averaging the pre- and post-calibrations of all pressure, flow, and volume measurements. Pre- and post-calibrations were averaged to mitigate any electrical drift that may have occurred during the experiment. Although minimal electrical drift was seen between the pre- and post-calibrations for each parameter, the average was still used to create the calibration factor in LabChart for each parameter recorded during the experiment. Once normalized, the hemodynamic data were exported from LabChart into text files. These texts files were saved as DAT-files, and imported into MatLab (R2016, Mathworks, Natick, MA) for post-processing and data reduction using a Hemodynamic Estimation and Analysis Research Tool (HEART) software (Schroeder et al., 2004). Once imported into the HEART program, each data file was "beat picked" using the LVP as the reference signal and a "beat picking method" that selected end-diastolic landmark using a threshold detection and slope algorithm, as

previously reported (Schroeder et al., 2004). This point on the LVP waveform corresponds to end diastole was used as the reference point for starting and ending each beat. The reference point was selected using an upper threshold, a lower threshold, a bad beat threshold, and an end-diastolic threshold. Sample LVP and AoP distal waveforms with each beat start and end point landmark identified by a red circle on the LVP waveform is shown in Figure 16.

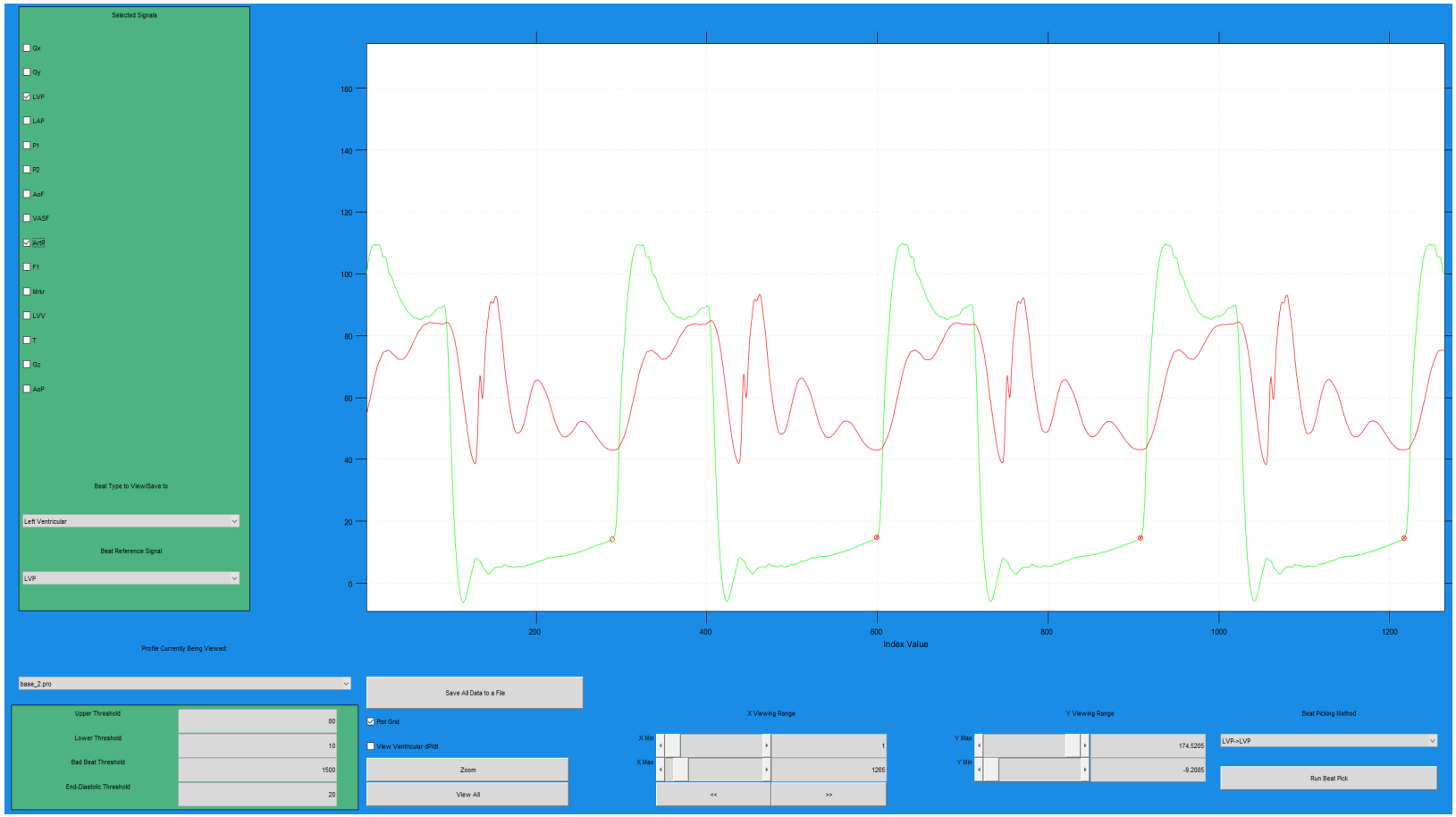

Figure 16. Hemodynamic Estimation and Analysis Research Tool (HEART) with left ventricular pressure (LVP, green waveform) and aortic pressure (AoP distal, red waveform) waveforms. Beginning and end of each beat are depicted by red circle on the LVP waveform corresponding to end diastole. Beginning and end of each beat were selected using an upper threshold, lower threshold, and end diastolic threshold.

Once each data file was "beat picked", the file was exported as a MAT-file for analysis by a custom MatLab script as listed in **Appendix III**. The MatLab script was used to analyze beat-to-beat parameters for each of the 12 recorded hemodynamic waveforms. The script was able to produce calculations, including max-min flow, max-min pressure, as well as mean pressures and flows during each part of the cardiac cycle (systole-diastole).

Pulse pressure (ΔP), mean arterial pressure (MAP), surplus hemodynamic energy (SHE), energy equivalent pressure (EEP), and arterial impedance (ZART) were calculated from the recorded hemodynamics to quantify the impact the intelligent HVAD control system had on pulsatility. EEP is defined as the hemodynamic energy of a given volume of fluid passing through a given tubing cross section as expressed by Equation 2 (Soucy et al., 2013).

$$EEP = \frac{\int Q * P * dt}{\int Q * dt} \tag{2}$$

SHE is defined as the additional energy that exists when there is some degree of pulsatility in the pressure or flow waveform (Ündar et al., 2005), SHE is represented as the difference of EEP and MAP multiplied by 1,332 (Equation 3).

$$SHE\ (ergs/cm^3) = 1{,}332 * (EEP - MAP) \tag{3}$$

ZART (vascular load impedance) is a function of resistance, compliance, and inertance, and regulates the dissipation of hemodynamic energy (Soucy et al., 2013). ZART is expressed as the fast Fourier transform (FFT) of arterial pressure divided by the FFT of arterial flow (Equation 4). For this experiment the resistance component of ZART was analyzed and is the quotient of mean pressure divided by mean flow.

$$Z_{ART} = \frac{FFT(P)}{FFT(Q)} \tag{4}$$

LV stroke volume, LV external work (PV loop area), LV end diastolic pressure, and LV end systolic pressure were calculated to determine the effect of the intelligent LVAD control strategy had on ventricular volume unloading. Intrinsic pump parameters including speed (rpm) and current were recorded from the intelligent controller and analyzed. Power was calculated by multiplying the current and voltage supplied to the HVAD during pump operation. These parameters were used in correlation with hemodynamic data to visualize trends associated with increasing (and decreasing) flows and pressures during pump speed modulation with each cardiac cycle. Data are presented as means and percent differences between equivalent means for pump power comparison.

III. RESULTS

A. Key Findings

In this study, we successfully demonstrated that a novel intelligent LVAD control algorithm was able to increase and decrease the operating pump speed (rpm) of a Medtronic HVAD within a single cardiac cycle using an EKG waveform and R-wave threshold detection algorithm to trigger changes in pump speed. In addition, we identified two distinct time delays associated with the intelligent control strategy: (1) a time delay with initiation of changes in pump speed limitations associated with the R-wave detection and trigger algorithm(s), and (2) a hemodynamic time delay that occurs between the increase in pump speed and the increase in LVAD flow associated with fluid inertia. We also identified that improvements in hemodynamics with increasing levels and timing of pump speed modulation came at the expense of increased LVAD power consumption compared to operating at fixed speeds with equivalent mean flows. Notably, pump speed modulation improved hemodynamic performance as evidenced by dynamic LV volume unloading, increased cardiac output, and increased pulsatility with higher mean pump speed operating settings producing the greatest increases in LV volume unloading and cardiac output in this study, and the lower mean pump speed operating settings producing the greatest increases in pulsatility indices.

B. Mock Circulatory Loop (MCL) Model

We successfully demonstrated that the MCL model, used to test the performance of the intelligent LVAD control system, closely matched the blood viscosity and

hemodynamic waveforms and landmark parameters of a NYHA class IV HF patient (Table VI), and the viscosity of the blood analog solution was maintained at a mean of 3.01 cP and differences between pre- (3.05 cP) and post-calibrations (2.97 cP) were negligible.

TABLE VI
COMPARISON OF CLINICAL CLASS IV HEART FAILURE AND MOCK CIRCULATORY LOOP ACHIEVED HEMODYNAMICS

Comparison of Hemodynamic Paremeters		
Parameter	**Clinical Class IV HF**	**MCL Achieved**
Systolic Blood Pressure (mmHg)	98 ± 12	84
Mean Arterial Pressure (mmHg)	77 ± 9	63
Diastolic Blood Pressure (mmHg)	66 ± 8	46
Aortic Pulse Pressure (mmHg)	31 ± 9	38
Ejection Fraction (%)	25 ± 5	23
Cardiac Output (L/min)	<3	3
Left Atrial Pressure (mmHg)	20 ± 8	23
Heart Rate (BPM)	92 ± 15	78

Table VI. Clinical presentation of class IV heart failure hemodynamic parameters compared to achieved hemodynamics in mock circulatory loop. Clinical hemodynamic parameters are represented as mean +/- standard deviation (Yildiran et al., 2010; Melenovsky et al., 2015).

C. Intelligent LVAD Control –Engineering and Hemodynamic Performance

1. Pump Speed Modulation – Engineering Benchmarks

The intelligent LVAD control system successfully demonstrated the ability to rapidly increase and decrease HVAD pump speed within a single cardiac cycle during asynchronous operation, which also produced phases of synchronous co-pulsation and synchronous counter-pulsation profiles for all systolic durations (30, 35, 40%) at the highest pump speed profile (Δrpm = 2500), as shown in Figure 17. Specifically, the R-wave threshold detection algorithm demonstrated the ability to trigger an increase (or

decrease) in HVAD pump speed (by the change pump current as represented by the dotted vertical line for each beat) and decrease (or increase) in pump speed for specified systolic duration prior to the next cardiac cycle (EKG waveform – QRS complex). Key observations during the pump speed modulation study include the following: (1) pump speed (current) operated independently of LV end-systole or end-diastole during periods of asynchronous support, (2) during periods of synchronous co-pulsation pump speed (current) increased at LV end-diastole, (3) during periods of synchronous counter-pulsation pump speed (current) increased at LV end-systole, and (4) when R-wave detection is missed the pump speed remains at the higher operating speed until the next R-wave is detected. Sample asynchronous, synchronous co-pulsation, and synchronous counter-pulsation waveforms for all controller settings (systolic duration, Δrpm) are presented in **Appendix I**.

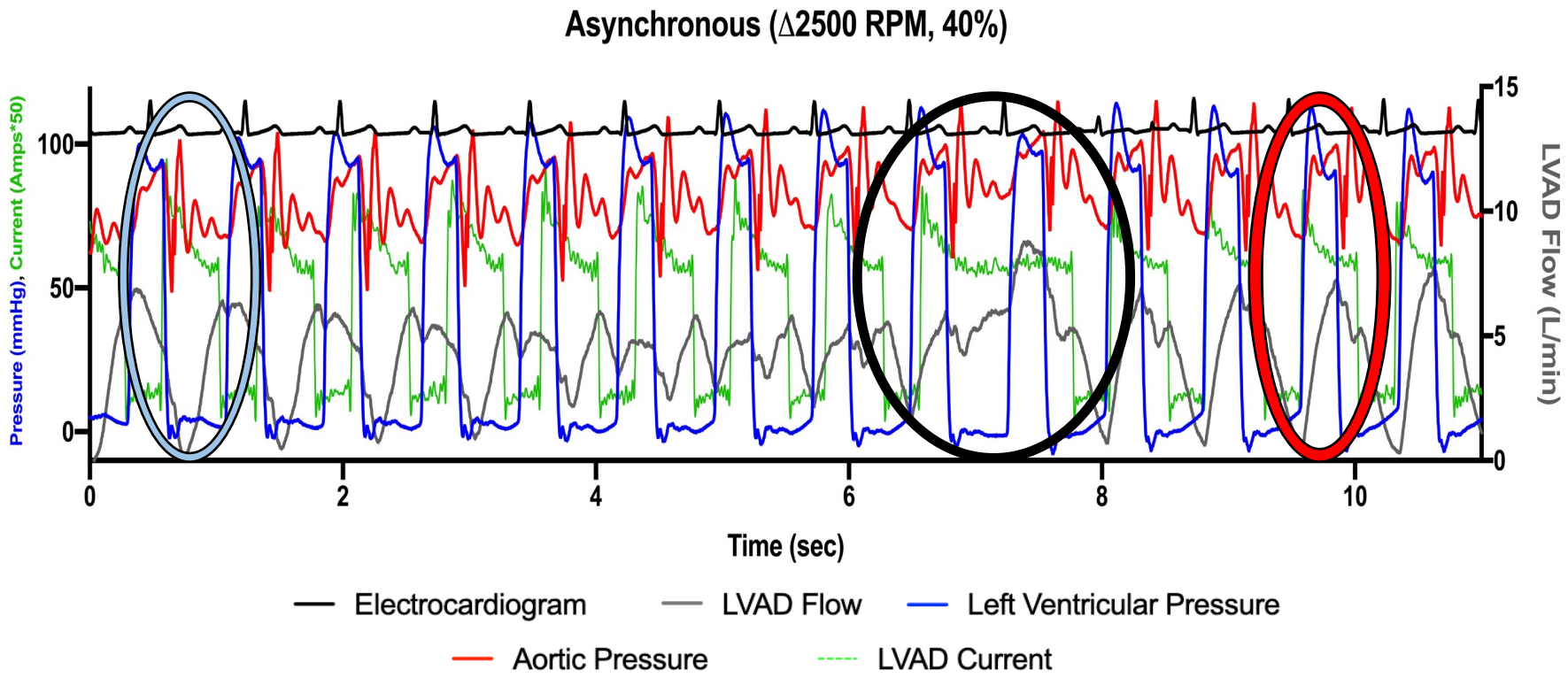

Figure 17. Asynchronous data recordings while operating the intelligent HVAD control at a Δ2500 RPM. Asynchronous beat-to-beat hemodynamic waveforms occur when increase (or decrease) in pump speed does not correlate with LV end-diastole or LV end-systole. Co-pulsation (red circle) beat-to-beat hemodynamic support occurs when pump speed increases (or decreases) at LV end-systole resulting in an increase in pulse pressure and LVAD flow. Counter-pulsation (blue circle) hemodynamic support occurs when pump speed increases (or decreases) at LV end-diastole and an increase in diastolic LVAD flow and a lowering of the LV end-diastolic pressure is seen. Missed R-wave detection is seen (black circle) with pump speed remaining at highest operating speed until next R-wave detection. Co-pulsation, counter-pulsation, asynchronous, and missed R-wave detection were consistent across all Δrpm and systolic durations (30%, 35%, 40%) tested. EKG: electrocardiogram, LVP: left ventricular pressure, AoP: distal aortic pressure, LVAD Flow: left ventricular assist device flow, Current: HVAD current (I, amps).

2. Time Delay

Two distinct time delays were observed during pump speed modulation with the intelligent LVAD control system: (1) a delay in pump speed modulation despite accurate R-wave threshold detection, and (2) a delay in increase in LVAD flow due to the fluid inertia of the blood analog solution in the MCL.

a. R-Wave Trigger Time Delay

Ideally, the intelligent control would increase (or decrease) the HVAD pump speed (current, dotted vertical line, Figure 19) instantaneously upon R-wave detection; however, a time delay between detection of the R-wave and trigger to initiate increase (or decrease) of pump speed for systolic durations of 35% and 40% (Figure 18, Figure 19) being 45 $\pm$ 3.0 ms and 82 $\pm$ 3.0 ms (Figure 16) was identified.

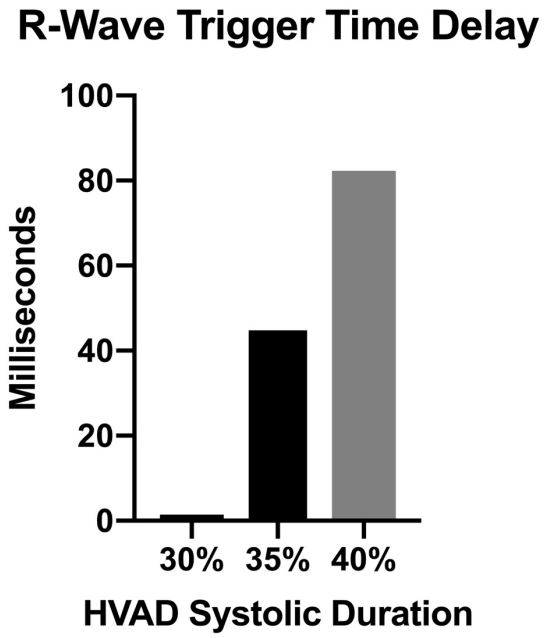

Figure 18. A time delay between detection of the R-wave trigger and subsequent pump speed modulation was seen while operating the intelligent LVAD control strategy at systolic durations of 35% and 40%. The data presented is displayed as the mean.

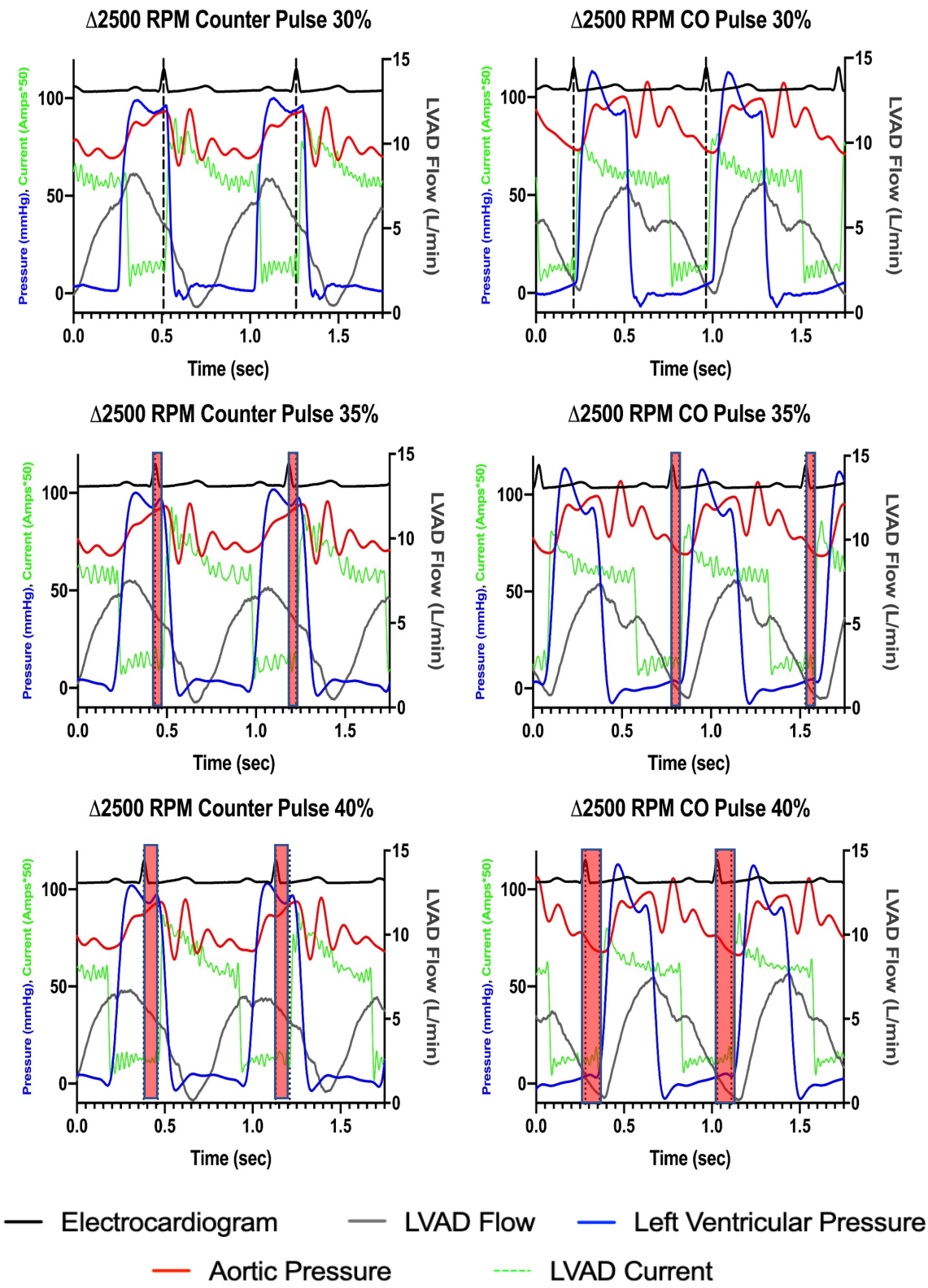

Figure 19. The graphs above show MCL-acquired counter-pulsation and co-pulsation hemodynamic waveforms for a Δ2500 RPM across the 30, 35, and 40% systolic durations tested. The R-wave trigger is depicted as a vertical dotted line overlaying the R-wave. The time delays for 35% and 40% systolic durations are depicted as the red area 45 ms and 82 ms, respectively, after the R-wave.

b. Fluid Inertia Time Delay

Additionally, a time delay between initiating the increase (or decrease) in pump speed and the resulting increase (or decrease) in LVAD flow was identified during co-pulsation and counter-pulsation phases (Figure 20). We hypothesize that this time delay may be associated with an inertial effect to rapidly increase (or decrease) blood flow (Figure 21). The flow inertia delays were 35 ms and 187 ms for co-pulsation and counter-pulsation, respectively. The inertia delay will also likely be a function of patient physiologic condition (ex. during hypervolemia, hypovolemia, etc).

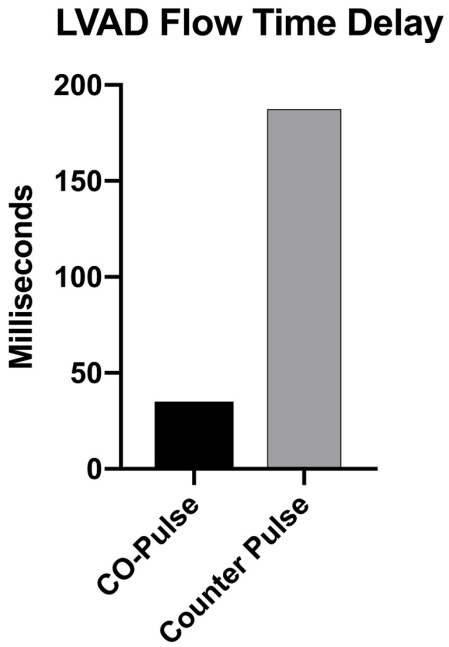

Figure 20. A time delay was observed between initiating the increase (or decrease) in pump speed modulation and the subsequent increase (or decrease) in LVAD flow for phases of co-pulsation and counter-pulsation support. The data presented is displayed as the mean.

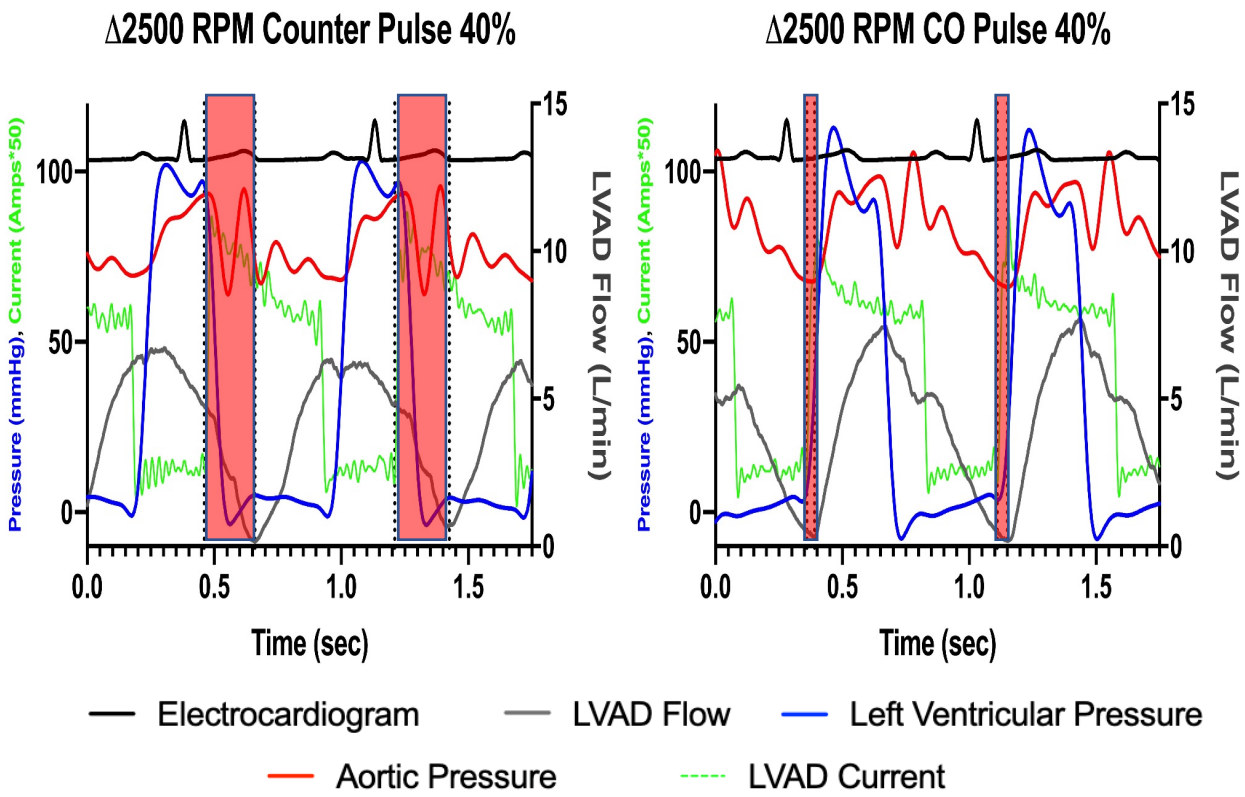

Figure 21. Hemodynamic waveforms for the Δ2500 rpm at a systolic duration of 40% operating setting to visualize the time delay created from the fluid inertia of the blood analog solution used in the mock circulatory loop. The fluid inertia delay is the delay between the increase (or decrease) in pump speed and the resulting increase in LVAD flow. The fluid inertia time delay is visualized as the red hued area on the waveform graph and varied between phases of co-pulsation (35 ms) and phases of counter-pulsation (187 ms) support. P

3. Slew Rate

The pump speed slew rate was calculated for each Δrpm operating setting. The pump speed slew rate is defined in classical engineering textbooks as the change in electrical current per unit time. In this study, the pump speed (rpm) was initially assumed to correlate with the electrical current; however, this relationship was shown to be non-linear (Figure 22). The ability to rapidly increase (or decrease) within a cardiac cycle is an important design criteria, especially with increasing heart rate, which is shown in Figure 22. The Δ2500 rpm demonstrated the most rapid change in pump speed (88.5

rpm/ms). The current slew rate (Figure 22) was also calculated and showed that the highest slew rate of 49 Amps/sec was achieved while operating the intelligent LVAD control at a Δ2500 rpm. The current slew rate increased with each increasing Δrpm testing condition similar to the pump speed slew rate which is expected as current is the input to the LVAD that controls which speed the device is operating. In this study we demonstrated the ability to rapidly increase (or decrease) pump speed to achieve the desired Δrpm target values.

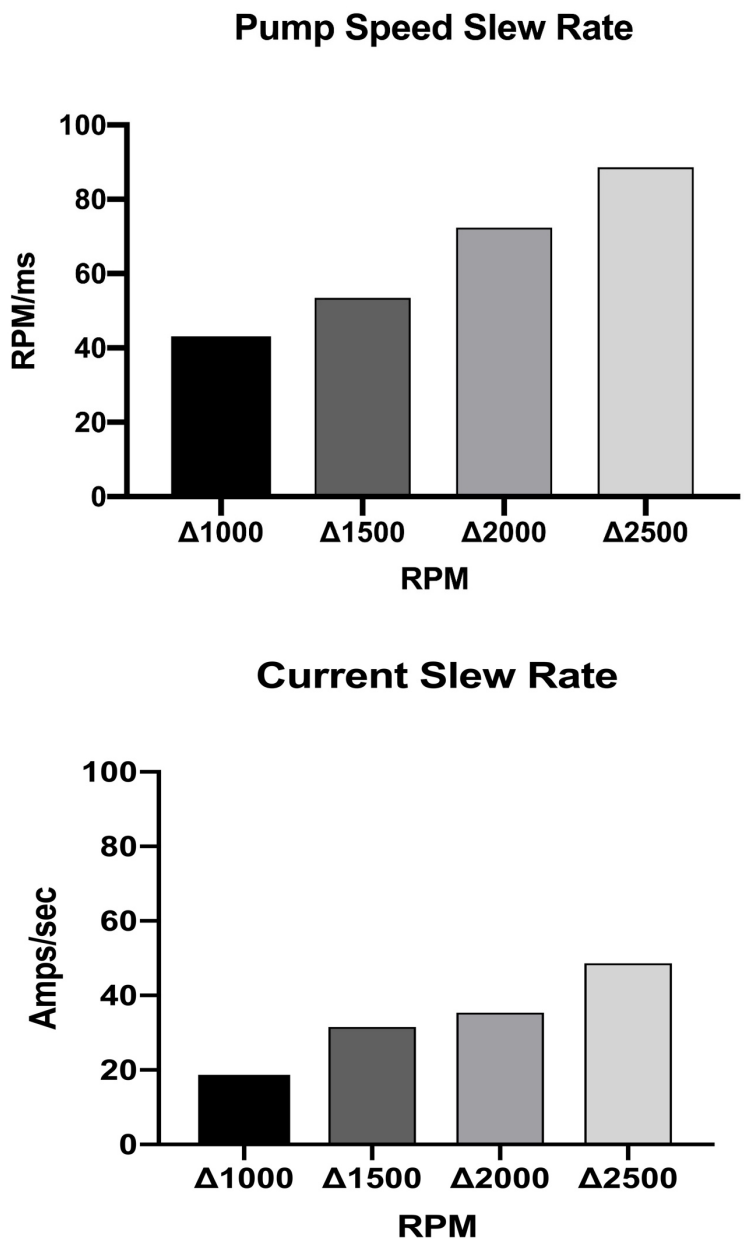

Figure 22. Pump speed slew rate (top) and current slew rate (bottom) were calculated to evaluate if the intelligent LVAD control strategy had the ability to increase the rate at which pump speed is modulated at higher Δrpm operating settings. The slew rate increased for each increase in Δrpm resulting in the ability of the intelligent LVAD control strategy to modulate pump speed and current within a single cardiac cycle while operating at either high or low pump speed. The data presented is displayed as the mean.

D. Intrinsic Pump Parameters

Intrinsic pump parameters (HVAD pump speed, current, and power usage) were obtained for all recorded test conditions. HVAD pump speed and current were recorded to confirm that HVAD pump speed was increasing (or decreasing) in response to increasing (or decreasing) the current supplied by the HVAD controller to the pump. HVAD power usage was recorded to evaluate if there was a penalty of increased power consumption while operating the HVAD in a pulsatile manner using the intelligent LVAD control strategy. Our results demonstrate that HVAD pump speed did increase (or decrease) in response to increasing (or decreasing) current and that there was a penalty of increased power usage when operating the HVAD in a pulsatile manner when compared to fixed speed operation at equivalent mean pump speeds (Table VII).

1. Mean HVAD Pump Speed

Mean LVAD pump speed was recorded throughout the duration of the experiment when operating the HVAD using the intelligent LVAD control strategy, as shown below in Figure 23. The highest mean pump speed while operating the HVAD using the intelligent control strategy in a pulsatile manner was during 30% systolic duration at a Δ2500 rpm. The mean pump speed was determined to not only be a function of the Δrpm, but also a function of the systolic duration (or the time spent at each high and low operating setting), which can be visualized by the lowered mean pump speed with increasing systolic duration that corresponds to a shorter time spent at the higher operating rpm. Corresponding mean fixed speeds, depicted as horizontal red dotted lines, are also shown in Figure 23. Additionally, individual mean rpm values for each pulsatile operating setting tested using the intelligent LVAD control strategy were plotted with the red line depicting the mean of the data set. This graph shows the overshoot (or

undershoot) that occurs when operating the HVAD in a pulsatile manner with the intelligent LVAD control strategy. The two distinct clusters of mean rpm data points above and below the overall mean rpm represent the overshooting (or undershooting) of the desired operating rpm during pump speed modulation.

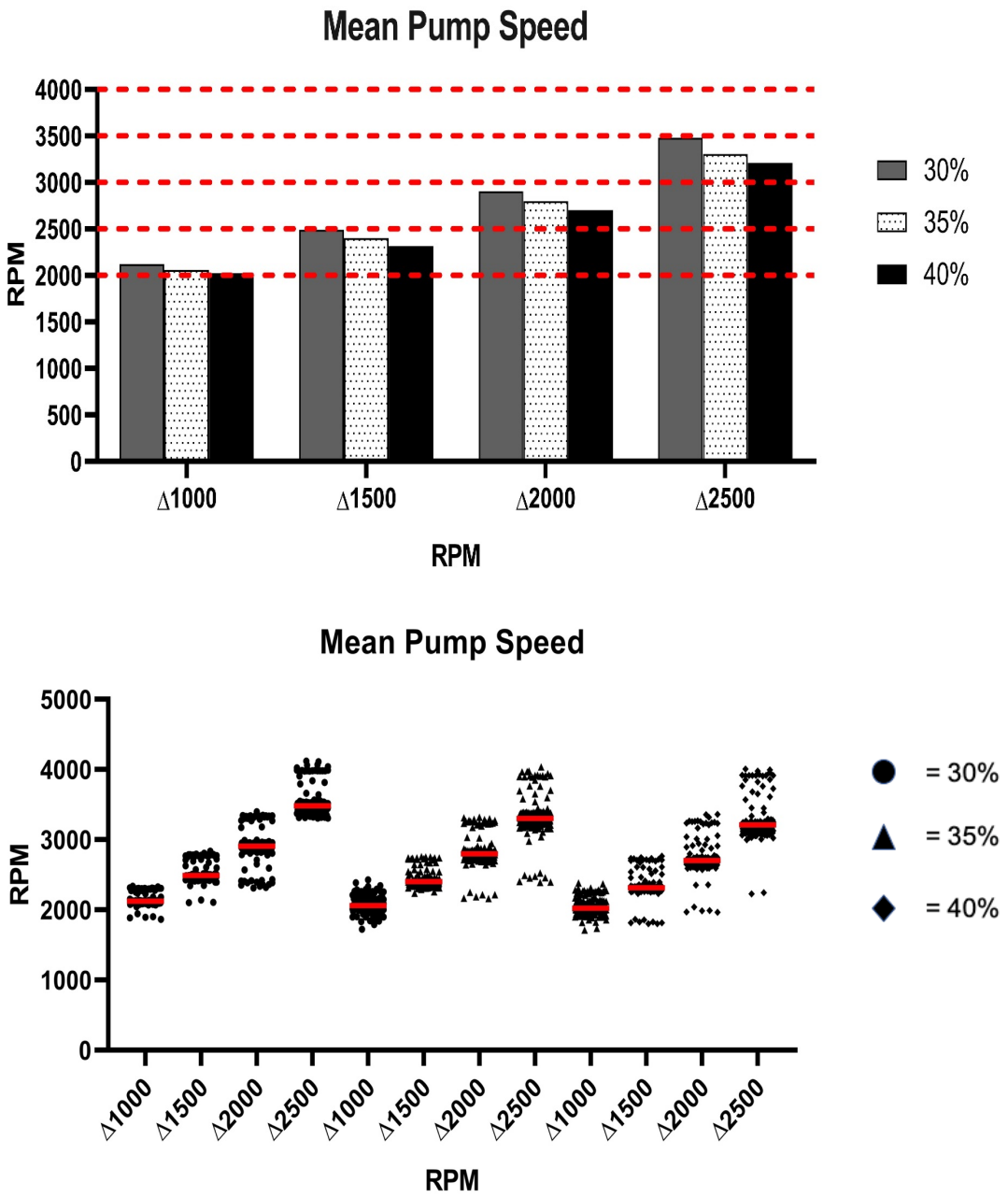

Figure 23. Mean pump speed (top) was plotted for each Δrpm and systolic duration. Mean pump speed increased with increasing Δrpm and was the highest at 30% systolic duration for each Δrpm. The red dashed line (top) represents the fixed pump speed the HVAD was operated at during the intelligent LVAD control strategy experiment. Mean pump speed (bottom) was plotted as individual values on a beat-to-beat basis to show undershoot and overshoot of pump speed modulation throughout the entire four-minute data recording during pulsatile operation using the intelligent LVAD control strategy. Clusters above and below overall mean pump speed (red line, bottom graph) represent the over- and undershoot of the desired pump speed while operating in a pulsatile manner using the intelligent LVAD control strategy. It was determined that mean pump speed is not solely a function of the high and low pump speed settings but also as a function of the time spent (systolic duration) at the high and low pump speeds. Data is presented as the mean for the top graph and individual means for each ventricular beat on the bottom graph.

2. HVAD Current

The current supplied to the HVAD from the intelligent controller was recorded throughout the experiment. As expected, the current increased with increasing pump speed operation (Figure 24). The current supplied to the HVAD is the input that either increases (or decreases) pump speed during operation. The highest current recorded during the pulsatile operation of the intelligent LVAD control strategy was during 30% systolic duration at a pump amplitude of Δ2500 rpm, which corresponds with the highest mean pump speed setting. Current also decreased with increasing systolic duration, corresponding to a lower total time spent at the higher rpm during pulsatile operation. As seen in the individual data point graph (Figure 24) the overshoot (or undershoot) of the current corresponded to the intelligent LVAD control strategy either over (or undershooting) the desired pump speed while operating the HVAD in a pulsatile manner.

Also shown in Figure 24, the current and increasing pump speed (rpm) was not linear when operating the HVAD using the intelligent LVAD control strategy. It would have been expected that by increasing the magnitude of pump speed by 500 rpm each operating setting that the current magnitude would have increased linearly with respect to pump speed, due to current being the input that controls pump speed. Also, the current to power relationship is more curvilinear than the current to rpm relationship due to power being derived by squaring the current and then multiplying it by the internal coil resistance of the HVAD.

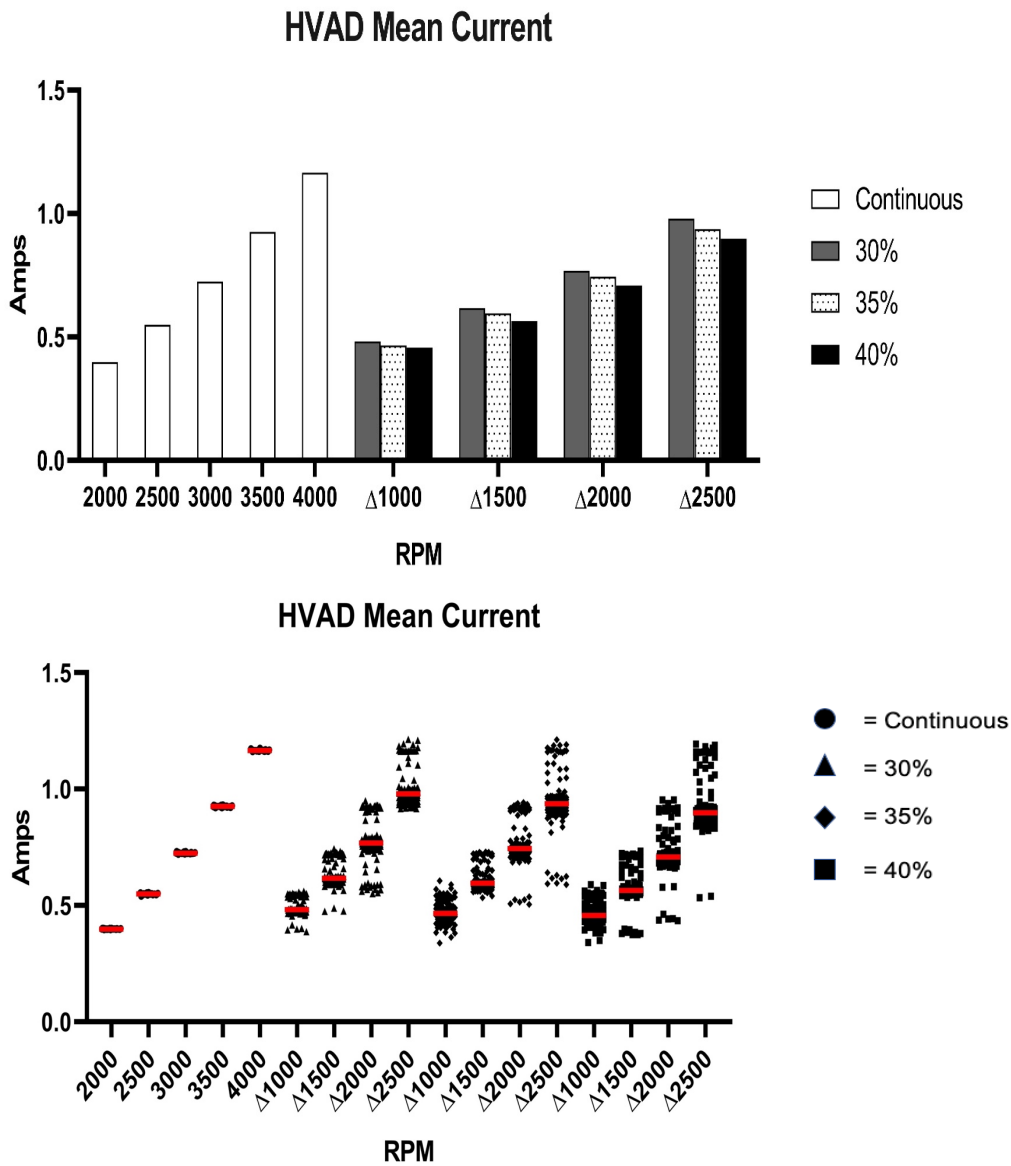

Figure 24. Mean current (top) supplied to the HVAD was plotted for each Δrpm and systolic duration during pulsatile operation and at each fixed speed operating setting during continuous operation. Mean current supplied to the HVAD increased with increasing Δrpm and was the highest at 30% systolic duration for each Δrpm and follows the same trend as mean pump speed. Current supplied to the HVAD is the input that dictates what pump speed the LVAD will operate at. Mean current (bottom) supplied to the HVAD was also plotted as individual values on a beat-to-beat basis to show over- and undershoot of current supplied to the HVAD during pump speed modulation throughout the entire four-minute data recording for each pulsatile operating setting. As seen in the bottom graph continuous operation does not demonstrate any over- or undershoot of current supplied to the HVAD, but while operating in a pulsatile manner the clusters of data above and below the overall mean current (red line, bottom graph) indicate an over- or undershoot of current supplied to the HVAD during pump speed modulation. Data is presented as the mean for the top graph and individual means for each ventricular beat on the bottom graph.

3. HVAD Power

The power of the HVAD during this experiment was derived by multiplying the current squared by the internal resistance of the HVAD pump used in this study. The internal coil resistance of the HVAD was 4.8 ohms and was multiplied by the current squared that was supplied to the HVAD to acquire total estimated power. HVAD power usage on average was greater while operating in a pulsatile manner using the intelligent LVAD control strategy when compared to mean pump speeds at equivalent mean pump flows (Table VII) with the exception of operating the intelligent control strategy at a systolic duration of 40% with Δ2000 and Δ2500 rpms. This could be explained due to these two operating settings not corresponding exactly to a fixed speed operating setting tested in this experiment. Power followed the same trend as mean pump speed, and current with the higher the Δrpm had the higher power requirement compared to systolic durations (Figure 25). By plotting the data points individually, we are able to demonstrate intelligent LVAD control over- and undershooting desired operating pump speed (Figure 25) leading to a larger range of power use when compared to fixed speed operation. By correcting this over (or undershoot) of pump speed while in pulsatile operation, the power difference between pulsatile operation and corresponding fixed speed mean pump speed may be reduced and the percent increase in pump power decreased while operating in a pulsatile manner.

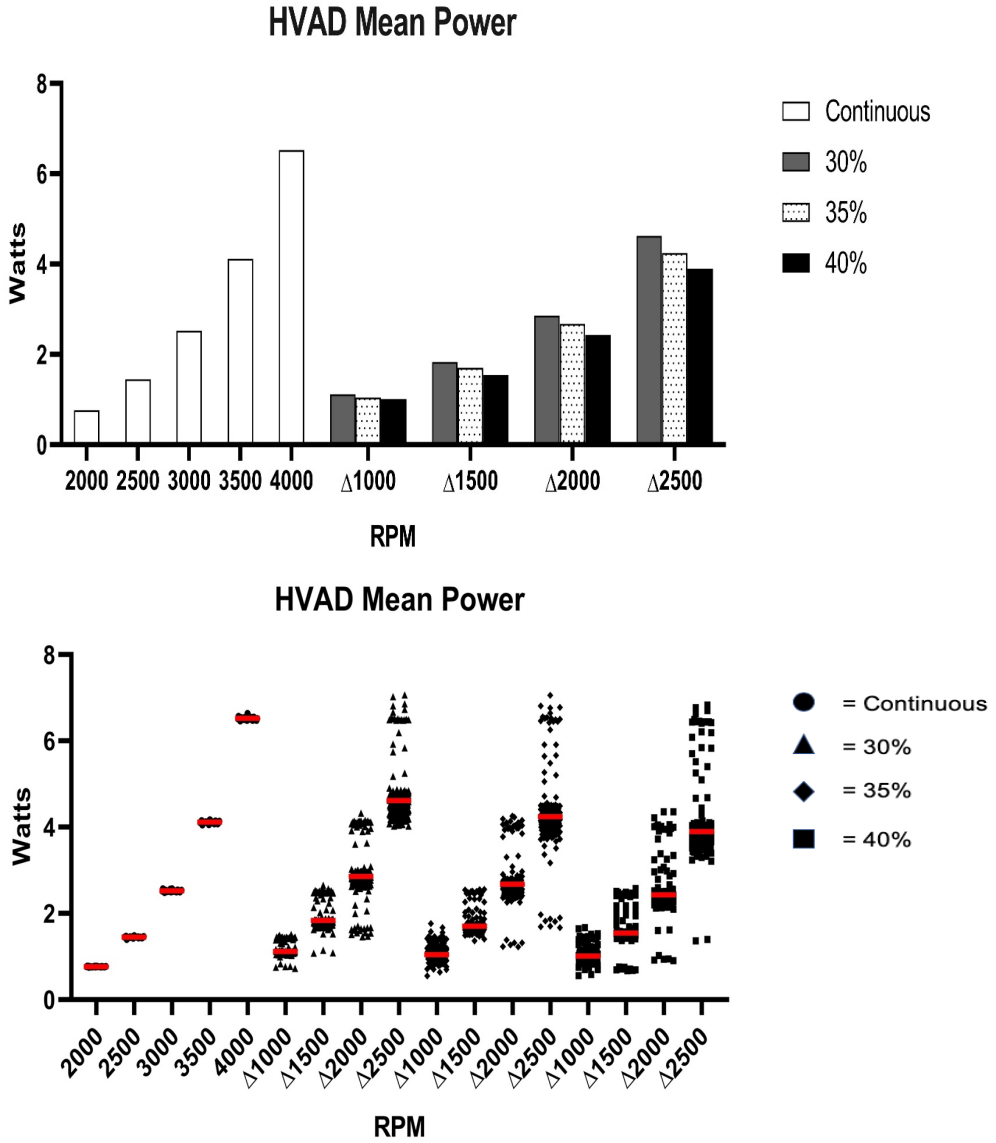

Figure 25. Mean HVAD power usage (top) was plotted for Δrpm and systolic duration during pulsatile operation and at each fixed speed operating setting during continuous operation. Mean HVAD power usage increased with increasing Δrpm and was the highest at 30% systolic duration for each Δrpm and follows the same trend as mean pump speed and current supplied to the HVAD. HVAD power usage on average is higher during pulsatile operation while modulating pump speed using the intelligent LVAD control strategy when compared to an equivalent mean pump speed. Mean HVAD power usage (bottom) was also plotted as individual values on a beat-to-beat basis to show over- and undershoot of HVAD power usage during pump speed modulation throughout the entire four-minute data recording for each pulsatile operating setting. As seen in the bottom graph continuous operation does not demonstrate any over- or undershoot of power usages, but while operating in a pulsatile manner the clusters of data above and below the overall mean HVAD power usage (red line, bottom graph) indicate an over- or undershoot of HVAD power during pump speed modulation. Data is presented as the mean for the top graph and individual means for each ventricular beat on the bottom graph.

TABLE VII
POWER DIFFERENCE BETWEEN PULSATILE OPERATION USING THE INTELLIGENT LVAD CONTROL STRATEGY AND EQUIVALENT FIXED SPEED MEAN RPM

		Power Difference	
		Percent Change (%)	Equivalent Fixed Speed (RPM)
30%	Δ1000	46	2000
	Δ1500	26	2500
	Δ2000	13	3000
	Δ2500	12	3500
35%	Δ1000	37	2000
	Δ1500	18	2500
	Δ2000	6	3000
	Δ2500	3	3500
40%	Δ1000	32	2000
	Δ1500	6	2500
	Δ2000	-4	3000
	Δ2500	-5	3500

Table VII. Power usage difference of each pulsatile operating setting compared to its equivalent mean fixed pump speed operating setting. Power usage on average was higher for pulsatile operation when compared to continuous operation of the HVAD using the intelligent LVAD control strategy. The negative power usage difference for Δ2000 and Δ2500 while operation at a systolic duration of 40% may be attributed to these settings not having a true equivalent fixed speed to compare against, as these two settings mean pump speeds lying in between the fixed speed operating settings tested. Data is presented as the percent difference between pulsatile operating settings and equivalent fixed speed operating settings.

E. Pump Speed Modulation – Hemodynamic Performance

Within a select 10-second data epoch of asynchronous operation phases during co-pulsation and counter-pulsation support were achieved for single, isolated cardiac cycles. In between these time points, asynchronous support occurred independent of the cardiac cycle to produce beat-to-beat changes in hemodynamic parameters. The hemodynamic support achieved for pulsatility, LV volume unloading, and cardiac output were determined for each type of support (co-pulsation, counter-pulsation, and fixed speed). The operating condition that provided the greatest degree of ventricular volume unloading, highest increase of total and LVAD flow, highest preserved aortic flow, and

greatest degree of pulsatility with its specific achieved hemodynamic values (Table VIII). Overall, operating the intelligent control at a Δ2500 rpm (highest mean rpm) resulted in the greatest degree of ventricular volume unloading, the highest increase in total flow, and the highest increase in LVAD flow. The greatest increase in aortic flow and greatest degree of pulsatility parameters were achieved by operating the intelligent control at a Δ1000 rpm (lowest mean rpm).

TABLE VIII
OPERATING SETTINGS AND HEMODYNAMIC PARAMETERS ACHIEVED USING INTELLIGENT LVAD CONTROL STRATEGY

	Operating Settings				Hemodynamics Achieved			
	Parameter	Fixed Speed	Co-Pulsation	Counter-Pulsation	Parameter	Fixed Speed	Co-Pulsation	Counter-Pulsation
Volume Unloading	Stroke Volume	4000 RPM	Δ2500 RPM, 30% sys	Δ2000 RPM, 40% sys	Stroke Volume (mL)	23	23	25
	LVESP	4000 RPM	Δ2500 RPM, 30% sys	Δ2000 RPM, 30% sys	LVESP (mmHg)	100	93	96
	LVEDP	4000 RPM	Δ2500 RPM, 30% sys	Δ2500 RPM, 30% sys	LVEDP (mmHg)	-0.5	6	2
	LVEDV	4000 RPM	Δ2500 RPM, 30% sys	Δ2500 RPM, 40% sys	LVEDV (mL)	155	157	158
	LVEW	4000 RPM	Δ2500 RPM, 35% sys	Δ2500 RPM, 30% sys	LVEW (mmHg*mL)	2069	2081	1842
Flows	LVAD	4000 RPM	Δ2500 RPM, 30% sys	Δ2500 RPM, 30% sys	VAD (L/min)	6.5	4.7	4.6
	Aortic	2000 RPM	Δ1000 RPM, 40% sys	Δ1000 RPM, 40% sys	Aortic (L/min)	1.3	1.4	1.2
	Total	4000 RPM	Δ2500 RPM, 30% sys	Δ2000 RPM, 30% sys	Total (L/min)	4.8	4.5	4.1
Pulsatility	AoP ΔP	2000 RPM	Δ1000 RPM, 40% sys	Δ1000 RPM, 40% sys	AoP ΔP (mmHg)	32	34	30
	AoP PI	2000 RPM	Δ1000 RPM, 35% sys	Δ1000 RPM, 40% sys	AoP PI	0.45	0.36	0.41
	Total Flow PI	2000 RPM	Δ1000 RPM, 40% sys	Δ1000 RPM, 40% sys	Total Flow PI	0.47	0.44	0.41
	SHE	2000 RPM	Δ1000 RPM, 40% sys	Δ1000 RPM, 35% sys	SHE (ergs/cm^3)	1546	1575	1226
	Vascular Resistance	4000 RPM	Δ2500 RPM, 30% sys	Δ2000 RPM, 30% sys	Vascular Resistance (dynes-sec/cm^5)	94	89	84

Table VIII. Operating settings for the greatest degree of ventricular volume unloading, increase in total flow and LVAD flow, and greatest degree of pulsatility are shown on the left side of the table with the hemodynamics achieved for each operating setting listed on the right side of the table. Operating settings that have higher mean pump speeds produced the greatest degree of ventricular volume unloading and increases in total and LVAD flow. Operating settings that have lower mean pump speeds produced the greatest degree of pulsatility and greatest forward flow through the aortic valve. Data is presented as the mean.

1. Left Ventricular (LV) Volume Unloading

Stroke volume decreased for all HVAD pump speed modulation operating conditions compared to baseline (HF, HVAD off) as shown in Figure 26. However, our experimental findings did not demonstrate the large reductions in LV unloading we had hypothesized (smallest stroke volume, achieved at 4000 rpm fixed speed). This may have been due in part to a significant error associated with LV volume measurement we identified during data analysis and troubleshooting. This error as well as a potential calculation error (MatLab script, **Appendix III**) likely resulted in erroneous LV external work (equals ΔLV volume * ΔLV pressure) results. First error, the LV volume admittance catheter did not have the required number of segments and appropriate spacing to accurately measure the volume of the mock ventricle. Second error, calculation of LV systolic and diastolic pressures (average) and forward flow (LV stroke volume) may have resulted in an under estimation of these values. To address this error, we modified our methods and performed additional data analysis using LabChart's software. The LabChart calculation of LV external work appeared to be a better estimation based upon the rough estimation of the area within the PV loop (LV stroke volume * (LV end systolic pressure – LV end diastolic pressure)).

LV end diastolic pressure was also reduced with increasing mean rpm for all pump settings (fixed, pulsatile asynchronous operation), as shown in Figure 26. Additionally, increasing Δrpm provides a greater degree of volume unloading during both phases of co-pulsation and counter-pulsation support (Figure 26), which may also be attributed to the increase in mean pump speed when increasing Δrpm in this study. The mean pump speed (rpm) for counter-pulsation and co-pulsation is a function of the systolic duration (time spent at each rpm) and Δrpm.

Pressure-volume (PV) loops recorded for each operating setting tested while operating the intelligent LVAD control strategy at a fixed speed are shown in Figure 27. The PV loops did not produce a downward shift to the left as would be expected with increasing LVAD support for any testing condition (fixed or pulsatile operation). It is believed that the size of the LV volume catheter used in this study was inadequate and did not allow for the measuring of LV volume throughout the entirety of the artificial ventricle. The LV volume catheter limitations may explain (in part) why the end diastolic and end systolic volumes appear to condense around the center of the NYHA class IV HF baseline (HVAD off) PV loop.

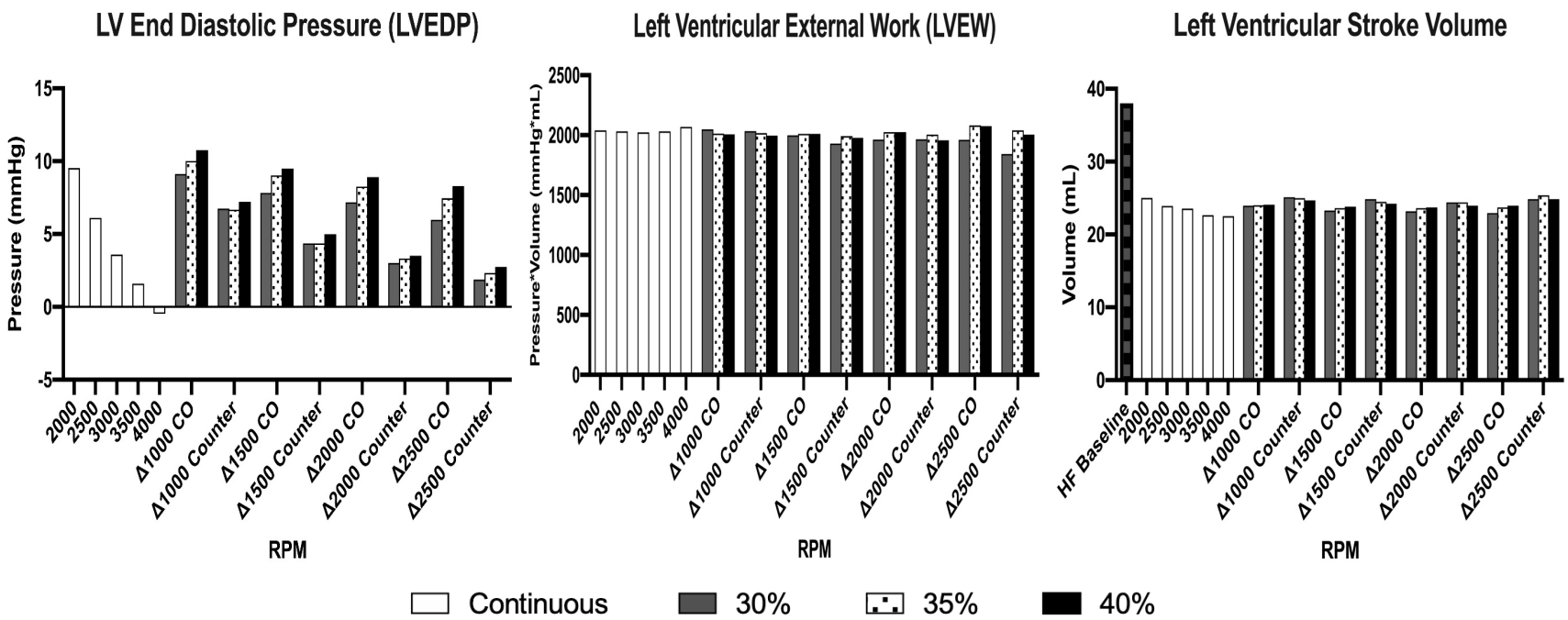

Figure 26. Left ventricular stroke volume (right) shows a reduction in stroke volume for all operating settings during the intelligent LVAD control strategy experiment. Left ventricular end diastolic pressure (LVEDP, left) indicates a greater degree of volume unloading (reduction in LVEDP) with increasing ΔRPM with counter-pulsation having a greater reduction than co-pulsation at equal ΔRPM. Left ventricular external work (LVEW, middle) shows a trend of reducing LVEW with increasing ΔRPM. Counter-pulsation appears to have the largest reduction in LVEW when compared to co-pulsation at the same ΔRPM. Fixed speed is represented on the left side of the x-axis with increasing ΔRPM progressing to toward the right side of the x-axis. The data presented is displayed as the mean.

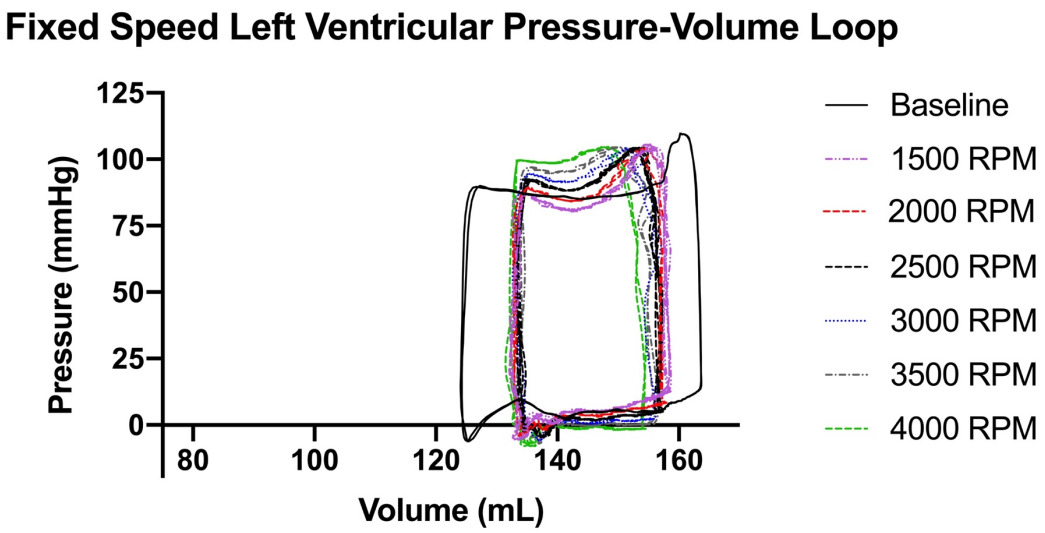

Figure 27. Left ventricular pressure-volume (PV) loops recorded during fixed speed operation of the HVAD using the intelligent LVAD control strategy. The PV loops for the fixed speed operation are representative of each operating setting tested during this study. The PV loops did not shift downward or to the left with increasing LVAD support as would be expected. The limitations (inadequate of number and spacings of electrodes) of the LV volume catheter used in this study may explain (in part) why the PV loops did not respond to increasing LVAD support as would have been expected.

2. Cardiac Output

As shown in Figure 28, the highest flow was achieved with the HVAD operated at a fixed speed of 4000 rpm; however, during phases of asynchronous co-pulsation pump speed modulation at the largest pump speed differential (low = 1500, high = 4000, Δrpm = 2500, systolic duration 30%) mean pump speed was the greatest (3,300 ± 1,200 rpm). The forward flow at a fixed pump speed of 4,000 rpm was 4.8 L/min compared to a mean co-pulsation rpm of 4.5 L/min. Mean total flow increased for all pump speed modulation operating settings with increasing mean rpm and Δrpm. Co-pulsation on average yielded

the highest total forward flow at equivalent mean pump speed (rpm) when compared to counter-pulsation at the same mean pump speed (rpm). Increasing systolic duration (lower total time spent at higher rpm) flow decreased due to the reduction in mean pump speed (rpm), as shown in Figure 28.

The operating setting that had the greatest aortic flow occurred at a Δ1000 rpm and a systolic duration of 40%, with phases of co-pulsation having a greater preservation of aortic flow when compared to phases of counter-pulsation at the same Δrpm (Figure 28). Regurgitant flow was seen through the aortic valve when operating the HVAD at fixed pump speeds greater than 3,500 rpm. In contrast to fixed speed operation of the HVAD, there was no regurgitant flow observed when modulating pump speed in a pulsatile manner with the intelligent LVAD control strategy, independent of Δrpm or systolic duration.

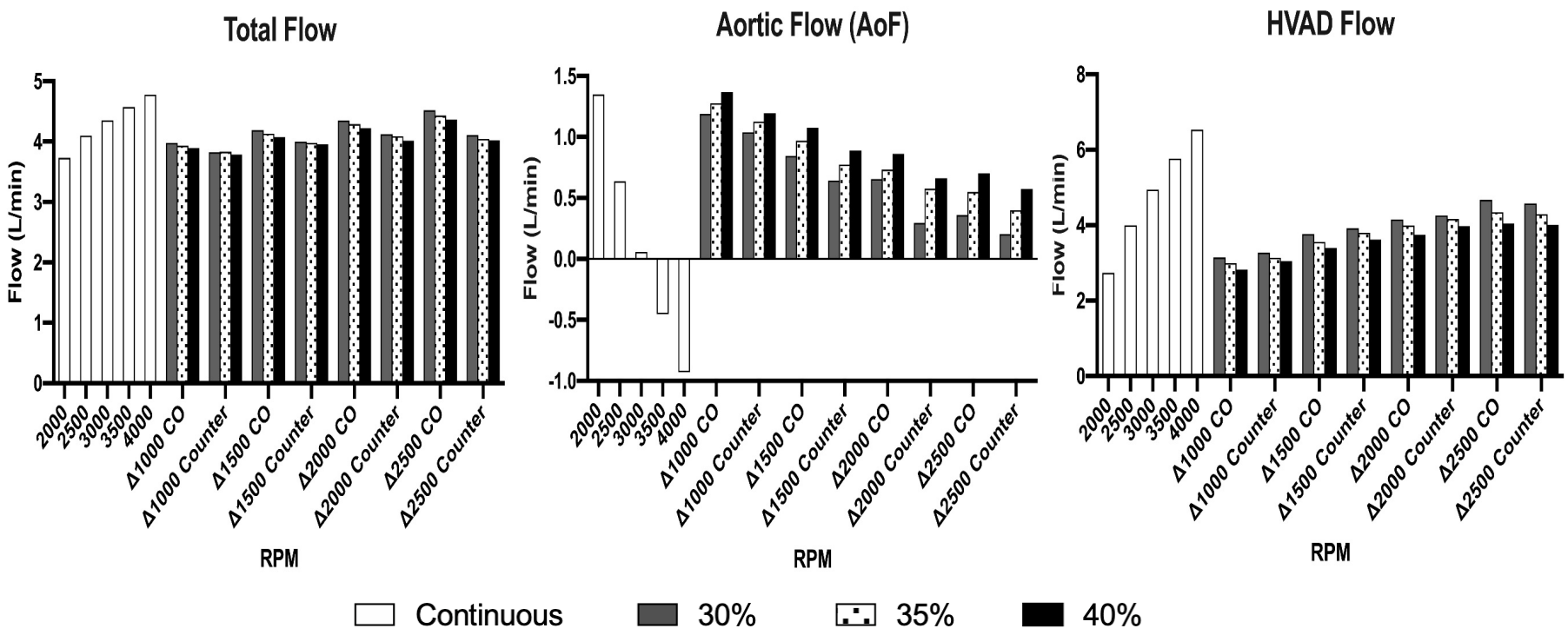

Figure 28. Mean total flow (left) shows greater augmentation of total flow with increasing ΔRPM for all operating settings. LVAD flow (right) has the greatest improvement with increasing ΔRPM as expected across all operating conditions. Aortic flow (AoF, middle) is diminished with increasing ΔRPM due to increased LVAD flow, while operating at fixed speeds of 3,500 and 4,000 rpm AoF is negative due to regurgitation through the aortic valve. Fixed speed is represented on the left side of the x-axis with increasing ΔRPM progressing to toward the right side of the x-axis. The data presented is displayed as the mean.

3. Pulsatility

Pulse pressure (ΔP) decreased with increasing mean pump speed (rpm) for all operating settings (fixed speed and modulating pump speed asynchronously). The operating setting that achieved the smallest reduction in pulse pressure from HF baseline occurred at a Δ1000 rpm and 40% systolic duration, with phases of co-pulsation producing higher pulse pressures than counter-pulsation at the same Δrpm (Figure 29). The operating setting that resulted in the greatest aortic pressure pulsatility index (PI) was achieved using the intelligent HVAD control strategy at a Δ1000 rpm with a systolic duration of 35%, with phases of co-pulsation producing greater PI than phases of counter-pulsation.

SHE, a measure of the extra energy that is produced by pulsatile blood flow, is reduced in HF patients that are implanted with a CF-LVAD (Soucy et al., 2013). The operating setting that produced the greatest SHE was at a Δ1000 RPM at a systolic duration of 40%, with phases of co-pulsation generating higher SHE values than phases of counter-pulsation. Vascular resistance was also calculated and increased with increasing mean rpm from baseline in all operating settings and was higher in co-pulsation when compared to counter-pulsation at the same mean pump rpm. Increasing mean pump speed (rpm) decreased pulsatility parameters (Figure 29). When operating at the same operating setting (equivalent mean pump speed), phases of co-pulsation showed increases in pulsatility as evidenced by increases in AoP ΔP, PI, and SHE compared to phases of counter-pulsation and fixed speed operation.

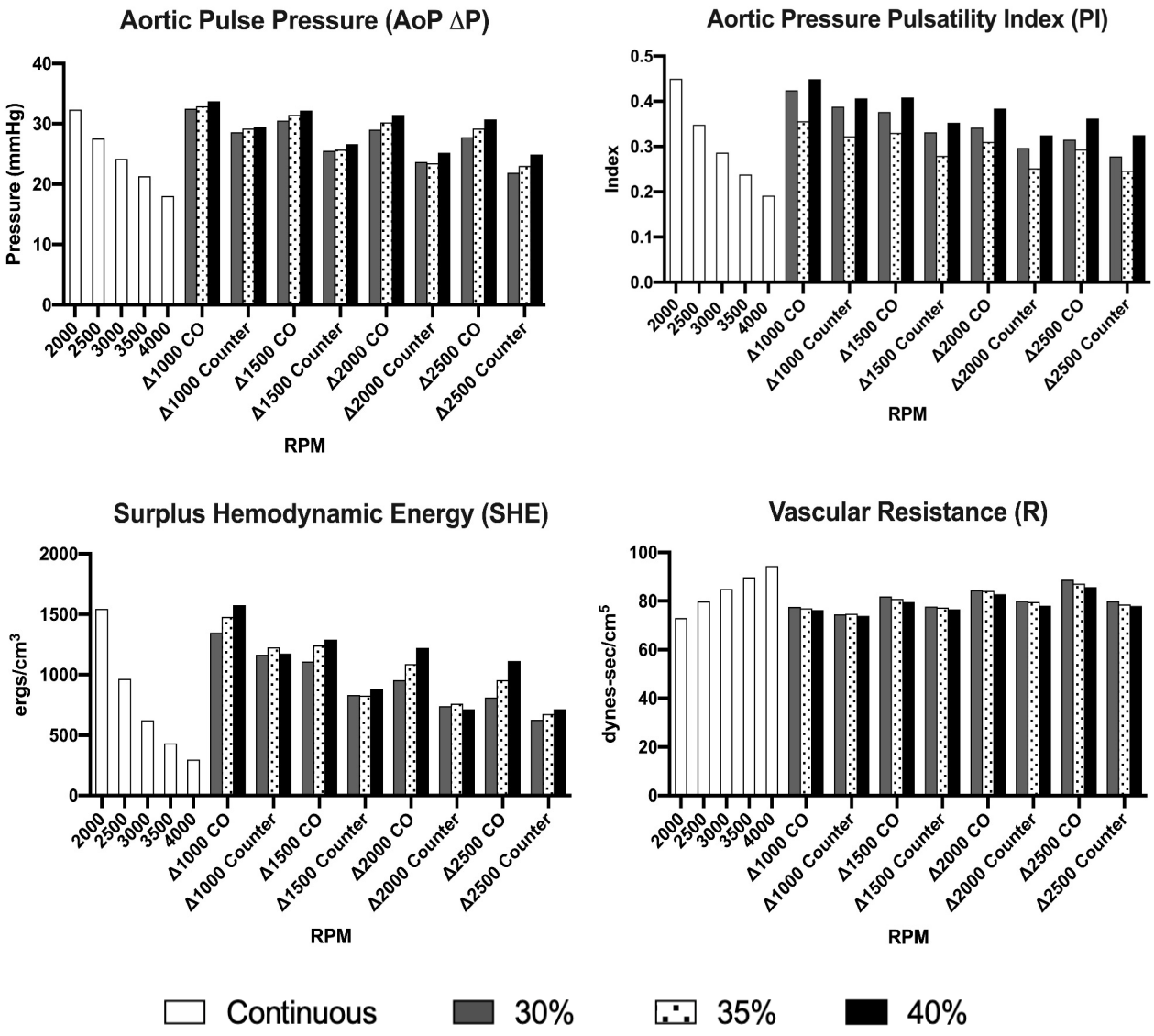

Figure 29. Aortic pulse pressure (AoP ΔP, top-left) reduced with increasing ΔRPM as expected due to the subsequent increase in mean pump speed as well. Phases of co-pulsation produced greater pulse pressures than counter-pulsation and fixed speed operation at equivalent mean pump speeds. Surplus hemodynamic energy (SHE, bottom-left) reduced with increasing ΔRPM and followed the same trend as the AoP ΔP with co-pulsation producing greater SHE values at equivalent pump speeds. The aortic pressure pulsatility index (PI, top-right) reduced with increasing operating RPM due to the decrease in AoP ΔP. Vascular resistance (R, bottom-right) increased with increasing ΔRPM with fixed speed operation producing greater vascular resistance than co-pulsation and counter-pulsation at equivalent mean pump speeds. The data presented is displayed as the mean.

F. Hemodynamic Trade-Offs

While evaluating the hemodynamics achieved using the intelligent LVAD control strategy, hemodynamic trade-offs were observed between operating settings that gave the highest degree of LV volume unloading, largest increase in cardiac output, and highest degree of pulsatility achieved. Our results indicate it may be possible to operate the intelligent LVAD control strategy to target specifically LV volume unloading, cardiac output, and/or pulsatility support directly. But with the ability to target each type of hemodynamic support directly there may also be hemodynamic trade-offs incurred.

1. Left Ventricular Volume Unloading

During this experiment the operating setting that produced the greatest degree of LV volume unloading by evaluating reductions in LV stroke volume, LV end diastolic pressure, and LV external work was operating the intelligent LVAD control strategy asynchronously at a Δ2500 rpm at a 30% systolic duration while in phases of counter-pulsation. This operating setting corresponded to the highest mean pump speed throughout the experiment and produced the greatest degree of LV volume unloading while also increasing cardiac output but came with the limitations of decreasing pulsatility and increasing the power the HVAD used as shown in Table IX.

TABLE IX
LEFT VENTRICULAR VOLUME UNLOADING HEMODYNAMIC TRADE-OFFS

Δ2500 RPM at 30% Systolic Duration: during Counter-Pulsation Phases	
Cardiac Output	↑
Pulsatility	↓
Power	↑
↑ = Increases; ↓ = Decreases	

Table IX. Hemodynamic trade-offs of operating the intelligent LVAD control strategy to produce the greatest degree of left ventricular (LV) volume unloading. Cardiac output is also increased while operating the intelligent LVAD control strategy to produce the greatest LV volume unloading but diminished pulsatility and increased power usage of the LVAD.

2. Cardiac Output

Cardiac output had the greatest augmentation in total flow, LVAD flow, and aortic flow when the intelligent LVAD control strategy was operating asynchronously, during phases of co-pulsation at a Δ2500 rpm with a systolic duration of 30%. Operating at this setting gave the largest increase in cardiac output and greatest degree of LV volume unloading but came at the limitations of reduced pulsatility and increased HVAD power usage, as shown in Table X. The aortic flow did not follow this trend (increase in mean pump speed results in increased total and LVAD flow), as it was generally greater at lower mean pump speeds. Due to the aortic flow always having a mean forward flow, the operating setting that gave the highest degree of augmentation in cardiac output occurred with pump setting of Δ2500 rpm, systolic duration of 30%, and during phases of co-pulsation support.

TABLE X
CARDIAC OUTPUT HEMODYNAMIC TRADE-OFFS

Δ2500 RPM at 30% Systolic Duration: during Co-Pulsation Phases	
LV Volume Unloading	↑*
Pulsatility	↓
Power	↑
↑ = Increases; ↓ = Decreases	

Table X. Hemodynamic trade-offs of operating the intelligent LVAD control strategy to produce the greatest increase in cardiac output. Left ventricular volume unloading also increased while operating the intelligent LVAD control strategy to produce the greatest increase in cardiac output but diminished pulsatility and increased power usage of the LVAD. The * designates that LV volume unloading would be expected to increase in this operating setting due to operating at a high mean pump speed; but due to limitations associated with the LV volume catheter the degree to which the LV is unloaded cannot be specified.

3. Pulsatility

The highest degree of pulsatility was achieved while operating the intelligent LVAD control strategy asynchronously at a Δ1000 rpm at 40% systolic duration during phases of co-pulsation as evidenced by increases in AoP ΔP, PI, SHE, and vascular resistance. This operating setting corresponded to the lowest mean pump speed tested while operating the HVAD in a pulsatile manner using the intelligent LVAD control strategy. The highest degree of pulsatility had hemodynamic trade-offs, including lower LV volume unloading and cardiac output with the increased power requirements while operating the HVAD in a pulsatile manner (Table XI).

TABLE XI
PULSATILITY HEMODYNAMIC TRADE-OFFS

Δ1000 RPM at 40% Systolic Duration: during Co-pulsation Phases	
LV Volume Unloading	↓ *
Cardiac Output	↓
Power	↑
↑ = Increases; ↓ = Decreases	

Table XI. Hemodynamic trade-offs of operating the intelligent LVAD control strategy to produce the highest degree of pulsatility. Left ventricular volume unloading and cardiac output decreased in order to obtain the highest degree of pulsatility in this study while operating the HVAD using the intelligent LVAD control strategy. In addition to reducing the degree of left ventricular volume unloading and augmentation of cardiac output there was also an increase in power usage of the LVAD. The * designates that LV volume unloading would be expected to decrease in this operating setting due to operating at a lower mean pump speed; but due to limitations associated with the LV volume catheter the degree to which the LV is unloaded cannot be specified.

IV. DISCUSSION

A. Key Findings

In this study, we successfully demonstrated that a novel intelligent LVAD control strategy reliably detected an R-wave from an external EKG and triggered pump speed (rpm) modulation (rapidly increase and decrease) of a Medtronic HVAD within a single cardiac cycle. However, unexpectedly the relationship between electrical current and pump speed (rpm) was non-linear for unknown reasons, which may be associated with limitations of the intelligent LVAD controller. The results of this study also demonstrated that mean operating pump speed (rpm) is a function of (1) magnitude of change in pump speed (Δrpm) and (2) time spent at the high and low operating pump speeds (rpm). The HVAD pump speed modulation settings that produced the greatest ventricular volume unloading, greatest increase in cardiac output, and greatest pulsatility (ΔP, SHE) were identified. Counter-pulsation provided the greatest ventricular volume unloading compared to co-pulsation at the same mean pump speed (rpm) as characterized by a greater reduction in LV end diastolic pressure and LV external work. Phases of co-pulsation support produced the greatest pulsatility and cardiac output compared to phases of counter-pulsation at the same mean pump speed (rpm) as characterized by a greater aortic pulse pressure, pulsatility index, surplus hemodynamic energy, total flow, and LVAD flow. During post-processing and data analysis of the recorded hemodynamic waveforms for all test conditions, two unexpected time delays were identified: (1) a computational time delay (ms) between the detection of the R-wave threshold landmark

and the command to initiate rapid increase in pump speed associated with an algorithm implementation error, and (2) a hemodynamic time delay between the increase in pump speed and increase in LVAD flow associated with fluid inertia.

B. Pump Speed Modulation

1. Thoratec HeartMate 3: Artificial Pulse

The Thoratec HeartMate 3 (Burlington, MA) is a clinically-approved centrifugal LVAD that is implanted inside the chest with the inflow cannula sutured to the LV and the outflow cannula routinely grafted to the aorta. The HeartMate 3 provides an artificial pulse by lowering the operating rpm of the pump by 2000 rpm for 0.15 seconds, followed by an increase in operating rpm by 4000 rpm for 0.20 seconds, and then lowered to the original fixed pump speed (Figure 30). The HeartMate 3 pump speed modulation algorithm operates asynchronously to the native heart to create an artificial pulse that transitions in and out of phase with the native heart cardiac cycle resulting in flow reduction (counter-pulsation) phase and flow augmentation (co-pulsation) phases (Castagna et al., 2017), but cannot be set to function continuously in co-pulsation and counter-pulsation for a pre-set period of time.

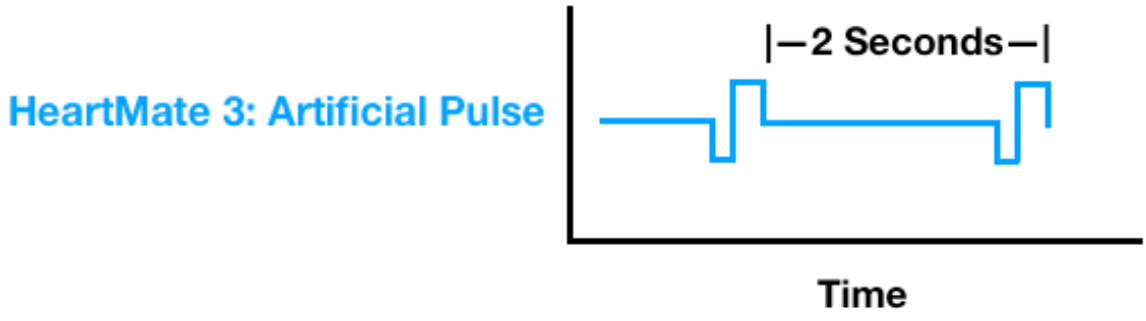

Figure 30. Graphical representation of the Thoratec HeartMate 3 pump speed modulation technique. Pump speed modulation occurs once every two seconds independent of the cardiac cycle with a 2000 rpm decrease in pump speed for 0.15 seconds followed by a 4000 rpm increase in pump speed for 0.20 seconds and then returning to original fixed speed until next pump speed modulation cycle.

In a study performed by Krabatsch et al., clinical outcomes data for 50 patients implanted with the HeartMate 3 were follow-up at one-year post-implant to evaluate incidence of adverse events, re-hospitalizations, device malfunction, and survival (Krabatsch et al., 2017). The study concluded lower rates of pump thrombosis (no incidence), GI bleeds (12%), and no pump failures (mechanical) compared to the reported adverse events (INTERMACS) of patients supported with other currently available CF-LVADs. Although the author reports no incidence of hemolysis and/or pump thrombosis, the overall rate of stroke was 18% (Krabatsch et al., 2017). The findings in the study conducted by Krabatsch et al., may support that the pump speed modulation of the HeartMate 3 may reduce the risks of GI bleeds and pump thrombosis. Additional studies with durations spanning longer than a year may need to be done in order to see if pump speed modulation is the main contributing factor to the reduced incidence of adverse events for the patients implanted with the HeartMate 3.

2. Lavare Cycle: Medtronic HVAD

The Lavare cycle is a control strategy integrated into the Medtronic HVAD controller designed to provide intermittent pump washing to help reduce the risk of pump thrombosis. The Lavare cycle is a pump speed modulation algorithm that rapidly decreases pump operating speed by 200 rpm for a period of two seconds, followed by a rapid increase of 400 rpm for one second, and then rapid decrease back to the initial set pump speed (Figure 31). The Lavare cycle is intended to reduce the occurrence of thrombus formation by potentially decreasing the areas of blood stasis within the LV by dynamically varying ventricular volume and pump flow (LaRose et al., 2010).

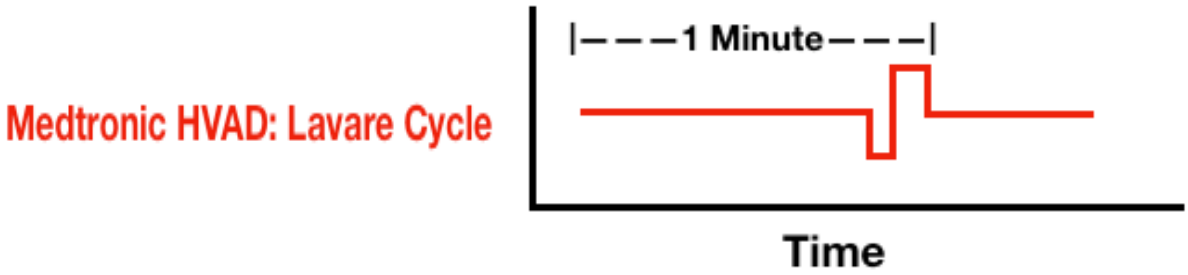

Figure 31. Graphical representation of the Medtronic HVAD pump speed modulation technique using the Lavare cycle. The Lavare cycle operates asynchronously to the native heart with a pump speed modulation cycle that occurs once per minute. The Lavare cycle decreases pump speed by 200 rpm for two seconds and then increases the operating rpm by 400 rpm for one second before returning to the original fixed pump speed.

The hypothesis that the Lavare cycle may decrease the potential for thrombus formation by reducing blood stasis in the LV is supported by the findings of Zimpfer et al. They demonstrated that operating a Medtronic HVAD with the Lavare cycle decreased the stagnation index of the LV by 22% compared to operating at a fixed pump speed in a MCL model with particle image velocimetry (PIV) analyses (Zimpfer et al., 2016). They also found that a drop-in pump speed greater than 400 rpm produced negative flow at the inflow cannula. It is theorized that larger drops in pump speed and/or longer periods of support at low pump speed settings may promote aortic valve opening and reduce the risk of GI bleeds by promoting pulsatile flow compared to CF-LVADs (Zimpfer et al., 2016).

3. Jarvik 2000: Intermittent Low Speed (ILS)

The Jarvik 2000 (Jarvik Heart, New York, NY) is a clinically-approved axial flow LVAD that is implanted with the inflow and outflow grafts attached to the LV and ascending aorta, respectively. The Jarvik 2000 was the first LVAD to use cyclic pump speed rotation (one cycle per minute) to minimize the risk of thrombus formation by promoting periodic ejection through the aortic valve, as described in the Jarvik 2000's

operating manual (Figure 32). By reducing the operating pump speed of the Jarvik 2000 for a short period of time with the ILS controller, the amount of pump flow and LV unloading is reduced, and the workload of the heart is increased. During this short period of time, in which the Jarvik pump operates at lower pump speeds, the heart adapts to the increase in preload by increasing contractility (Selzman et al., 2018). The native heart is able to eject a greater volume of blood through the aortic valve, which may result in better washing of the aortic valve and root, thereby reducing the risk of aortic thrombus. The Jarvik 2000 ILS controller may also have the added benefit of an increase in pulsatility at the lowered pump speed setting (Selzman et al., 2018).

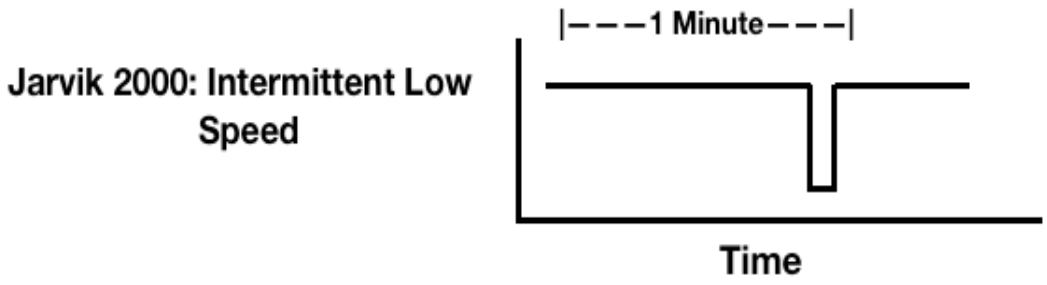

Figure 32. Graphical representation of the Jarvik 2000 intermittent low speed (ILS) pump speed modulation technique. The ILS pump speed modulation technique operates asynchronously to the native cardiac cycle and reduces operating rpm of the Jarvik 2000 for a short period of time each minute to allow the native heart to retake the majority of work in pumping blood to the body before returning to the original fixed pump speed.

Stanfield et al. conducted a study implementing a MCL to compare two bearing designs for the Jarvik 2000 during support with the ILS algorithm (Stanfield et al., 2013), and demonstrated average flow was reduced by up to 68% but produced up to 360% increase in PI for both bearing designs (Stanfield et al., 2013). The finding in this in vitro study evaluating the intelligent LVAD control strategy supports the theory that a

reduction in pump speed should result in increased pulsatility that may offer the benefits of a more physiologic flow pattern and potentially a reduced risk of AI formation, but at the potential expense of decreasing the degree of LV volume unloading and cardiac output.

C. Clinical Impact

The potential clinical impact of this study is the implementation of an intelligent LVAD control strategy to provide pump speed modulation of CF-LVADs with the ability to provide pulsatile flow in an asynchronous manner with phases of counter-pulsation and co-pulsation support. Pump speed modulation is a function of mean pump speed (rpm) as well as magnitude of rapid changes in pump speed (Δrpm) and time period (T, ms) at high and low pump speed settings. Additionally, effective pump modulation settings may also be able programmed to provide greatest LV volume unloading, cardiac output, and/or pulsatility based upon patient-specific needs. If the time delays (or advances) are implemented into the intelligent LVAD control strategy, pump speed modulation may target specific phases of the cardiac cycle, such as co-pulsation or counter-pulsation. For example, if the mean pump speed (rpm) during a pulsatile mode (pump speed modulation) was kept constant and the magnitude (Δrpm) increased around that mean setting, then counter-pulsation would be expected to have greater hemodynamic benefit with respect to LV external work and LV end-diastolic pressure compared to the same co-pulsation mean pump speed (rpm). Also, co-pulsation would be expected to have a greater hemodynamic benefit for pulsatility and cardiac output when evaluating pulse pressure, PI, SHE, and total flow if the mean pump speed (rpm) if pulsatile operation of the intelligent control was kept constant and the Δrpm was increased around the same mean compared to counter-pulsation support. The ability to specify type of pump speed

modulation support (co-pulsation, counter-pulsation, and asynchronous) specific to a patient's need (ex. activity level and time of day) may also be possible to achieve.

A complication that is often present in long-term CF-LVAD support is the development or progression of aortic insufficiency (AI). AI can develop as a result of the pressure gradient applied across the aortic valve limiting the opening of the valve due to the implantation of CF-LVADs. This can result in partial opening or closure of the aortic valve followed by subsequent distortion of the aortic valves anatomy. (Cowger et al., 2010). In our mock loop study, we did not identify any regurgitant flow through the mechanical aortic valve in the MCL model while operating the Medtronic HVAD in a pulsatile fashion, but regurgitant flow was observed when operating the HVAD at fixed speeds greater than 3,500 rpm (regurgitant flow up to ~0.75 L/min). This finding supports the concept that pump speed modulation allows better aortic valve opening by allowing the heart to produce forward flow through the aortic valve as a result of a lowered pressure gradient across the aortic valve and may help to reduce the incidence of AI but needs to be evaluated further utilizing in vivo testing platforms to see the effect on a biological aortic valve.

Although there are potential benefits to pump speed modulation, a drawback associated with operating CF-LVADs in a pulsatile manner may be the incidence of bleeding from the potential of increasing the shear stress that is applied to the blood and platelets. Bleeding has been hypothesized to occur due to high shear stress on blood causing acquired von Willebrand syndrome from the continuous rotation of CF-LVAD impellers (Eckman et al., 2012). Additional studies evaluating the intelligent LVAD control strategy for blood trauma should be done to evaluate if pump speed modulation of CF-LVADs increases the risk of bleeding due to the shear stress that can be applied to

blood and platelets during pump speed modulation. Also, with the high shear stresses applied on blood hemolysis and platelet damage may occur leading to thrombus formation may result.

D. Limitations

By testing the intelligent LVAD control strategy in a MCL model, many assumptions and associated limitations may impact interpretation of key findings. First, the MCL model was configured and tuned to mimic key hemodynamic parameters of a class IV HF patient. Although the MCL model is a valuable tool in the pre-clinical testing of MCS devices, it cannot reproduce the interactions between a biological system and the device (HVAD). Second, the MCL is a lumped parameter model and does not have the to simulate the complex branching network of the circulatory system (multiple vessels, length, diameter, wall thickness), which may impact vascular pulsatility. Third, the MCL model does not account for physiologic feedback mechanisms (i.e. Frank Starling, baroreceptor), thereby limiting evaluation of how intelligent control algorithm performance and physiologic responses to a dynamic cardiovascular system (ex. vasoconstriction and vasodilation). Fourth, a blood analog (glycerol-saline) solution rather than human blood was used, subsequently biological considerations such as blood trauma, hemolysis, and clotting, were not investigated. Despite these limitations, the MCL provides a valuable benchtop testing platform to test the feasibility of pump speed modulation algorithm and hemodynamic performance of the intelligent LVAD control strategy as an initial step in the pre-clinical development phase required to demonstrate function, efficacy, reliability, and safety (verification and validation) prior to clinical implementation.

A technical limitation of this study was the inability to reliably synchronize the intelligent control algorithm with the cardiac cycle of the mock ventricle, which limited operation to asynchronous mode. However, short periods of co-pulsation and counter-pulsation phases were achieved when setting mock ventricle (78 bpm) and intelligent control algorithms (80 cycles/sec), which were instrumental in elucidating the two unexpected time delays (trigger, inertia effect). The computational delay (trigger) can be easily corrected in software, and the inertial delay may be corrected by enabling user to adjust initiation (advance or delay) of pump speed increase (or decrease), similar to an IABP console. The ability to modulate pump speed comes at the expense of requirement for increase in power, which may reduce the amount of time the device can be operated solely on battery power.

An instrumentation limitation of this study was the use of the volume admittance catheter which did not have the appropriate number of segments and spacings required to accurately measure the entire volume of the mock ventricle. The volume catheter used in this study did not allow for the measurement of volume throughout the entirety of the artificial ventricle, but only at the apex. Additionally, the MatLab calculation of LV external work from the product of the LV systolic and diastolic pressures (averages) and forward flow (LV stroke volume) may have resulted in an under estimation of the LV external work. To address this error, we modified our methods and performed additional data analysis using LabChart's software. These limitations may explain why the LV stroke volume, LV external work, and PV loops did not vary largely with increasing mean pump speeds as would have been expected.

Finally, a limitation of the study design was that only single recordings for each test condition were completed. Subsequently, it did not allow the ability to test for reproducibility (larger sample size) and statistical analysis between operating settings.

E. Future Considerations

Next steps for the intelligent LVAD control strategy include additional testing in a MCL to evaluate the ability to reproduce the data gathered in this experiment and also increase the sample size to allow for statistical analysis of the data collected. Additionally, a time delay (or advance) could be implemented to account for the time delays observed in this study; (1) a computational time delay (ms) between the detection of the R-wave threshold landmark and the command to initiate rapid increase in pump speed associated with an algorithm implementation error, and (2) a hemodynamic time delay between the increase in pump speed and increase in LVAD flow associated with fluid inertia. This delay (or advance) would facilitate more accurate pump speed ramping in response to specific points in the cardiac cycle that would allow pump speed modulation not only in an asynchronous manner but also specifically for co-pulsation and counter-pulsation support. A time delay (or advance) that allows for specified support would allow the ability to gather data for co-pulsation, counter-pulsation, and asynchronous support independently, giving the ability to compare and contrast each type of support for LV volume unloading, cardiac output, and pulsatility. In future experiments in which the intelligent LVAD control strategy is able to target support based on specific points in the cardiac cycle the heart rate at which pump speed modulation is triggered can be altered. The study design of future experiments can also be changed to evaluate the intelligent LVAD control strategy at varying heart rates to

investigate if the intelligent control strategy can modulate pump speed within a cardiac cycle at higher heart rates. The effect of arrhythmias on the intelligent LVAD control strategy should be investigated to see how the control algorithm responds to various arrhythmias such as ventricular tachycardia. Finally, safety measures should be implemented into the intelligent control algorithm for events such as ventricular wall suction so the pump speed modulation can be adjusted automatically without having to be manually manipulated.

V. CONCLUSION

The results of this study show the ability of the intelligent LVAD control strategy to increase and decrease pump speed within a single cardiac cycle. This study showed through asynchronous modulation that phases of co-pulsation can generate near physiologic pulse pressure and pulsatility when compared to phases of counter-pulsation. Counter-pulsation phases generated greater ventricular volume unloading when compared to phases of co-pulsation. Furthermore, the clinical impact of pump speed modulation of CF-LVADs may result in lower incidence of adverse events associated with CF-LVAD support such as bleeding and aortic insufficiency but additional testing needs to be performed in order evaluate the effectiveness of pump speed modulation in living systems. Additional studies implementing the time delays (or advances) need to be done in order to show proof of concept in providing co-pulsation and counter-pulsation support. Also, with the ability to specify pump support the hemodynamic benefits can be evaluated for each type of support, as well as investigating if it is more beneficial to modulate pump speed asynchronously to receive the benefits of both co-pulsation and counter-pulsation support.

BIBLIOGRAPHY

Abebe TB, Gebreyohannes EA, Tefera YG, Abegaz TM. Patients with HFpEF and HFrEF have different clinical characteristics but similar prognosis: a retrospective cohort study. *BMC Cardiovasc Disord*. 2016;16(1):1-8.

Androne AS, Katz SD, Lund L, LaManca J, Hudaihed A, Hryniewicz K, Mancini D.. Hemodilution is common in patients with advanced heart failure. *Circulation*. 2003;107(2):226-229.

Argiriou M, Kolokotron SM, Sakellaridis T, et al. Right heart failure post left ventricular assist device implantation. *J Thorac Dis.* 2014;6 Suppl 1(Suppl 1):S52-S59.

Athilingam P, D 'aoust R, Zambroski C, Mcmillan SC, Sahebzemani F. Predictive validity of NYHA and ACC/AHA classifications of physical and cognitive functioning in heart failure. *Int J Nurs Sci*. 2013;3(1):22-32.

Azevedo PS, Polegato BF, Minicucci MF, Paiva SA, Zorn off LA. Cardiac remodeling: concepts, clinical impact, pathophysiological mechanisms and pharmacologic treatment. *Arq Bras Cardiol*. 2016;106(1):62–69.

Benjamin EJ, Blaha MJ, Chiuve SE, et al. Heart disease and stroke statistics'2017 update: A aeport from the American Heart Association. *Circulation.* 2017; 135(10):e146-e603.

Benjamin EJ, Virani SS, Callaway CW, et al. Heart disease and stroke statistics - 2018 update: A report from the American Heart Association. *Circulation*. 2018; 137:e67-e492.

Benjamin, E Paul M, Alvaro A, et al. Heart disease and stroke statistics—2019 update: A report from the American Heart Association. *Circulation*. 2019;139(10):e56-e528.

Berliner D, Bauersachs J. Current drug therapy in chronic heart failure - The new guidelines of the European Society of Cardiology (ESC). *Korean Circ J*. 2017;47(5):543-554.

Boulate D, Marques MA, Ha R, Banerjee D, Haddad F. Biventricular VAD versus LVAD for right heart failure. *Ann Cardiothorac Surg*. 2014;3(6):585-588.

Burgess A, Shah K, Hough O, Hynynen K. Focused ultrasound-mediated drug delivery through the blood-brain barrier. *Expert Rev Neurother*. 2015; 15(5):477-491.

Carlsson M, Andersson R, Bloch KM, et al. Cardiac output and cardiac index measured with cardiovascular magnetic resonance in healthy subjects, elite athletes and patients with congestive heart failure. *J Cardiovasc Magn Reson.* 2012; 14(1):51

Castagna F, Stöhr EJ, Pinsino A, et al. The unique blood pressures and pulsatility of LVAD patients : Current challenges and future opportunities. *Curr Hyperrens Rep.* 2017; 19(10):85.

Chatterjee K, Rame JE. Systolic heart failure: Chronic and acute syndromes. *Crit Care Med*. 2008;36(1 Suppl):S44-S51

Cheng NS. Formula for the viscosity of a glycer-watermixture. *Ind Eng Chem Res.* 2008;47(9):3285-3288.

Clifford R, Kim YD, Robson D, et al. Effect of the Lavare cycle on pump function, aortic valve opening, autonomic function and activity outcomes in continuous flow LVAD patients. *J Hear Lung Transplant*. 2017;36(4):S82.

Cook JA, Shah KB, Quader MA, et al. The total artificial heart. *J Thorac Dis*. 2015;7(12):2172-2180.

Maron BJ, Towbin JA, Thiene G, et al. Contemporary definitions and classification of the cardiomyopathies. *Circulation*. 2006;113(14):1807-1816.

Cowger J, Pagani FD, Haft JW, Romano MA, Aaronson KD, Kolias TJ. The development of aortic insufficiency in left ventricular assist device-supported patients. *Circ Heart Fail*. 2010;3(6):668–674.

De Jonge N, Kirkels JH, Klöpping C, et al. Guidelines for heart transplantation. *Netherlands Hear J*. 2008;16(3):79-87.

Delgado RM, MD, James T. Willerson M. Pathophysiology of heart failure: A look at the future. *J KONES Powertrain Transp*. 2011;18(3):149-154.

Demers C, Mody A, Teo KK, McKelvie RS. ACE inhibitors in heart failure: What more do we need to know? *Am J Cardiovasc Drugs*. 2005;5(6):351-359.

den Uil CA, Akin S, Jewbali LS, Dos Reis Miranda D, Brugts JJ, Constantinescu AA, Kappetein AP, Caliskan K.Short-term mechanical circulatory support as a bridge to durable left ventricular assist device implantation in refractory cardiogenic shock: a systematic review and meta-analysis. *Eur J Cardio-Thoracic Surg*. 2017;52(1):14-25.

Koenig SC, Woolard C, Drew G, et al. Integrated data acquisition system for medical device testing and physiology research in compliance with good laboratory practices. *Biomed Instrum Technol*. 2004;38(3):229-40.

Eckman PM, John R. Bleeding and thrombosis in patients with continuous-flow ventricular assist devices. *Circulation*. 2012;125(24):3038-3047.

Edwards Lifesciences. Normal hemodynamic parameters and laboratory values. *EdwardsCom*. 2014;AR10523:1-3. http://ht.edwards.com/scin/edwards/sitecollectionimages/products/mininvasive/ar10523- normalcard1lr.pdf

Ergle K, Parto P, Krim SR. Percutaneous ventricular assist devices : A novel approach in the management of patients with acute cardiogenic shock. *Ochsner J.* 2016:243-249.

Fida N, Loebe M, Estep JD, Guha A. Predictors and management of right heart failure after left ventricular assist device implantation. *Methodist Debakey Cardiovasc J*. 2015;11(1):18-23.

Frohlich ED, Quinlan PJ. Coronary heart disease risk factors: public impact of initial and later-announced risks. *Ochsner J*. 2014;14(4):532-537.

Gheorghiade M, Bonow RO. Chronic heart failure in the United States. A manifestation of coronary artery disease.*Circulation*. 1998;97(3):282-289.

Gilotra NA, Stevens GR. Temporary mechanical circulatory support: A review of the options, indications, and outcomes. *Clinical Medicine Insights: Cardiology*. 2015;8:75-85

Guglin M, Darbinyan N. Relationship of hemoglobin and hematocrit to systolic function in advanced heart failure. 2012:187-194.

Heidenreich PA, Albert NM, Allen LA, et al. Forecasting the impact of heart failure in the united states a policy statement from the american heart association. *Circ Hear Fail*. 2013;6(3):606-619.

Hernandez GA, Nunez Breton JD, Chaparro S V. Driveline infection in ventricular assist devices and its implication in the present era of destination therapy. *Open J Cardiovasc Surg*. 2017;9:117906521771421.

Inamdar AA, Inamdar AC. Heart failure: Diagnosis, management and utilization. *J Clin Med*. 2016;5(7):62.

Ising MS, Sobieski MA, Slaughter MS, Koenig SC, Giridharan GA. Feasibility of pump speed modulation for restoring vascular pulsatility with rotary blood pumps. *ASAIO J*. 2015;61(5):526-532.

Katz JN, Waters SB, Hollis IB, Chang PP. Advanced therapies for end-stage heart failure. *Curr Cardiol Rev*. 2015;11(1):63-72.

Kawashima D, Gojo S, Nishimura T, et al. Left ventricular mechanical support with impella provides more ventricular unloading in heart failure than extracorporeal membrane oxygenation. *ASAIO J*. 2011;57(3):169-76

Kirklin JK, Pagani FD, Kormos RL, et al. Eighth annual INTERMACS report: Special focus on framing the impact of adverse events. *J Heart Lung Transplant*. 2017;36(10):1080-1086

Kemp CD, Conte JV. The pathophysiology of heart failure. *Cardiovasc Pathol*. 2012;21(5):365-371.

Koomalsingh K, Kobashigawa JA. The future of cardiac transplantation. *Ann Cardiothorac Surg*. 2018;7(1):135-142.

Krabatsch T, Netuka I, Schmitto JD, et al. Heartmate 3 fully magnetically levitated left ventricular assist device for the treatment of advanced heart failure - 1-year results from the Ce mark trial. *J Cardiothorac Surg*. 2017;12(1):23.

Kumar J, Elhassan A, Dimitrova G, Essandoh M. The Lavare cycle: A novel pulsatile feature of the HVAD continuous-flow Left Ventricular Assist Device. *J Cardiothorac Vasc Anesth*. 2019;33(4):1170-1171.

LaRose JA, Tamez D, Ashenuga M, Reyes C. Design concepts and principle of operation of the HeartWare ventricular assist system. *ASAIO J*. 2010:285-9.

Lund LH, Edwards LB, Dipchand AI, et al. The Registry of the International Society for Heart and Lung Transplantation: Thirty-third adult heart transplantation report—2016; Focus theme: Primary diagnostic indications for transplant. *J Hear Lung Transplant*. 2016;35(10):1158-1169.

Lund LH, Khush KK, Cherikh WS, et al. The Registry of the International Society for Heart and Lung Transplantation: Thirty-fourth adult heart transplantation report-2017; Focus theme: Allograft ischemic time. *J Heart Lung Transplant*. 2017;36(10):1037-1046.

Makdisi G, Wang I. Extra corporal membrane oxygenation (ECMO) review of a livesafing techonoloy. *J Thorac Dis*. 2015;7(7):166-176.

Maniar S, Kondareddy S, Topkara VK. Left ventricular assist device-related infections: Past, present and future. *Expert Rev Med Devices*. 2011;8(5):627-634.

Melenovsky V, Hwang S, Redfield MM, Zakeri R, Lin G, Borlaug BA. Left atrial remodeling and function in advanced heart. *Circ Heart Fail*. 2015;8(2):295-303.

Monreal G, Gerhardt MA, Kambara A, Abrishamchian AR, Bauer JA, Goldstein AH. Selective microembolization of the circumflex coronary artery in an ovine model: Dilated, ischemic cardiomyopathy and left ventricular dysfunction. *J Card Fail*. 2004;10(2):174-83.

Mosterd A, Hoes AW. Clinical epidemiology of heart failure. *Heart*. 2007; 93(9):1137–1146.

Mukku VK, Cai Q, Barbagelata A, Gilani S. Use of Impella ventricular assist device in patients with severe coronary artery disease presenting with cardiac arrest. *Int J Angiol*. 2012;21(3):163-6.

Nascimbene A, Neelamegham S, Frazier OH, Moake JL, Dong JF. Acquired von Willebrand syndrome associated with left ventricular assist device. *Blood*. 2016;127(25):3133-3141.

Operator Manual Jarvik 2000 ® Adult Ventricular Assist System , Post-Auricular. 2000;(212).

Puehler T, Ensminger S, Schoenbrodt M, et al. Mechanical circulatory support devices as destination therapy—current evidence. *Ann Cardiothorac Surg*. 2014;3(5):513-524.

Wexler R, Elton T, Pleister A, Feldman D. Cardiomyopathy: An overview. *Am Fam Physician* 2010;79(9):778-784.

Sarkar K, Annapoorna S Kini MD MF. Percutaneous left ventricular support devices. *Cardiol Clin*. 2010;28(1):169-184.

Savarese G, Lund LH. Global public health burden of heart failure. *Card Fail Rev.* 2017;3(1):7–11.

Schroeder MJ, Perreault B, Ewert DL, Koenig SC, Perreault WG. HEART: An automated beat-to-beat cardiovascular analysis package using Matlab®. *Comput Biol Med*. 2004;34(5):371-388.

Sequeira V, van der Velden J. Historical perspective on heart function: the Frank–Starling law. *Biophys Rev*. 2015;7(4):421-447.

Selzman C, Koliopoulou A, Glotzbach J, McKellar SH. Evolutionary improvements in the Jarvik 2000 left ventricular assist device. *ASAIO J*. 2018;64(6):827-830.

Shah A, Gandhi D, Srivastava S, Shah KJ, Mansukhani R. Heart failure: A class review of pharmacotherapy. *P T*. 2017;42(7):464-472.

Slaughter MS, Pagani FD, Rogers JG, et al. Clinical management of continuous-flow left ventricular assist devices in advanced heart failure. *J Hear Lung Transplant*. 2010;29(9):1081.

Soucy K, Giridharan G, Choi Y, Sobieski M, Monreal G, Cheng A, et al. Rotary pump speed modulation for generating pulsatile flow and phasic left ventricular volume unloading in a bovine model of chronic ischemic heart failure. *J Hear Lung Transplant*. 2015;34(1):122-31.

Soucy KG, Koenig SC, Giridharan GA, Sobieski MA, Slaughter MS. Defining pulsatility during continuous-flow ventricular assist device support. *J Hear Lung Transplant*. 2013;32(6):581-587.

Soucy KG, Slaughter MS, Sobieski MA, Koenig SC, Giridharan GA. Rotary pumps and diminished pulsatility: do we need a pulse?. *ASAIO J*. 2013;59(4):355-366.

Stanfield JR, Selzman CH. In vitro pulsatility analysis of axial-flow and centrifugal-flow left ventricular assist devices. *J Biomech Eng*. 2013;135(3):34505

Toda K, Sawa Y. Clinical management for complications related to implantable LVAD use. *Gen Thorac Cardiovasc Surg*. 2015;63(1):1-7.

Taylor DO, Edwars LB, Boucek MM, et al. Registry of the International Society for Heart and Lung Transplantation: twenty-third official adult lung and heart-lung transplantation report-2006. *J Heart Lung Transplant*. 2006;25(8):880-892.

Ündar A, Rosenberg G, Myers JL. Major factors in the controversy of pulsatile versus nonpulsatile flow during acute and chronic cardiac support. *ASAIO J*. 2005;51(3):173-175.

Paulus WJ, Tschöpe C, Sanderson JE, et al. How to diagnose diastolic heart failure: a consensus statement on the diagnosis of heart failure with normal ventricular ejection fraction by the Heart Failure and Echocardiography Associations of the European Society of Cardiology. *European Heart J*. 2007;28(20):2539-2550.

Wu A. Cardiomyopathy N. Management of patients with non-ischaemic cardiomyopathy. *Heart*. 2007;93(3):403-408.

Yildiran T, Koc M, Bozkurt A, Sahin DY, Unal I, Acarturk E. Low pulse pressure as a predictor of death. *Tex Heart Inst J.* 2010;37(3):284-90.

Zimpfer D, Strueber M, Aigner P, Schmitto JD, Fiane AE, Larbalestier R. Evaluation of the HeartWare ventricular assist device Lavare cycle in a particle

image velocimetry model and in clinical practice. *Eur J Cardiothorac Surg*. 2016;50(5):839-848.

APPENDIX I HEMODYNAMIC WAVEFORMS:

Asynchronous waveforms for a 30% systolic duration:

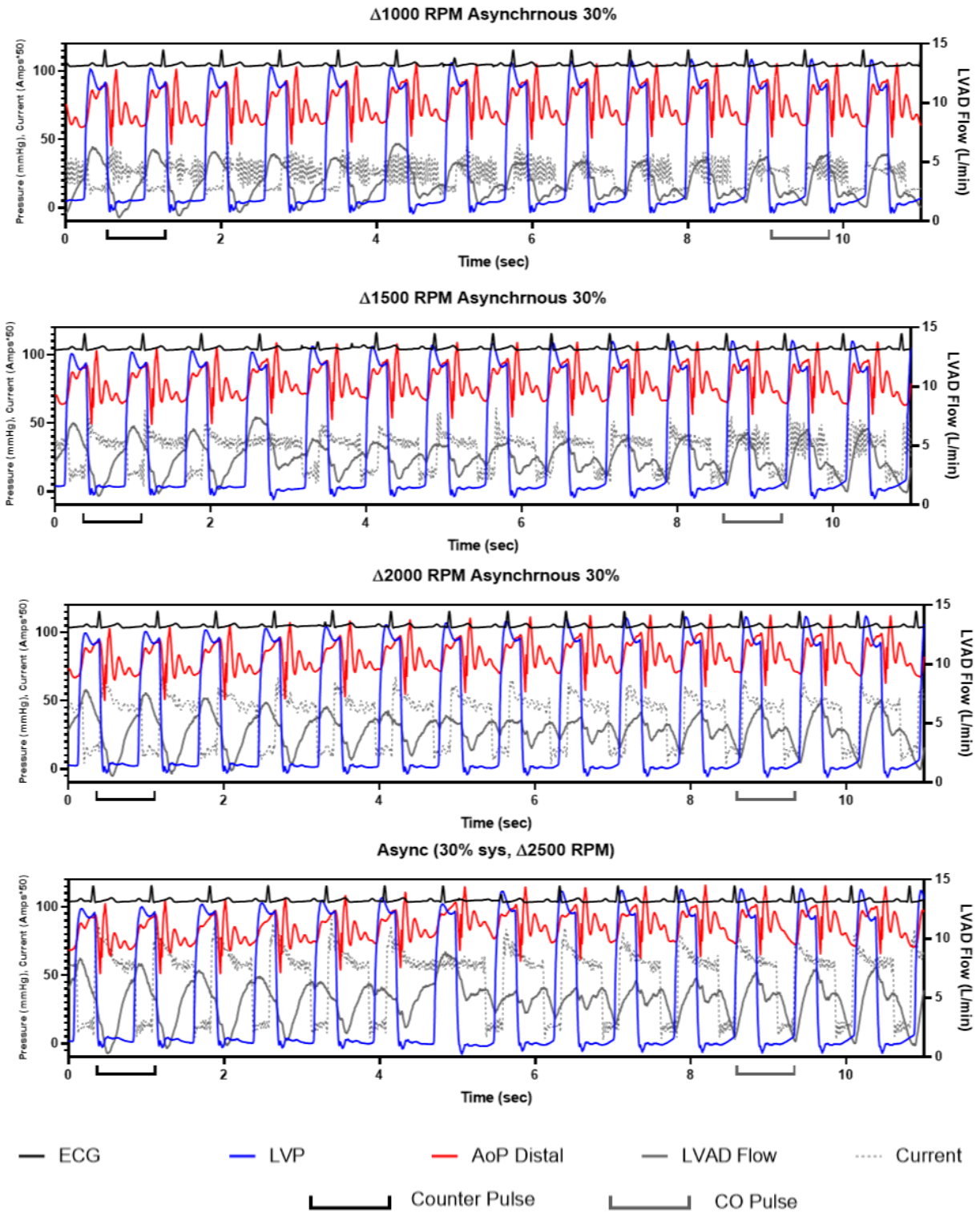

Asynchronous waveforms for a 35% systolic duration:

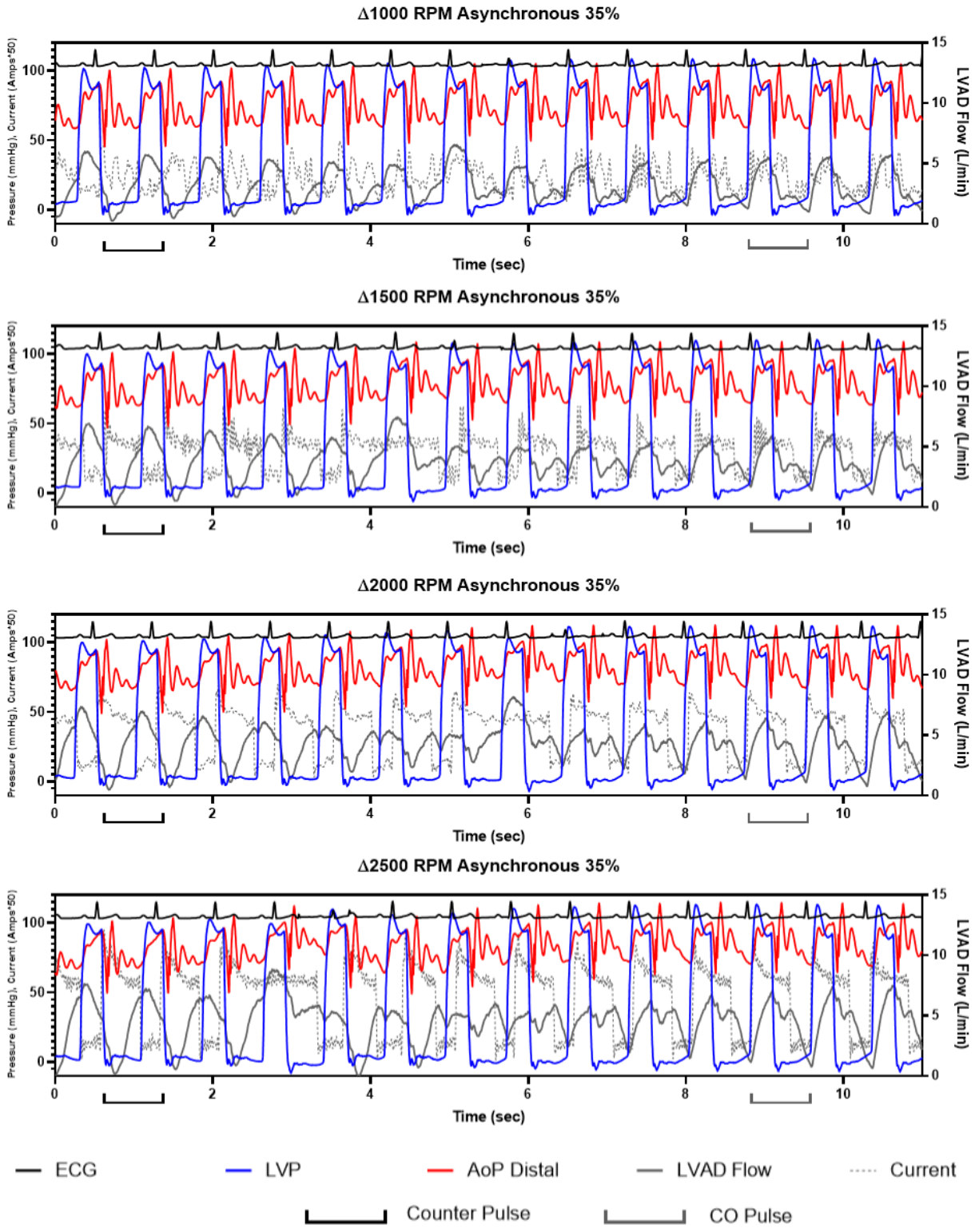

Asynchronous wavefroms for a 40% systolic duration:

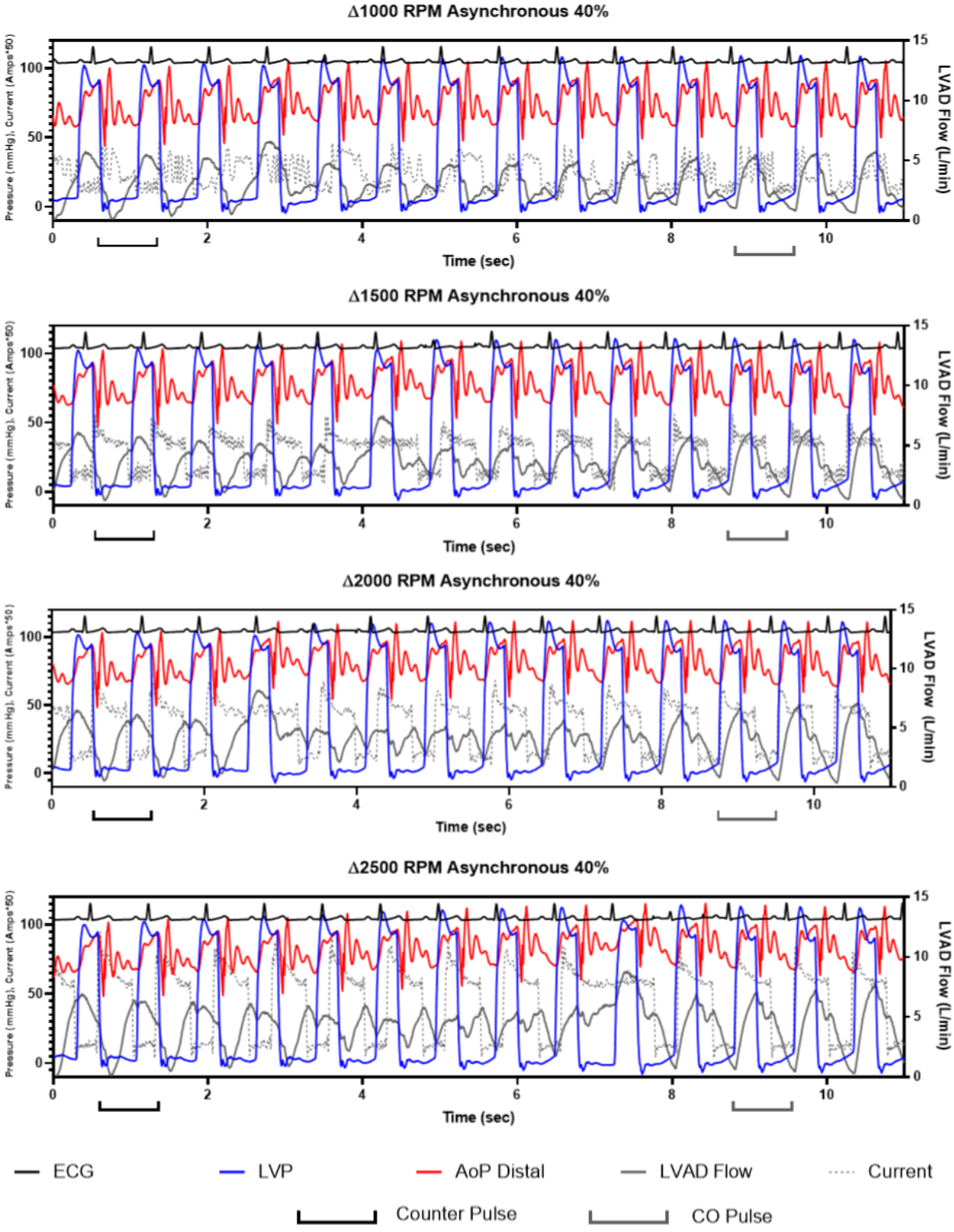

Counter-pulsation & CO-pulsation waveforms for a 30% systolic duration:

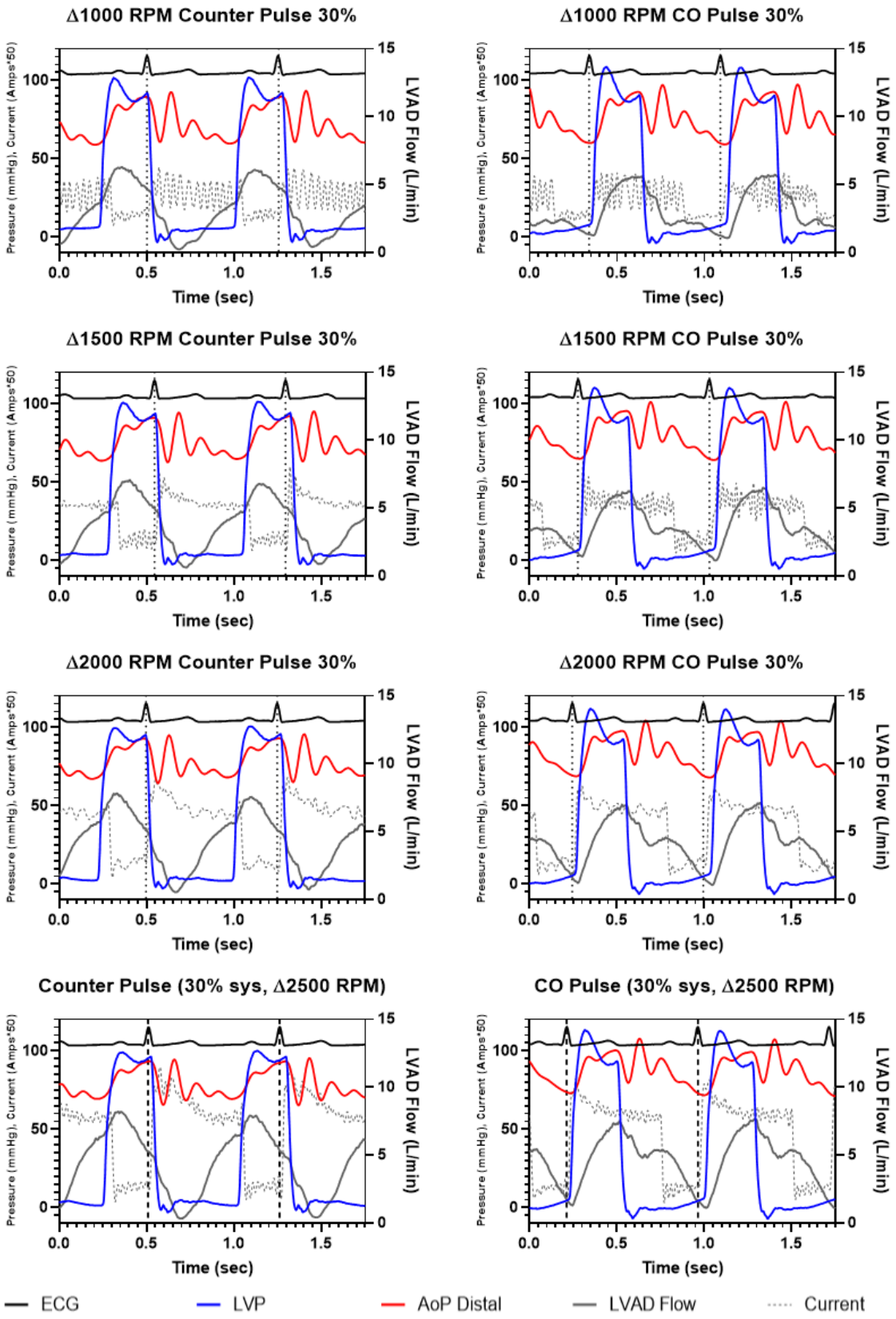

Counter-pulsation & CO-pulsation waveforms for a 35% systolic duration:

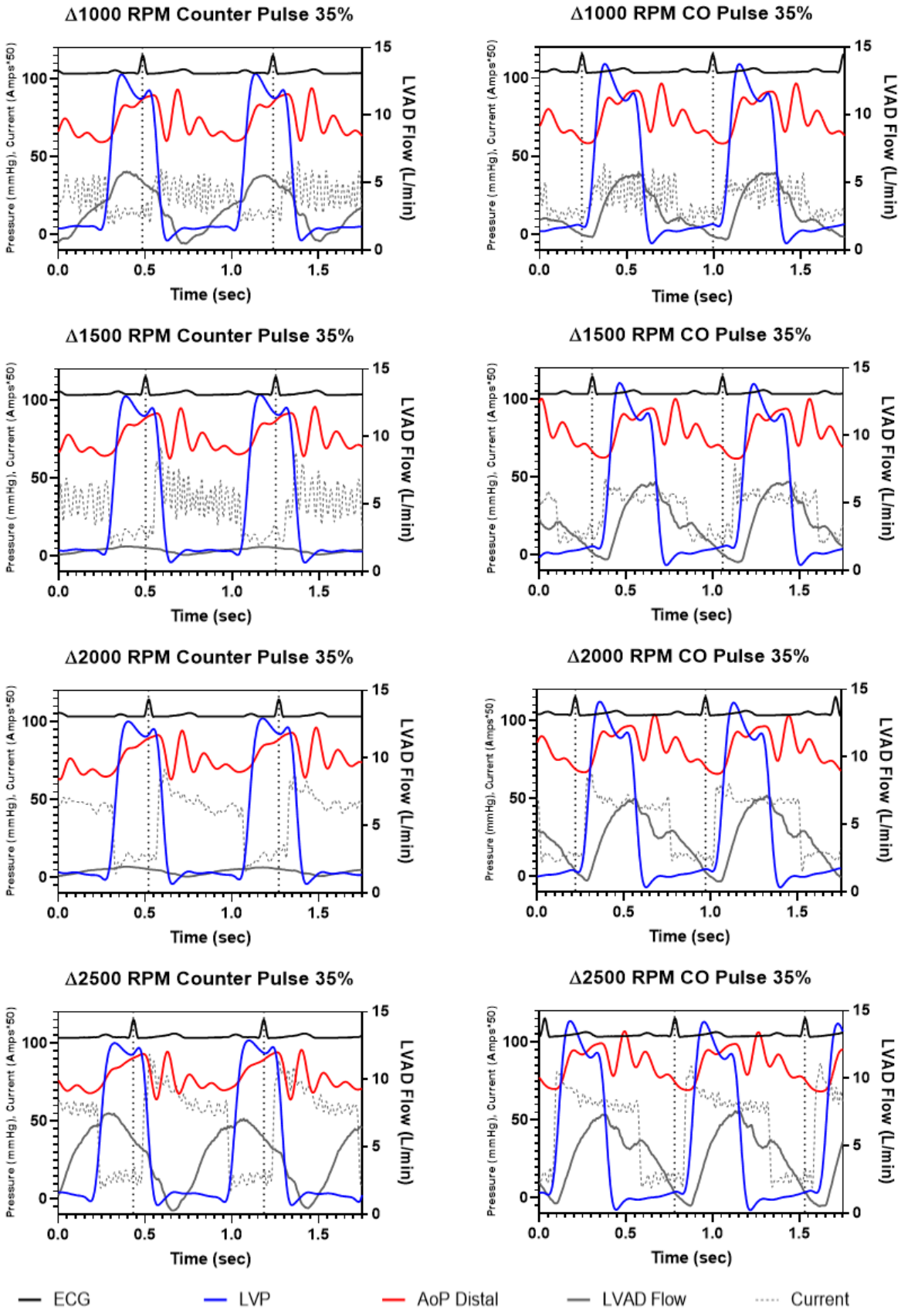

Counter-pulsation & CO-pulsation waveforms for a 40% systolic duration:

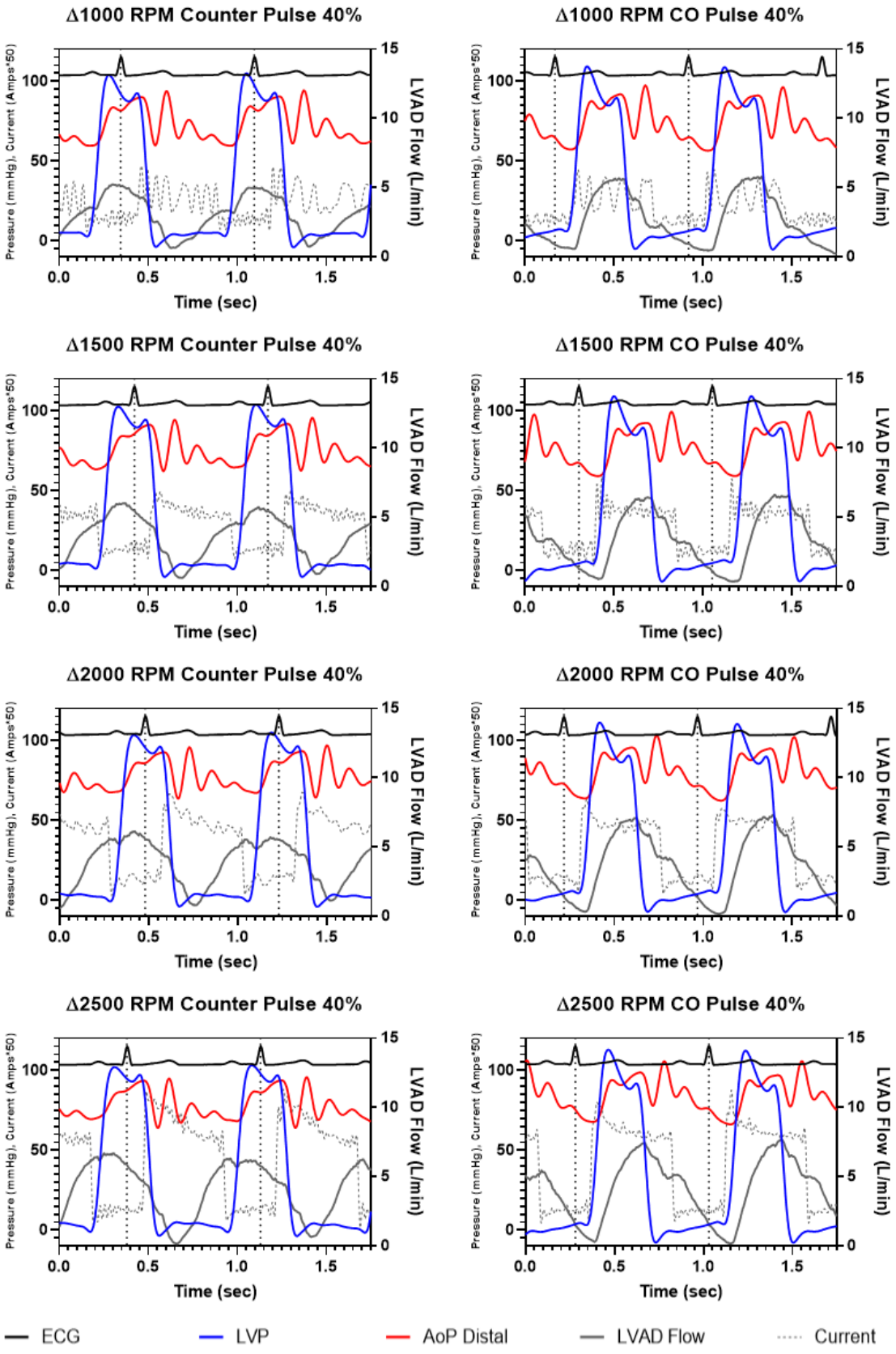

Fixed Speed Waveforms:

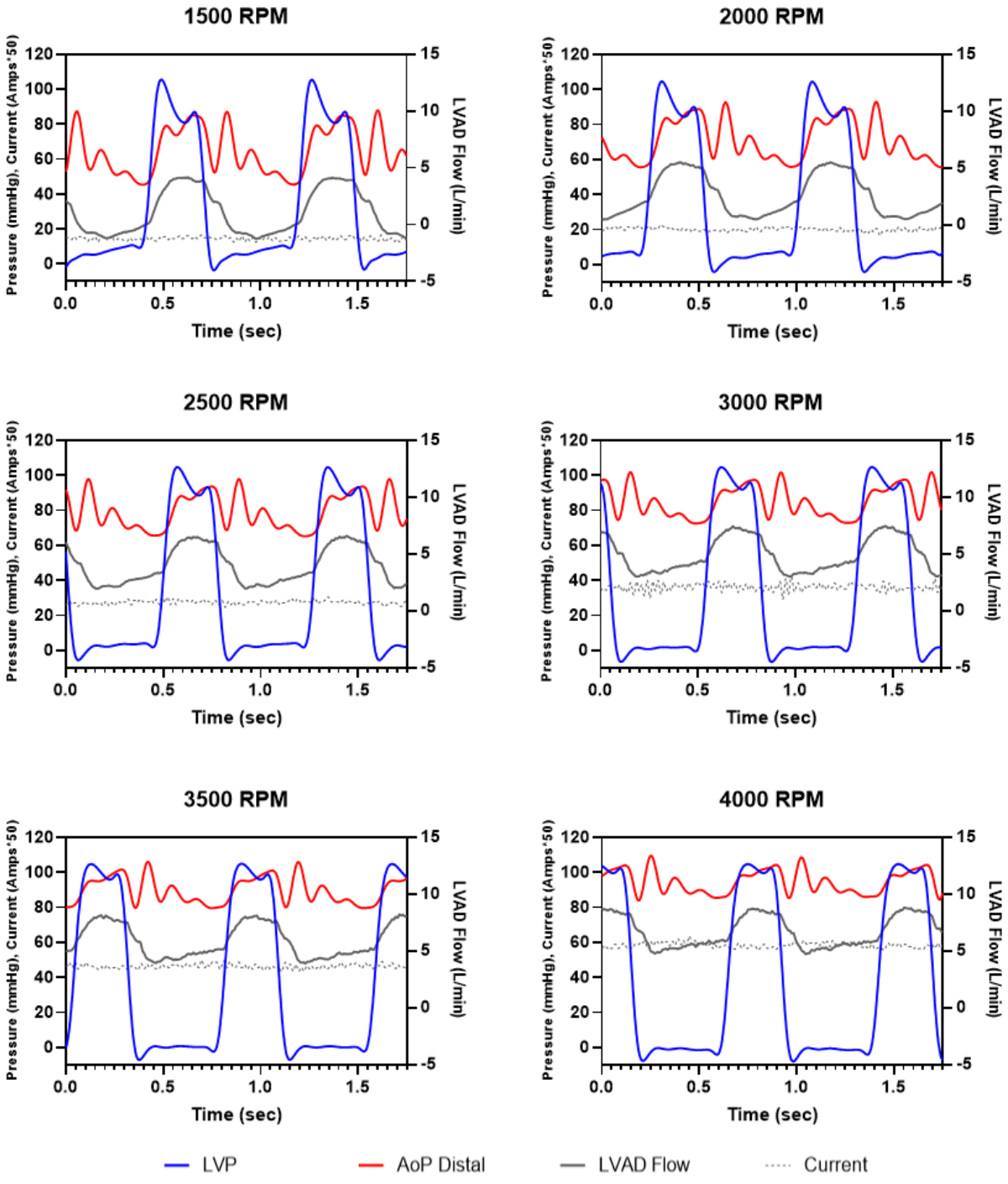

APPENDIX II HEMODYNAMIC GRAPHS:

Ventricular Volume Unloading Hemodynamic Graphs:

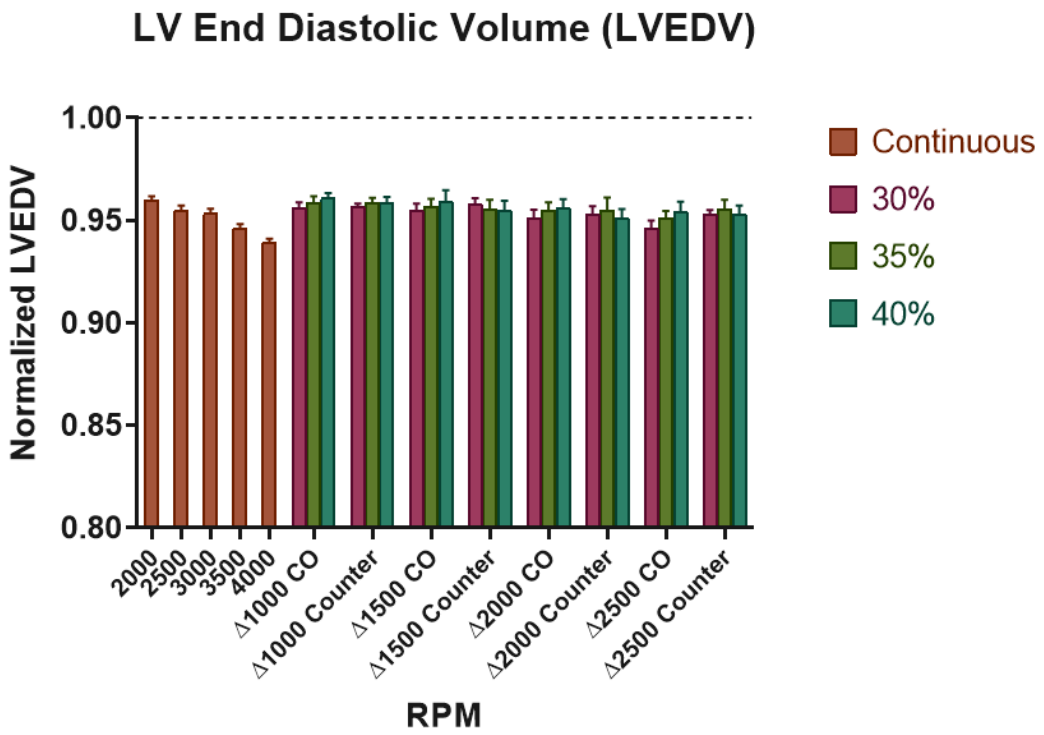

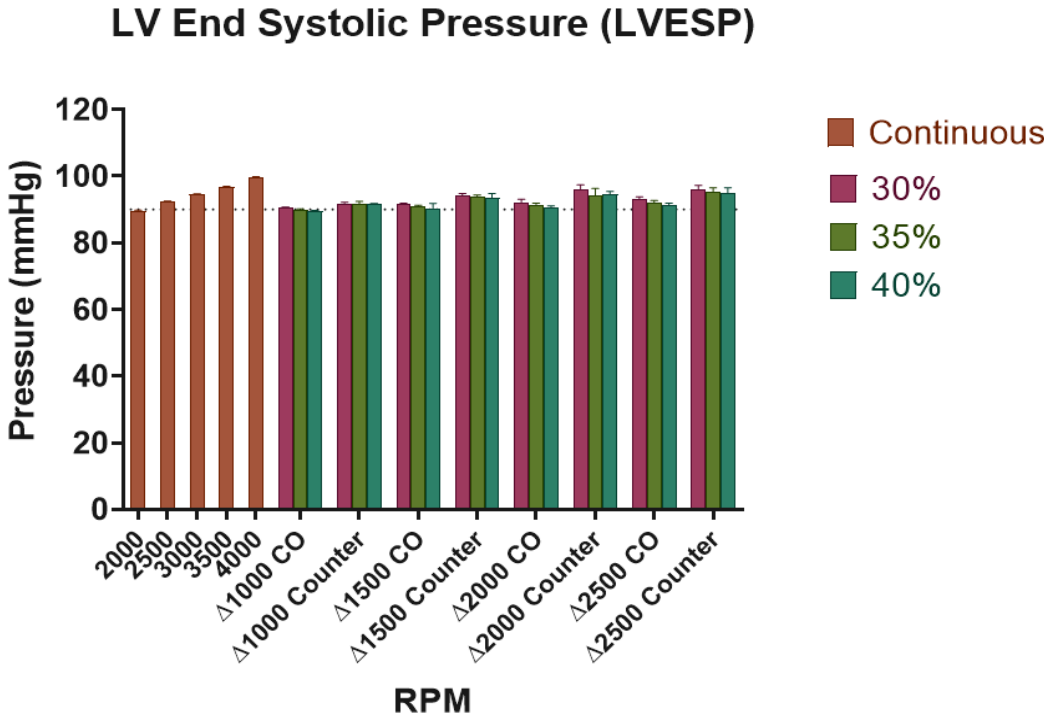

Pulsatility Hemodynamic Graphs:

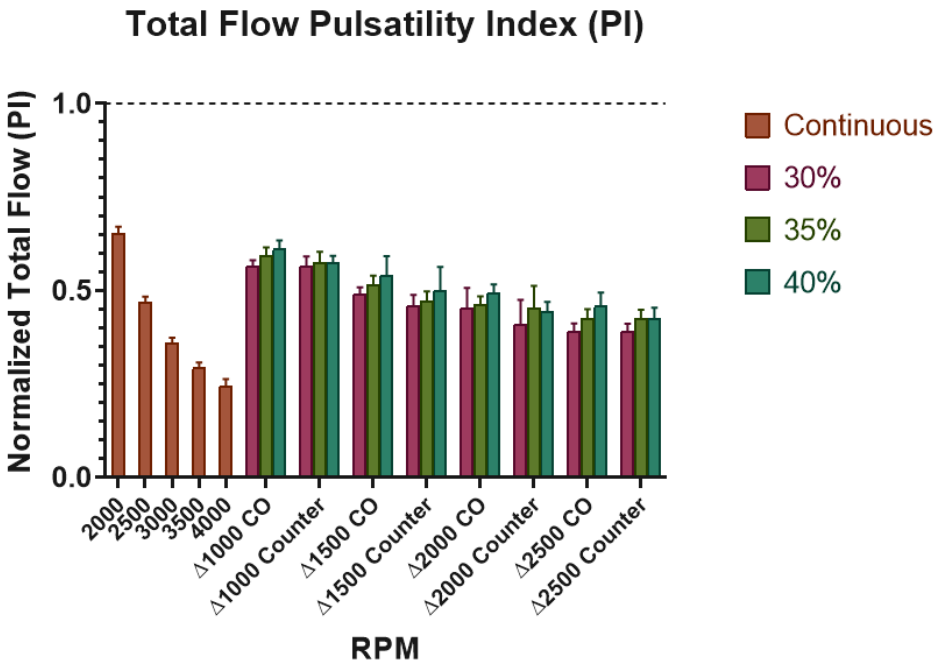

APPENDIX III MATLAB SCRIPT FOR INTELLIGENT CONTROL ANALYSIS:

```
MatLab Script for Intelligent Control experiment analysis
% This file is adapted from hrt_VAD.m which was originally written by
% Steven Koenig, Ph.D. on November 6, 2001 for the HEART program to
analyze
% Mock Circulatory Loop data from CorWave initial testing.
%
% This file calculates beat-to-beat hemodynamic parameters of mat files
% that were outputted by HEART. AoP or LVP beats must have been picked in
% HEART.
%
% Update 2/28/17 - Calculations for AOP, SHE, EEP have been changed to used
% LVP beat indices (more reliable), and LVP end systolic pressure is now
% calculated based on timing (mock loop timing is more reliable; less noise).
%
% Update 3/37/17 - Added AOP dP/dt and ZART calculations

clear all;
clc;
warning('off','MATLAB:xlswrite:AddSheet');

folderpath = 'S:\CII Unrestricted\Cary Data Dump
Zone\2019_Data\Jake_Thesis\30sys\mat\'; % Set to directory of mat files **NEED
trailing \
d=what(folderpath);  % Get everything in directory
filename=d.mat; % Gets all .mat files in the current folder

errors = 0; % initialize to no errors

% List all output labels that you are saving in heartData at the bottom of
% the code. This is to set up an output matrix for later export to Excel
% document. DO NOT REMOVE 'Recording'.
labelList = {'Recording' 'Heart Rate' 'Cardiac Output' 'Ejection Fraction',...
        'Mean LAP' 'LAP Systolic' 'LAP Diastolic',...
        'Mean LVP' 'LVP Peak Systolic' 'LVP End Systolic' 'LVP End Diastolic'
'LVP +dP/dt' 'LVP -dP/dt',...
        'LVV End Systole' 'LVV End Diastole' 'LVV Stroke Volume' 'LV External
Work',...
        'Mean AoP' 'AoP Systolic' 'AoP Diastolic' 'DeltaP_AoP'  'Mean AoF',...
        'Max AoF' 'Min AoF' 'AoF Systolic Avg' 'AoF Diastolic Avg',...
        'Mean AoPd' 'AoPd Systolic' 'AoPd Diastolic',...
        'Mean VAD P' ' VAD P Systolic' 'VAD P Diastolic' 'Mean VAD F' 'Max
VAD F' 'Min VAD F' 'VAD F Systolic Avg' 'VAD F Diastolic Avg',...
        'Mean TotalFlow' 'TotalFlow peak (+)' 'TotalFlow peak (-)' 'TotalFlowPI'
'ZART' 'SHE' 'EEP' 'ArtPavg' 'ArtPsys' 'ArtPdia' 'DeltaP_ArtP' 'ArtP_PI' 'LVCO'};
```

```
% Set up output matrix for later export to Excel document.
for i=1:length(labelList)
   output(i,1) = labelList(i);
end

for i=2:length(labelList)
   beatOutput(1,i-1) = labelList(i);
end


numFiles = length(filename);
progress = 0;
h = waitbar(progress,'Initializing data...');

for k=1:length(filename)                    % Run for all files in folder
   load(strcat(folderpath,filename{k}))       % Load the .mat files one by one
   n=filename{k};                          % Get filename of current .mat file
   outputName = strcat(n(1:end-15),'-analysis');
   if k == 1
      prevName = outputName;
      currentFile = 1;
   else
      if (strcmp(outputName,prevName) == 0)
         output = output.';
         xlswrite(prevName, output, 'Sheet1');
         output = {};
         for i=1:length(labelList)
            output(i,1) = labelList(i);
         end
         prevName = outputName;
         currentFile = 1;
      else
         currentFile = currentFile + 1;
      end
   end


   if isempty(LVPbeatindices) == 1
      % return error of no data to analyze
      disp(strcat('No LVP beat indices found in .mat file: ',n))
      errors = 2;
   else % analyze
      numbeats = size(LVPbeatindices,1);

      % Change HEART variables to real names
       AoPd = P1; % AOP Distal
```

```
VADF = VASF; % VAD Flow
VADP = P2; % VAD Pressure
TotalFlow = F1; %Total Flow
AOPRF = AoF % %Root Flow
AOPRM = ArtP % Root Millar
Current = Mrkr
Phase = T
MAG = Gz
AOPRF = AoP

% Initialize data variables
LVHR = zeros(numbeats,1)*NaN;
LVppdPdt = zeros(numbeats,1)*NaN;
LVpndPdt = zeros(numbeats,1)*NaN;
LVPbd = zeros(numbeats,1)*NaN;
LVPavg = zeros(numbeats,1)*NaN;
LVPed = zeros(numbeats,1)*NaN;
LVPpksys = zeros(numbeats,1)*NaN;
LVPes = zeros(numbeats,1)*NaN;
LVEW = zeros(numbeats,1)*NaN;
LVVes = zeros(numbeats,1)*NaN;
LVVed = zeros(numbeats,1)*NaN;
LVVSV = zeros(numbeats,1)*NaN;
LVEF = zeros(numbeats,1)*NaN;
AoPavg = zeros(numbeats,1)*NaN;
AoPsys = zeros(numbeats,1)*NaN;
AoPdia = zeros(numbeats,1)*NaN;
ArtPavg = zeros(numbeats,1)*NaN;
ArtPsys = zeros(numbeats,1)*NaN;
ArtPdia = zeros(numbeats,1)*NaN;
ArtP_PI = zeros(numbeats,1)*NaN;
LAPsys = zeros(numbeats,1)*NaN;
LAPdia = zeros(numbeats,1)*NaN;
LAPavg = zeros(numbeats,1)*NaN;
AoPdsys = zeros(numbeats,1)*NaN;
AoPddia = zeros(numbeats,1)*NaN;
AoPdavg = zeros(numbeats,1)*NaN;
LCAPsys = zeros(numbeats,1)*NaN;
LCAPdia = zeros(numbeats,1)*NaN;
LCAPavg = zeros(numbeats,1)*NaN;
CdAPsys = zeros(numbeats,1)*NaN;
CdAPdia = zeros(numbeats,1)*NaN;
CdAPavg = zeros(numbeats,1)*NaN;
SpinalPsys = zeros(numbeats,1)*NaN;
SpinalPdia = zeros(numbeats,1)*NaN;
SpinalPavg = zeros(numbeats,1)*NaN;
RenalPsys = zeros(numbeats,1)*NaN;
RenalPdia = zeros(numbeats,1)*NaN;
```

```
RenalPavg = zeros(numbeats,1)*NaN;
AoFavg = zeros(numbeats,1)*NaN;
AoFpkpos = zeros(numbeats,1)*NaN;
AoFpkneg = zeros(numbeats,1)*NaN;
AoFsys = zeros(numbeats,1)*NaN;
AoFdia = zeros(numbeats,1)*NaN;
LAFavg = zeros(numbeats,1)*NaN;
LAFpkpos = zeros(numbeats,1)*NaN;
LAFpkneg = zeros(numbeats,1)*NaN;
LAFsys = zeros(numbeats,1)*NaN;
LAFdia = zeros(numbeats,1)*NaN;
CAFavg = zeros(numbeats,1)*NaN;
CAFpkpos = zeros(numbeats,1)*NaN;
CAFpkneg = zeros(numbeats,1)*NaN;
CAFsys = zeros(numbeats,1)*NaN;
CAFdia = zeros(numbeats,1)*NaN;
CdAFavg = zeros(numbeats,1)*NaN;
CdAFpkpos = zeros(numbeats,1)*NaN;
CdAFpkneg = zeros(numbeats,1)*NaN;
CdAFsys = zeros(numbeats,1)*NaN;
CdAFdia = zeros(numbeats,1)*NaN;
SAFavg = zeros(numbeats,1)*NaN;
SAFpkpos = zeros(numbeats,1)*NaN;
SAFpkneg = zeros(numbeats,1)*NaN;
SAFsys = zeros(numbeats,1)*NaN;
SAFdia = zeros(numbeats,1)*NaN;
RAFavg = zeros(numbeats,1)*NaN;
RAFpkpos = zeros(numbeats,1)*NaN;
RAFpkneg = zeros(numbeats,1)*NaN;
RAFsys = zeros(numbeats,1)*NaN;
RAFdia = zeros(numbeats,1)*NaN;
AoFdavg = zeros(numbeats,1)*NaN;
AoFdpkpos = zeros(numbeats,1)*NaN;
AoFdpkneg = zeros(numbeats,1)*NaN;
AoFdsys = zeros(numbeats,1)*NaN;
AoFddia = zeros(numbeats,1)*NaN;
LVCO = zeros(numbeats,1)*NaN;
VADPsys = zeros(numbeats,1)*NaN;
VADPdia = zeros(numbeats,1)*NaN;
VADPavg = zeros(numbeats,1)*NaN;
VADFavg = zeros(numbeats,1)*NaN;
VADFpkpos = zeros(numbeats,1)*NaN;
VADFpkneg = zeros(numbeats,1)*NaN;
VADFsys = zeros(numbeats,1)*NaN;
VADFdia = zeros(numbeats,1)*NaN;
TotalFlowavg = zeros(numbeats,1)*NaN;
TotalFlowpkpos = zeros(numbeats,1)*NaN;
TotalFlowpkneg = zeros(numbeats,1)*NaN;
```

```
TotalFlowpulse = zeros(numbeats,1)*NaN;
TotalFlowsv = zeros(numbeats,1)*NaN;
TotalFlowPI = zeros(numbeats,1)*NaN;
ZARTbt = zeros(numbeats,1)*NaN;
SHE =zeros(numbeats,1)*NaN;
SHEbt = zeros(numbeats,1)*NaN;
EEP =zeros(numbeats,1)*NaN;
EEPbt = zeros(numbeats,1)*NaN;

fs = 400
dt = 1/fs;  % Fetch sampling interval and create dt (time interval)

% Filters - requires Signal Processing Toolbox
% See https://www.mathworks.com/help/curvefit/smooth.html
AoPfilt = fastsmooth(AoP,20,2);
AoPfilt = fastsmooth(AoPfilt,20,2);
ArtPfilt = fastsmooth(ArtP,20,2);
ArtPfilt = fastsmooth(ArtPfilt,20,2);
LAPfilt = fastsmooth(LAP,20,2);
LAPfilt = fastsmooth(LAPfilt,20,2);


% Force flow units to be ml/sec
AoF = AoF*1000/60;      % Aortic flow
VADF = VADF*1000/60;    % VAD flow
TotalFlow = TotalFlow*1000/60



plotcheck = 0;                % Set to 1 to see verification plots and values.

for counter = 1:(numbeats)
   if LVPbeatindices(counter,3) == 1                        % Do only 'good'
beats
      btstart = LVPbeatindices(counter,1);                  % Beginning of
LVP beat
      btend = LVPbeatindices(counter,2);                     % End of LVP beat
      btlen = btend-btstart+1;

      % Calculate heart rate
      LVHR(counter,1) = 60/((btend-btstart)*dt);
      percentSystole = .35; % percent systole set on the ventricle driver, will
change between heart conditions
      indexEndSys = round(btstart +
((60/LVHR(counter,1))*percentSystole)/dt);

      index35 = round(btstart + 0.35*(btend-btstart));      % Index at 35% of
beat length (ref. to pt 1)
```

```
                index80 = round(btstart + 0.8*(btend-btstart));       % Index at 80% of
beat length (ref. to pt 1)
                index120 = round(btstart + 1.2*(btend-btstart));      % Index at 120% of
beat length (ref. to pt 1)

        % Stroke volume routine not needed in SecondHeart study
                % Calculate stroke volume in mL
                % Use TotalFlow for mock loop testing
                if exist('TotalFlow') == 1
                  %  Offset flow
                  AoFoffset=mean(TotalFlow(index80:btend));
                  AoFnew = TotalFlow;%-AoFoffset;          % offsets flow
                  [fmax ifmax] = max(AoFnew(btstart:btend));

                  % find start pt. of flow
                  indexback=0;
                  while AoFnew(btstart+ifmax+indexback-1)>0 &&
(btstart+ifmax+indexback-1)>btstart
                     indexback = indexback-1;
                  end
                  flowb=btstart+ifmax+indexback-1;

                  % find end pt. of flow
                  indexfor=0;
                  while AoFnew(btstart+ifmax+indexfor-1) > 0 &&
(btstart+ifmax+indexfor-1) < btend
                     indexfor = indexfor+1;
                  end
                  flowe=btstart+ifmax+indexfor-1;

                  %   Calculate the SV in mL
                  % LVSV(counter,1) = trapz(AoFnew(flowb:flowe))*dt; % IGNORES
NEGATIVE FLOW
                  LVSV(counter,1) = trapz(AoFnew(btstart:btend))*dt;
                end

                % Calculate left ventricular parameters (+dP/dt,-dP/dt,Pbd,Ped,Ppksys)
                if exist('LVP') == 1
                   % Calculate the slope of LVP at each data point for beat 'counter'
                   LVslopes=[];
                   LVslopes(1:(btlen),1) = [1/(12*dt)]*[LVP(btstart-2:btend-2,1)-
8*LVP(btstart-1:btend-1,1)+8*LVP(btstart+1:btend+1,1)-LVP(btstart+2:btend+2,1)];

                   % Calculate peak positive (dP/dt) and peak negative (-dP/dt) LVP
pressure as an
                   % index of contractility using previous 'slope' routine
                   [LVppdPdt(counter,1),LVmaxsi] = max(LVslopes); % LVmaxsi =
max slope index  (within bt. index)
```

```
                    [LVpndPdt(counter,1),LVminsi] = min(LVslopes); % LVminsi = min
slope index  (within bt. index)

                    % Calculate LV diastolic beginning (LVPbd) and ending
(LVPed)pressures and LV systolic pressure
                    postol = 100;     % set high threshold for LVPed
                    negtol = 0;       % set low threshold for LVPbd
                    maxLVPbd=30;      % set max. LVPbd pressure threshold
                    LVPbtstep = LVminsi; %create pt by pt increment counter 'step' to
find LVPbd pt
                    while LVslopes(LVPbtstep,1) < negtol % find LVPbd pt
                       LVPbtstep = LVPbtstep + 1;
                       if LVPbtstep >= btlen, break, end; % error check - if can't find
LVPbd at slope = 0
                    end

                    LVPbd(counter,1) = LVP(btstart+LVPbtstep-1);                 %
Calculate Pbd = LVP beginning diastole
                    LVPavg(counter,1) = mean(LVP(btstart:btend));
                    LVPed(counter,1) = LVP(btend);        % Calculate Ped = LVP end
diastole at end of beat
                    [LVPpksys(counter,1),indexMaxLVP] = max(LVP(btstart:btend-1));
% Calculate LVPsys = LV systolic pressure (max LVP)
                    %[LVPpksys(counter,1),indexES] = max(LVP(btstart:btend-1));
                    [LVPes(counter,1),indexEnS] = max(LVP(indexEndSys-
15:indexEndSys+15));
                    indexED = btend;
                    indexES = indexEndSys - 15 + indexEnS;
                 end

                 % Calculate LV external work 'LVEW'(ref Sunagawa, 1983)
                 % Use TotalFlow for mock loop testing
                 if exist('LVP') == 1 && exist('AoF') ==1
                    negtol = 0;
                    bstep = LVminsi;
                    while LVslopes(bstep,1) < negtol;  bstep = bstep + 1;  if bstep >=
btlen,    break, end; end

                    [fmax ifmax] = max(AoF(btstart:btend));
                    % find start pt. of flow
                    indexback=0;
                    while AoF(btstart+ifmax+indexback-1)>0 &&
(btstart+ifmax+indexback-1)>btstart
                       indexback = indexback-1;
                    end
                    flowb=btstart+ifmax+indexback-1;

                    % find end pt. of flow
```

```
                    indexfor=0;
                    while AoF(btstart+ifmax+indexfor-1) > 0 &&
(btstart+ifmax+indexfor-1) < btend
                       indexfor = indexfor+1;
                    end
                    flowe=btstart+ifmax+indexfor-1;

                    LVPdavg = mean(LVP(btstart+bstep-1:btend));     % LVP avg.
diastolic pressure. Temp. variable.
                    LVPsavg = mean(LVP(flowb:flowe));               % LVP avg. systolic
pressure. Temp. variable.
                    LVEW(counter,1) = sum((LVP(flowb:flowe)-
LVPdavg).*AoF(flowb:flowe)).*dt;    % New EW method.
                 end

                 % Calculate LV end-systolic, end-diastolic, and stroke volumes
                 if exist('LVV') == 1
                    LVVed(counter,1) = max(LVV(btstart:btend));
                    LVVes(counter,1) = min(LVV(btstart:btend));
                    LVVSV(counter,1) = LVVed(counter,1)-LVVes(counter,1);
                    LVEF(counter,1) = LVVSV(counter,1) / LVVed(counter,1) * 100;
                 end


                 % This routine is used to calculate aortic root peak systolic, min
diastolic, and mean pressures
                 if exist('AoP') == 1
                    if LVPbeatindices(counter,3) == 1
                      btstartAo = LVPbeatindices(counter,1);
                     btendAo = LVPbeatindices(counter,2);
                     btlenAo =  btendAo-btstartAo+1;
                       AoP(indexES+5:indexED) = AoPfilt(indexES+5:indexED);
                     AoPavg(counter,1) = mean(AoP(btstartAo:btendAo));
                       % Grab AoPsys point using the LVPsys index
                       AoPsys(counter,1) = AoP(indexES);
                       AoPdia(counter,1) = AoP(indexED);
                       DeltaP_AoP = AoPsys - AoPdia;
                    end
                 end

                  if exist('ArtP') == 1
                    if LVPbeatindices(counter,3) == 1
                      btstartArt = LVPbeatindices(counter,1);
                     btendArt = LVPbeatindices(counter,2);
                     btlenArt =  btendArt-btstartArt+1;
                       ArtP(indexES+5:indexED) = ArtPfilt(indexES+5:indexED);
                     ArtPavg(counter,1) = mean(ArtP(btstartArt:btendArt));
                       % Grab AoPsys point using the LVPsys index
```

```
                ArtPsys(counter,1) = ArtP(indexES);
                ArtPdia(counter,1) = ArtP(indexED);
                DeltaP_ArtP = ArtPsys - ArtPdia;
                ArtP_PI = DeltaP_ArtP/ArtPavg
            end
        end

        progress = progress + ((1 / numFiles) * .325 * (1 / numbeats));
        progressText = num2str(progress*100,'%.2f');
        waitText = strcat(progressText,'% complete...
(',num2str(k),'/',num2str(numFiles),' files analyzed)');
        waitbar(progress,h,waitText)

        % This routine is used to calculate LA max systolic, min diastolic, and
mean pressures
        if exist('LAP') == 1
            %LAP(indexES+5:indexED) = LAPfilt(indexES+5:indexED);
            LAPsys(counter,1) = LAP(indexES);
            LAPdia(counter,1) = LAP(indexED);
            LAPavg(counter,1) = mean(LAP(btstart:btend-1));
        end

        if exist('AoPd') == 1
            AoPdsys(counter,1) = AoPd(indexES);
            AoPddia(counter,1) = AoPd(indexED);
            AoPdavg(counter,1) = mean(AoPd(btstart:btend-1));
        end
        if exist('VADP') == 1
            VADPsys(counter,1) = VADP(indexES);
            VADPdia(counter,1) = VADP(indexED);
            VADPavg(counter,1) = mean(VADP(btstart:btend-1));
        end

        if exist('AoF') ==1
            AoFavg(counter,1) = mean(AoF(btstart:btend))*60/1000;          %
calculate mean flow
            AoFpkpos(counter,1) = max(AoF(btstart:btend))*60/1000;         %
calculate peak positive flow
            AoFpkneg(counter,1) = min(AoF(btstart:btend))*60/1000;         %
calculate peak positive flow
            AoFsys(counter,1) = mean(AoF(btstart:indexES));                %
calculate average systolic flow
            AoFdia(counter,1) = mean(AoF(indexES:btend));                  %
calculate average diastolic flow
        end

        if exist('VADF') ==1
```

```
                    VADFavg(counter,1) = mean(VADF(btstart:btend))*60/1000;
% calculate mean flow
                    VADFpkpos(counter,1) = max(VADF(btstart:btend))*60/1000;
% calculate peak positive flow
                    VADFpkneg(counter,1) = min(VADF(btstart:btend))*60/1000;
% calculate peak positive flow
                    VADFsys(counter,1) = mean(VADF(btstart:indexES));                    %
calculate average systolic flow
                    VADFdia(counter,1) = mean(VADF(indexES:btend));
% calculate average diastolic flow
                end

                 if exist('TotalFlow') ==1
                    TotalFlowavg(counter,1) = mean(TotalFlow(btstart:btend))*60/1000;
% calculate mean flow
                    TotalFlowpkpos(counter,1) =
max(TotalFlow(btstart:btend))*60/1000;          % calculate peak positive flow
                    TotalFlowpkneg(counter,1) =
min(TotalFlow(btstart:btend))*60/1000;          % calculate peak positive flow
                    TotalFlowsys(counter,1) = mean(TotalFlow(btstart:indexES));
% calculate average systolic flow
                    TotalFlowdia(counter,1) = mean(TotalFlow(indexES:btend));
% calculate average diastolic flow
                    TotalFlowPI = ((TotalFlowpkpos - TotalFlowpkneg)/TotalFlowavg);
                end


                % Calculate SHE and EEP and ZART beat-to-beat
                if exist('ArtP') == 1 && exist('TotalFlow') ==1
                    if LVPbeatindices(counter,3) == 1
                      btstartArtP = LVPbeatindices(counter,1);
                      btendArtP = LVPbeatindices(counter,2);
                      ArtPmbt(counter,1) = mean(ArtP(btstartArtP:btendArtP));
                      EEPbt(counter,1) =
(trapz(ArtP(btstartArtP:btendArtP).*TotalFlow(btstartArtP:btendArtP))*dt)/(trapz(TotalF
low(btstartArtP:btendArtP))*dt); %in mmHg
                      if EEPbt(counter,1) < 0
                         EEPbt(counter,1) = NaN;
                      end
                      SHEbt(counter,1)=1332*(EEPbt(counter,1)-ArtPmbt(counter,1));
%units = ergs/cm^3
                      if SHEbt(counter,1) < 0
                         SHEbt(counter,1) = NaN;
                      end
                      EEP (counter,1) =
(trapz(AoP.*TotalFlow)*dt)/(trapz(TotalFlow)*dt);
                      MAP (counter,1)= mean(AoP);
                      SHE (counter,1)= 1332*(EEP(counter,1)-MAP(counter,1));
```

```
                    % BEGIN ZART beat-to-beat
                    ArtPdynes=ArtP*1333;        %converting to dynes/cm^2
                    thresh = 0.02; % set fractional threshold on flow fft magnitude
                    fftstart=btstartArtP;
                    fftend=btendArtP;
                    epochl = fftend-fftstart+1;                    % length of epoch being
analyzed
                    xxx=fft(ArtPdynes(fftstart:fftend-1))/(epochl-1);        % pressure
fft
                    yyy=fft(TotalFlow(fftstart:fftend-1))/(epochl-1);   % flow fft
                    ZZZ=xxx./yyy;                                % input impedance in
dyne-sec/cm5
                    ZARTbt(counter,1) = ZZZ(1);                    % ZART is the input
impendence at 0Hz (first harmonic; DC term)
                  end
                end

                %Plotting routine to verify correction waveform analysis
                if plotcheck==1; figure
                  %Check LVP
                  plotys(LVP(btstart:btend)); hold on
                  hline = refline([0 LVPavg(counter,1)]); hline.Color = 'r';

plot(find(LVP(btstart:btend)==LVPpksys(counter,1),1,'last'),LVPpksys(counter,1),'ro');

plot(find(LVP(btstart:btend)==LVPed(counter,1),1,'last'),LVPed(counter,1),'ro'); pause
                  close
                  % Check Ao
                  plotys(AoP(btstart:btend)); hold on
                  hline = refline([0 AoPavg(counter,1)]); hline.Color = 'r';

plot(find(AoP(btstart:btend)==AoPsys(counter,1),1,'last'),AoPsys(counter,1),'ro');

plot(find(AoP(btstart:btend)==AoPdia(counter,1),1,'last'),AoPdia(counter,1),'ro'); pause
                  close
                  % Check AoPd
                  plotys(AoPd(btstart:btend)); hold on
                  hline = refline([0 AoPdavg(counter,1)]); hline.Color = 'r';

plot(find(AoPd(btstart:btend)==AoPdsys(counter,1),1,'last'),AoPdsys(counter,1),'ro');

plot(find(AoPd(btstart:btend)==AoPddia(counter,1),1,'last'),AoPddia(counter,1),'ro');
pause
                  close
                end

              end % End of good beat if-statement
```

```
            end % End of beat by beat 'counter' loop


            progress = progress + (1 / numFiles * .325);
            progressText = num2str(progress*100,'%.2f');
            waitText = strcat(progressText,'% complete...
(',num2str(k),'/',num2str(numFiles),' files analyzed)');
            waitbar(progress,h,waitText)

            % Calculate cardiac output = sv x hr as a single matrix
            % multiplication. Use TotalFlow for mock loop with VAD study.
            if exist ('LVV') == 1
               LVCO = LVVSV.*LVHR/1000; % Use for flows recorded in L/min (that
were calculated into mL/sec)
        %           LVCO = LVSV.*LVHR;     % Use for flows recorded in mL/min (that
were converted to mL/sec)
            end

            heartData = [LVHR LVCO LVEF LAPavg LAPsys LAPdia, ...
                     LVPavg LVPpksys LVPes LVPed LVppdPdt LVpndPdt LVVes
LVVed LVVSV LVEW, ...
                     AoPavg AoPsys AoPdia DeltaP_AoP AoFavg AoFpkpos AoFpkneg
AoFsys AoFdia,...
                     AoPdavg AoPdsys AoPddia,...
                     VADPavg VADPsys VADPdia VADFavg VADFpkpos
VADFpkneg VADFsys VADFdia,...
                     TotalFlowavg TotalFlowpkpos TotalFlowpkneg TotalFlowPI EEPbt
SHEbt ZARTbt,...
                     ArtPavg ArtPsys ArtPdia DeltaP_ArtP ArtP_PI LVCO];



            for i=2:numbeats+1
               for j=1:length(labelList)-1
                  beatOutput{i,j} = heartData(i-1,j);
               end
            end

            xlswrite(outputName, beatOutput, n(1:end-4));

            beatOutput = {};
            for i=2:length(labelList)
               beatOutput(1,i-1) = labelList(i);
            end

            stats = [];
            [row,col] = size(heartData);
            for column = 1:col
```

```
            data = heartData(:,column);
            stats(column,1) = nanmean(data(isfinite(data)));
            stats(column,2) = std(data(isfinite(data)));
        end
        errors = 0;
    end % End of 'isempty' if statement for analysis block (LVP beat check)

    output{1,currentFile*2} = strcat(n(1:end-4),' Means');
    output{1,currentFile*2+1} = strcat(n(1:end-4),' Std Devs');
    for i=2:length(labelList)
        output{i,currentFile*2} = stats(i-1,1);
        output{i,currentFile*2+1} = stats(i-1,2);
    end

    if  (k == length(filename))
        output = output.';
        xlswrite(prevName, output, 'Sheet1');
    end

    waitText = strcat(progressText,'% complete...
(',num2str(k),'/',num2str(numFiles),' files analyzed)');
    waitbar(progress,h,waitText)
    progress = progress + (1 / numFiles * .35);
    progressText = num2str(progress*100,'%.2f');

end % End of main for loop

close(h)
warning('on','MATLAB:xlswrite:AddSheet');
clear all
```

APPENDIX IV MASTER MATLAB DATA SPREADSHEETS:

Fixed Speed:

	Recording						
Parameter	Baseline-Pre	Baseline-Post	2000 RPM	2500 RPM	3000 RPM	3500 RPM	4000 RPM
Heart Rate (BPM)	78	78	78	78	78	78	78
Cardiac Output (L/min)	3.2	3.2	3.7	4.1	4.4	4.6	4.8
Ejection Fraction (%)	24	23	16	15	15	15	15
Mean LAP (mmHg)	24	24	23	22	21	21	20
LAP Systolic (mmHg)	21	21	20	18	17	16	15
LAP Diastolic (mmHg)	23	23	23	22	22	21	21
Mean LVP (mmHg)	38	38	35	35	34	34	34
LVP Peak Systolic (mmHg)	110	110	104	104	104	104	105
LVP End Systolic (mmHg)	90	90	90	92	95	97	100
LVP End Diastolic (mmHg)	14	15	10	6	4	2	0
LVP +dP/dt (mmHg/sec)	3516	3499	3460	3454	3422	3375	3325
LVP -dP/dt (mmHg/sec)	-3435	-3429	-3333	-3378	-3382	-3415	-3426
LVV End Systole (mL)	124	127	133	133	133	133	132
LVV End Diastole (mL)	164	165	158	157	157	156	155
LVV Stroke Volume (mL)	40	38	25	24	24	23	23
LV External Work (mmHg*mL)	4321	4313	2764	2229	1756	1300	848
Mean AoP (mmHg)	63	63	72	79	84	89	94
AoP Systolic (mmHg)	84	84	90	94	98	102	105
AoP Diastolic (mmHg)	46	46	58	67	74	81	87
DeltaP_AoP (mmHg)	37	38	32	28	24	21	18
Mean AoF (L/min)	3.0	3.0	1.3	0.6	0.1	-0.5	-0.9
Max AoF (L/min)	15.2	15.2	10.3	8.3	6.7	5.1	3.4
Min AoF (L/min)	-8.4	-8.3	-9.5	-9.6	-9.9	-10.2	-10.4
Mean VAD P (mmHg)	49	51	81	92	102	111	120
VAD P Systolic (mmHg)	49	51	106	116	124	132	142
VAD P Diastolic (mmHg)	49	51	64	76	87	97	108
Mean VAD F (L/min)	0.0	0.0	2.7	4.0	4.9	5.8	6.5
Max VAD F (L/min)	0.0	0.0	5.5	6.6	7.4	8.1	8.8
Min VAD F (L/min)	0.0	0.0	0.5	2.0	3.0	3.9	4.8
Mean TotalFlow (L/min)	3.2	3.2	3.7	4.1	4.4	4.6	4.8
TotalFlow peak (+) (L/min)	4.4	4.4	4.6	4.8	4.9	5.1	5.2
TotalFlow peak (-) (L/min)	2.1	2.1	2.9	3.4	3.8	4.1	4.4
ZART (dynes-sec/cm^5)	65	65	73	80	85	90	94
SHE (ergs/cm^3)	2694	2651	1546	965	625	432	298
EEP (mmHg)	1567	1567	1542	1544	1552	1565	1577

30% systolic duration counter-pulsation:

	Recording																	
Parameter	Baseline-Pre	Baseline-Post	Counter Pulse 1500-2500							Counter Pulse 1500-3000								
Heart Rate (BPM)	78	78	78	78	78	78	78	78	78	78	78	78	78	78	78	78	78	78
Cardiac Output (L/min)	2.9	2.9	3.8	3.8	3.8	3.8	3.8	3.8	3.8	4.0	4.1	4.1	4.0	4.0	4.0	4.0	4.0	4.0
Ejection Fraction (%)	23	23	16	16	16	16	16	16	16	15	16	15	16	16	16	15	16	16
Mean LAP (mmHg)	23	23	23	23	23	23	23	23	22	22	22	22	22	22	22	22	22	22
LAP Systolic (mmHg)	21	21	19	19	19	19	19	19	19	19	18	18	19	19	19	18	18	19
LAP Diastolic (mmHg)	23	23	23	23	23	23	23	23	23	23	23	23	23	23	23	23	23	23
Mean LVP (mmHg)	38	38	35	35	35	35	35	35	35	35	36	35	35	35	35	35	35	35
LVP Peak Systolic (mmHg)	110	110	101	102	101	102	102	101	102	101	103	103	100	101	100	101	101	101
LVP End Systolic (mmHg)	90	90	92	92	92	92	92	92	92	94	95	95	94	94	94	94	94	94
LVP End Diastolic (mmHg)	15	14	7	6	7	7	7	7	7	4	4	5	4	4	4	4	4	4
LVP +dP/dt (mmHg/sec)	3499	3499	3438	3394	3442	3404	3441	3437	3435	3396	3413	3408	3401	3379	3433	3406	3418	3390
LVP -dP/dt (mmHg/sec)	-3434	-3434	-3348	-3364	-3357	-3360	-3354	-3352	-3365	-3397	-3401	-3405	-3390	-3363	-3384	-3394	-3391	-3371
LVV End Systole (mL)	128	128	133	133	134	134	134	134	134	135	134	135	134	134	134	134	134	134
LVV End Diastole (mL)	166	166	159	159	159	159	159	159	159	159	159	159	160	159	159	159	159	159
LVV Stroke Volume (mL)	38	38	26	25	25	25	25	25	25	25	25	24	26	25	25	25	25	25
LV External Work (mmHg*mL)	4317	4318	2449	2471	2468	2486	2474	2462	2493	2182	2101	2085	2153	2161	2151	2190	2177	2167
Mean AoP (mmHg)	63	63	73	74	74	74	74	74	74	77	79	78	76	77	76	77	77	77
AoP Systolic (mmHg)	84	84	90	90	91	90	91	90	90	92	93	94	92	92	92	92	92	92
AoP Diastolic (mmHg)	46	46	61	62	61	62	62	62	62	67	68	68	66	67	66	67	67	67
DeltaP_AoP (mmHg)	38	38	29	28	29	28	28	29	28	25	25	26	26	26	26	25	25	26
Mean AoF (L/min)	3.0	3.0	1.0	1.0	1.0	1.1	1.0	1.0	1.0	0.7	0.6	0.5	0.7	0.7	0.7	0.7	0.7	0.7
Max AoF (L/min)	15.2	15.2	9.0	9.0	9.0	9.1	9.0	9.0	9.1	7.9	7.7	7.6	7.8	7.8	7.9	7.9	7.9	7.9
Min AoF (L/min)	-8.2	-8.2	-9.2	-9.2	-9.4	-9.1	-9.0	-9.3	-9.4	-9.6	-9.0	-9.3	-9.3	-9.3	-9.5	-9.3	-9.2	-9.5
Mean VAD P (mmHg)	66	66	84	84	84	84	85	84	84	90	92	91	89	90	89	90	90	90
VAD P Systolic (mmHg)	66	66	102	102	101	103	103	102	103	104	107	106	105	105	105	105	104	105
VAD P Diastolic (mmHg)	66	66	72	72	72	73	73	72	73	82	82	82	81	80	80	81	80	81
Mean VAD F (L/min)	0.0	0.0	3.2	3.3	3.2	3.3	3.3	3.3	3.3	3.9	3.9	3.9	3.9	3.9	3.9	3.9	3.9	3.9
Max VAD F (L/min)	0.0	0.0	6.4	6.2	6.3	6.1	6.2	6.2	6.1	6.9	6.7	6.7	7.1	7.1	7.1	6.9	7.0	7.0
Min VAD F (L/min)	0.0	0.0	0.2	0.3	0.3	0.5	0.5	0.3	0.5	0.8	0.8	0.7	0.5	0.6	0.6	0.7	0.7	0.6
Mean TotalFlow (L/min)	3.2	3.2	3.8	3.8	3.8	3.8	3.8	3.8	3.8	4.0	4.1	4.1	4.0	4.0	4.0	4.0	4.0	4.0
TotalFlow peak (+) (L/min)	4.4	4.4	4.6	4.6	4.6	4.7	4.6	4.6	4.6	4.7	4.7	4.7	4.7	4.7	4.7	4.7	4.7	4.7
TotalFlow peak (-) (L/min)	2.1	2.1	3.1	3.1	3.1	3.1	3.1	3.1	3.1	3.4	3.5	3.5	3.4	3.4	3.3	3.4	3.4	3.4
ZART (dynes-sec/cm^5)	65	65	74	74	74	75	75	74	75	78	79	79	77	77	77	78	77	77
SHE (ergs/cm^3)	2642	2646	1221	1148	1197	1168	1144	1161	1115	798	800	791	881	847	838	834	826	870
EEP (mmHg)	1567	1567	1534	1543	1545	1544	1545	1540	1544	1542	1540	1541	1540	1539	1544	1546	1542	1544

30% systolic duration counter-pulsation:

	Recording													
Parameter	Baseline-Pre	Baseline-Post	Counter Pulse 1500 - 3500					Counter Pulse 1500 - 4000						
Heart Rate (BPM)	78	78	78	78	78	77	78	78	77	78	78	78	78	78
Cardiac Output (L/min)	2.9	2.9	4.1	4.1	4.2	4.2	4.1	4.1	4.1	4.1	4.1	4.1	4.2	4.1
Ejection Fraction (%)	23	23	15	15	15	15	16	16	16	16	16	16	16	16
Mean LAP (mmHg)	23	23	22	22	22	21	21	22	22	22	22	22	21	22
LAP Systolic (mmHg)	21	21	18	18	17	17	17	18	18	18	18	18	17	18
LAP Diastolic (mmHg)	23	23	23	23	23	23	23	23	23	23	23	23	23	23
Mean LVP (mmHg)	38	38	35	35	35	35	37	34	34	34	34	34	35	34
LVP Peak Systolic (mmHg)	110	110	100	100	102	102	103	98	99	99	99	99	100	99
LVP End Systolic (mmHg)	90	90	95	95	97	97	97	96	96	96	96	96	98	96
LVP End Diastolic (mmHg)	15	14	3	3	3	3	6	3	2	1	2	2	2	2
LVP +dP/dt (mmHg/sec)	3499	3499	3347	3403	3387	3353	3366	3353	3372	3351	3351	3362	3341	3343
LVP -dP/dt (mmHg/sec)	-3434	-3434	-3398	-3379	-3415	-3410	-3429	-3405	-3396	-3420	-3406	-3404	-3432	-3400
LVV End Systole (mL)	128	128	134	134	134	134	134	133	133	133	134	133	133	133
LVV End Diastole (mL)	166	166	158	158	158	158	159	158	158	158	158	158	158	158
LVV Stroke Volume (mL)	38	38	24	25	24	24	25	25	25	25	25	25	25	25
LV External Work (mmHg*mL)	4317	4318	1921	1887	1803	1766	1785	1735	1784	1798	1752	1737	1563	1782
Mean AoP (mmHg)	63	63	79	79	80	81	79	79	80	79	79	79	81	79
AoP Systolic (mmHg)	84	84	94	93	95	95	96	94	94	94	94	94	96	93
AoP Diastolic (mmHg)	46	46	71	70	71	71	67	72	73	72	72	72	72	72
DeltaP_AoP (mmHg)	38	38	23	24	24	24	28	22	22	22	22	22	24	21
Mean AoF (L/min)	3.0	3.0	0.4	0.4	0.2	0.2	0.3	0.2	0.2	0.3	0.2	0.2	0.0	0.2
Max AoF (L/min)	15.2	15.2	7.0	6.9	6.6	6.6	6.7	6.4	6.6	6.6	6.5	6.4	5.9	6.6
Min AoF (L/min)	-8.2	-8.2	-9.4	-9.2	-9.2	-9.9	-8.8	-9.2	-9.4	-9.3	-9.1	-8.9	-9.5	-9.4
Mean VAD P (mmHg)	66	66	94	94	95	96	92	96	96	96	96	96	98	96
VAD P Systolic (mmHg)	66	66	106	106	107	108	107	106	107	106	107	106	110	106
VAD P Diastolic (mmHg)	66	66	88	88	89	91	89	95	96	95	95	96	97	95
Mean VAD F (L/min)	0.0	0.0	4.4	4.4	4.3	4.3	3.6	4.6	4.6	4.6	4.5	4.6	4.5	4.6
Max VAD F (L/min)	0.0	0.0	7.7	7.8	7.5	7.5	7.2	8.5	8.2	8.3	8.3	8.4	8.3	8.2
Min VAD F (L/min)	0.0	0.0	0.8	0.6	0.7	0.7	-0.3	0.4	0.5	0.4	0.4	0.4	0.2	0.5
Mean TotalFlow (L/min)	3.2	3.2	4.1	4.1	4.2	4.2	4.1	4.1	4.1	4.1	4.1	4.1	4.2	4.1
TotalFlow peak (+) (L/min)	4.4	4.4	4.7	4.7	4.8	4.8	4.8	4.8	4.8	4.7	4.7	4.7	4.8	4.7
TotalFlow peak (-) (L/min)	2.1	2.1	3.6	3.5	3.7	3.7	3.4	3.6	3.6	3.6	3.6	3.6	3.7	3.6
ZART (dynes-sec/cm^5)	65	65	80	79	81	81	80	80	80	80	80	80	81	80
SHE (ergs/cm^3)	2642	2646	632	692	689	633	1164	650	594	589	614	640	724	580
EEP (mmHg)	1567	1567	1544	1545	1540	1541	1536	1544	1543	1543	1546	1548	1542	1544

30% systolic duration co-pulsation:

	Recording													
Parameter	Baseline-Pre	Baseline-Post	CO-Pulse 1500 - 2500					CO-Pulse 1500 - 3000						
Heart Rate (BPM)	78	78	78	78	78	78	78	78	78	78	78	78	78	78
Cardiac Output (L/min)	2.9	2.9	4.0	4.0	4.0	4.0	4.0	4.2	4.2	4.2	4.2	4.2	4.2	4.2
Ejection Fraction (%)	23	23	15	15	15	15	15	15	15	14	14	15	15	15
Mean LAP (mmHg)	23	23	22	22	22	22	22	22	22	22	22	22	22	22
LAP Systolic (mmHg)	21	21	19	19	19	19	19	18	18	18	18	18	18	18
LAP Diastolic (mmHg)	23	23	22	22	22	22	22	22	22	22	22	22	22	22
Mean LVP (mmHg)	38	38	36	36	36	36	36	35	35	35	35	35	35	35
LVP Peak Systolic (mmHg)	110	110	108	108	109	108	108	110	110	110	110	110	110	110
LVP End Systolic (mmHg)	90	90	90	90	90	91	90	91	92	92	91	91	92	91
LVP End Diastolic (mmHg)	15	14	9	9	9	9	10	8	8	8	8	8	8	8
LVP +dP/dt (mmHg/sec)	3499	3499	3527	3542	3519	3554	3556	3540	3557	3538	3552	3522	3564	3511
LVP -dP/dt (mmHg/sec)	-3434	-3434	-3346	-3328	-3360	-3342	-3357	-3351	-3362	-3365	-3375	-3362	-3377	-3362
LVV End Systole (mL)	128	128	135	135	135	135	135	135	135	136	136	135	135	135
LVV End Diastole (mL)	166	166	159	159	159	159	159	158	158	158	159	159	159	159
LVV Stroke Volume (mL)	38	38	24	24	24	24	24	23	23	23	23	24	23	24
LV External Work (mmHg*mL)	4317	4318	2796	2785	2790	2793	2780	2572	2579	2568	2598	2588	2586	2574
Mean AoP (mmHg)	63	63	77	77	77	77	76	81	81	81	81	81	81	81
AoP Systolic (mmHg)	84	84	93	93	93	93	93	96	96	96	96	96	96	96
AoP Diastolic (mmHg)	46	46	60	60	61	61	61	65	65	65	65	65	65	65
DeltaP_AoP (mmHg)	38	38	33	33	32	33	32	31	31	30	30	31	30	30
Mean AoF (L/min)	3.0	3.0	1.2	1.2	1.2	1.2	1.2	0.8	0.8	0.8	0.9	0.9	0.8	0.9
Max AoF (L/min)	15.2	15.2	10.2	10.2	10.2	10.2	10.1	9.3	9.4	9.3	9.4	9.4	9.4	9.4
Min AoF (L/min)	-8.2	-8.2	-9.3	-9.5	-9.4	-9.2	-9.4	-9.8	-9.6	-10.1	-9.3	-9.7	-9.6	-9.7
Mean VAD P (mmHg)	66	66	86	86	87	86	86	93	93	93	93	93	93	93
VAD P Systolic (mmHg)	66	66	114	114	114	113	114	122	121	122	121	122	121	122
VAD P Diastolic (mmHg)	66	66	62	61	61	61	62	65	65	65	64	65	65	66
Mean VAD F (L/min)	0.0	0.0	3.1	3.2	3.2	3.2	3.1	3.8	3.8	3.8	3.8	3.8	3.8	3.7
Max VAD F (L/min)	0.0	0.0	5.7	5.7	5.7	5.6	5.7	6.4	6.3	6.3	6.3	6.3	6.3	6.4
Min VAD F (L/min)	0.0	0.0	1.0	1.1	1.1	1.1	1.0	1.2	1.3	1.3	1.2	1.2	1.3	1.1
Mean TotalFlow (L/min)	3.2	3.2	4.0	4.0	4.0	4.0	4.0	4.2	4.2	4.2	4.2	4.2	4.2	4.2
TotalFlow peak (+) (L/min)	4.4	4.4	4.7	4.8	4.7	4.7	4.7	4.9	4.9	4.9	4.9	4.8	4.8	4.9
TotalFlow peak (-) (L/min)	2.1	2.1	3.2	3.1	3.1	3.1	3.1	3.4	3.4	3.4	3.4	3.4	3.4	3.3
ZART (dynes-sec/cm^5)	65	65	78	78	78	78	78	82	82	82	82	82	82	82
SHE (ergs/cm^3)	2642	2646	1367	1349	1328	1323	1375	1152	1083	1113	1056	1111	1077	1151
EEP (mmHg)	1567	1567	1540	1540	1543	1541	1543	1547	1549	1548	1544	1549	1544	1548

30% systolic duration co-pulsation:

	Recording													
Parameter	Baseline-Pre	Baseline-Post	CO- Pulse 1500 - 3500				CO-Pulse 1500 - 4000							
Heart Rate (BPM)	78	78	77	78	77	78	78	78	78	78	78	78	78	78
Cardiac Output (L/min)	2.9	2.9	4.4	4.4	4.4	4.2	4.5	4.5	4.5	4.5	4.5	4.5	4.5	4.5
Ejection Fraction (%)	23	23	15	15	15	15	15	15	14	15	15	15	15	14
Mean LAP (mmHg)	23	23	21	21	21	22	21	21	21	21	21	21	21	21
LAP Systolic (mmHg)	21	21	17	17	17	18	16	16	16	16	16	16	16	16
LAP Diastolic (mmHg)	23	23	21	21	21	22	21	21	21	21	21	21	21	21
Mean LVP (mmHg)	38	38	35	35	35	35	35	35	35	35	35	35	35	35
LVP Peak Systolic (mmHg)	110	110	111	112	112	109	113	113	113	113	113	113	113	113
LVP End Systolic (mmHg)	90	90	92	92	93	92	93	93	93	93	94	93	93	93
LVP End Diastolic (mmHg)	15	14	8	7	7	8	6	6	6	6	6	6	6	6
LVP +dP/dt (mmHg/sec)	3499	3499	3581	3580	3566	3539	3537	3546	3539	3563	3531	3556	3548	3524
LVP -dP/dt (mmHg/sec)	-3434	-3434	-3359	-3383	-3373	-3383	-3408	-3370	-3415	-3394	-3406	-3395	-3397	-3411
LVV End Systole (mL)	128	128	135	135	135	135	134	134	134	134	134	134	134	134
LVV End Diastole (mL)	166	166	158	158	158	159	157	157	157	157	157	157	157	157
LVV Stroke Volume (mL)	38	38	23	23	23	23	24	23	23	23	23	23	23	22
LV External Work (mmHg*mL)	4317	4318	2346	2399	2402	2614	2256	2260	2249	2270	2252	2251	2265	2267
Mean AoP (mmHg)	63	63	84	85	85	81	88	88	88	88	88	88	88	88
AoP Systolic (mmHg)	84	84	98	98	98	95	101	101	101	101	101	100	100	101
AoP Diastolic (mmHg)	46	46	69	69	70	66	73	73	73	73	73	72	73	73
DeltaP_AoP (mmHg)	38	38	30	29	29	29	28	28	28	28	27	28	28	27
Mean AoF (L/min)	3.0	3.0	0.5	0.6	0.6	0.9	0.4	0.4	0.3	0.4	0.3	0.4	0.4	0.3
Max AoF (L/min)	15.2	15.2	8.7	8.7	8.8	9.5	8.2	8.3	8.2	8.3	8.2	8.3	8.3	8.2
Min AoF (L/min)	-8.2	-8.2	-10.1	-10.1	-10.2	-10.4	-10.6	-10.4	-10.0	-9.7	-9.6	-10.4	-10.2	-10.3
Mean VAD P (mmHg)	66	66	99	99	99	93	105	104	105	104	105	104	104	105
VAD P Systolic (mmHg)	66	66	129	129	128	120	136	136	135	134	135	135	133	134
VAD P Diastolic (mmHg)	66	66	70	68	68	66	71	71	71	71	71	71	70	69
Mean VAD F (L/min)	0.0	0.0	4.2	4.3	4.3	3.9	4.7	4.7	4.7	4.7	4.7	4.6	4.6	4.7
Max VAD F (L/min)	0.0	0.0	7.1	7.0	6.9	6.2	7.4	7.5	7.5	7.3	7.3	7.5	7.4	7.3
Min VAD F (L/min)	0.0	0.0	1.0	1.2	1.3	1.1	1.2	1.2	1.2	1.3	1.3	1.1	1.2	1.3
Mean TotalFlow (L/min)	3.2	3.2	4.4	4.4	4.4	4.2	4.5	4.5	4.5	4.5	4.5	4.5	4.5	4.5
TotalFlow peak (+) (L/min)	4.4	4.4	5.0	5.0	5.0	4.8	5.1	5.1	5.1	5.1	5.1	5.1	5.1	5.1
TotalFlow peak (-) (L/min)	2.1	2.1	3.6	3.7	3.7	3.3	3.8	3.8	3.8	3.9	3.8	3.8	3.8	3.8
ZART (dynes-sec/cm^5)	65	65	85	85	86	81	89	89	89	89	89	88	89	89
SHE (ergs/cm^3)	2642	2646	1009	901	877	1049	806	846	819	792	780	819	823	801
EEP (mmHg)	1567	1567	1550	1549	1552	1552	1559	1559	1561	1560	1562	1561	1558	1563

35% systolic duration counter-pulsation:

	Recording																
Parameter	Baseline-Pre	Baseline-Post	Counter Pulse 1500 - 2500						Counter Pulse 1500 - 3000								
Heart Rate (BPM)	78	78	78	78	78	78	78	78	78	78	78	77	78	78	78	78	78
Cardiac Output (L/min)	2.9	2.9	2.0	2.0	1.9	2.0	2.0	1.9	1.9	1.9	1.9	1.9	1.9	1.9	1.9	1.9	2.0
Ejection Fraction (%)	23	23	16	16	15	16	16	16	16	15	15	16	15	15	15	15	16
Mean LAP (mmHg)	23	23	22	22	22	22	22	22	22	22	22	22	22	22	22	22	22
LAP Systolic (mmHg)	21	21	19	19	19	19	19	19	18	18	18	18	18	18	18	18	18
LAP Diastolic (mmHg)	23	23	23	23	22	23	23	23	23	23	23	23	23	23	23	23	23
Mean LVP (mmHg)	38	38	35	35	36	35	35	35	35	35	35	35	35	35	35	35	35
LVP Peak Systolic (mmHg)	110	110	102	102	109	102	102	103	101	102	102	103	101	102	102	104	101
LVP End Systolic (mmHg)	90	90	92	92	90	92	92	92	93	94	94	94	94	94	94	95	94
LVP End Diastolic (mmHg)	15	14	7	6	10	7	7	7	4	4	4	6	4	4	4	5	4
LVP +dP/dt (mmHg/sec)	3499	3499	3445	3411	3557	3431	3432	3456	3408	3423	3393	3435	3411	3427	3394	3437	3387
LVP -dP/dt (mmHg/sec)	-3434	-3434	-3350	-3357	-3363	-3359	-3374	-3348	-3370	-3396	-3369	-3421	-3375	-3419	-3373	-3407	-3369
LVV End Systole (mL)	128	128	134	134	135	134	134	134	134	134	134	134	134	135	134	134	134
LVV End Diastole (mL)	166	166	159	159	159	159	159	159	159	158	158	159	159	159	158	158	159
LVV Stroke Volume (mL)	38	38	25	25	24	25	25	25	25	24	24	25	24	24	24	24	25
LV External Work (mmHg*mL)	4317	4318	2542	2530	2865	2548	2544	2526	2276	2314	2307	2347	2284	2318	2312	2288	2289
Mean AoP (mmHg)	63	63	73	73	76	73	73	74	76	77	76	77	76	77	77	78	76
AoP Systolic (mmHg)	84	84	90	90	92	90	90	91	92	92	92	92	92	92	92	94	92
AoP Diastolic (mmHg)	46	46	61	61	59	61	61	62	66	66	66	67	66	66	67	67	66
DeltaP_AoP (mmHg)	38	38	29	29	33	29	29	29	26	26	26	25	26	26	26	27	25
Mean AoF (L/min)	3.0	3.0	1.1	1.1	1.3	1.1	1.1	1.0	0.8	0.8	0.8	0.8	0.8	0.8	0.8	0.7	0.8
Max AoF (L/min)	15.2	15.2	9.3	9.2	10.6	9.3	9.3	9.1	8.2	8.3	8.3	8.4	8.3	8.3	8.3	8.2	8.2
Min AoF (L/min)	-8.2	-8.2	-9.1	-8.9	-10.0	-8.9	-9.0	-8.9	-8.9	-9.8	-9.5	-9.0	-9.2	-9.1	-9.1	-9.3	-9.3
Mean VAD P (mmHg)	66	66	83	83	85	83	83	84	88	89	89	89	89	89	89	90	89
VAD P Systolic (mmHg)	66	66	103	102	113	102	103	104	104	104	104	106	104	106	105	106	104
VAD P Diastolic (mmHg)	66	66	72	72	60	72	72	72	80	80	80	78	81	79	80	78	81
Mean VAD F (L/min)	0.0	0.0	3.2	3.2	3.0	3.2	3.2	3.2	3.8	3.8	3.8	3.8	3.8	3.8	3.8	3.8	3.8
Max VAD F (L/min)	0.0	0.0	6.0	6.0	5.7	6.0	6.0	5.8	6.7	6.5	6.5	6.2	6.7	6.4	6.5	6.1	6.6
Min VAD F (L/min)	0.0	0.0	0.2	0.2	0.7	0.3	0.3	0.4	0.5	0.7	0.5	0.9	0.5	0.8	0.8	0.8	0.6
Mean TotalFlow (L/min)	3.2	3.2	3.8	3.8	3.9	3.8	3.8	3.9	4.0	4.0	4.0	4.0	4.0	4.0	4.0	4.1	4.0
TotalFlow peak (+) (L/min)	4.4	4.4	4.6	4.6	4.7	4.6	4.6	4.7	4.7	4.7	4.6	4.7	4.7	4.7	4.7	4.7	4.7
TotalFlow peak (-) (L/min)	2.1	2.1	3.1	3.0	3.1	3.1	3.1	3.1	3.3	3.3	3.3	3.4	3.3	3.4	3.4	3.5	3.3
ZART (dynes-sec/cm^5)	65	65	74	74	77	74	74	75	77	77	77	78	77	77	77	79	77
SHE (ergs/cm^3)	2646	2649	1135	1179	1524	1188	1188	1140	864	837	839	810	859	810	805	799	829
EEP (mmHg)	1567	1568	1542	1545	1539	1543	1538	1540	1540	1541	1546	1545	1544	1543	1544	1541	1545

35% systolic duration counter-pulsation:

	Recording																
Parameter	Baseline-Pre	Baseline-Post	Counter Pulse 1500 - 3500						Counter Pulse 1500 - 4000								
Heart Rate (BPM)	78	78	78	78	78	78	78	78	78	78	78	78	78	78	78	78	78
Cardiac Output (L/min)	2.9	2.9	1.8	2.0	1.8	1.8	2.0	1.9	1.9	2.0	1.9	1.9	1.9	2.0	2.0	2.0	2.0
Ejection Fraction (%)	23	23	15	16	15	15	16	16	16	16	16	16	16	16	16	16	16
Mean LAP (mmHg)	23	23	22	22	21	21	22	22	22	22	22	22	21	22	22	22	22
LAP Systolic (mmHg)	21	21	18	18	17	17	18	18	17	18	18	18	16	18	18	18	18
LAP Diastolic (mmHg)	23	23	23	22	21	23	23	23	23	23	23	23	23	23	23	23	23
Mean LVP (mmHg)	38	38	35	34	35	35	35	35	35	34	34	35	35	34	35	35	34
LVP Peak Systolic (mmHg)	110	110	101	100	112	102	100	100	100	99	99	99	101	98	99	99	98
LVP End Systolic (mmHg)	90	90	95	93	92	96	95	95	96	95	95	95	97	95	95	95	95
LVP End Diastolic (mmHg)	15	14	3	3	8	3	4	4	2	2	2	2	2	3	2	2	2
LVP +dP/dt (mmHg/sec)	3499	3499	3342	3396	3564	3398	3401	3376	3351	3358	3371	3364	3343	3361	3326	3380	3329
LVP -dP/dt (mmHg/sec)	-3434	-3434	-3396	-3376	-3385	-3418	-3390	-3409	-3415	-3403	-3398	-3393	-3421	-3400	-3384	-3410	-3381
LVV End Systole (mL)	128	128	134	134	135	134	133	134	133	133	133	134	133	133	133	133	133
LVV End Diastole (mL)	166	166	158	159	159	158	159	159	158	159	158	159	158	159	159	159	159
LVV Stroke Volume (mL)	38	38	24	25	24	24	26	25	25	25	25	25	25	25	26	26	26
LV External Work (mmHg*mL)	4317	4318	2114	2294	2530	1953	2020	2043	1961	1973	1962	1932	1737	1909	1991	1939	1951
Mean AoP (mmHg)	63	63	79	77	83	80	77	77	79	78	78	78	80	77	77	78	77
AoP Systolic (mmHg)	84	84	94	91	97	95	93	93	94	94	93	93	96	93	93	93	93
AoP Diastolic (mmHg)	46	46	70	69	67	70	69	69	71	71	70	70	71	70	70	70	70
DeltaP_AoP (mmHg)	38	38	24	22	30	24	24	24	23	23	23	23	24	23	23	23	23
Mean AoF (L/min)	3.0	3.0	0.5	0.8	0.7	0.4	0.5	0.5	0.4	0.4	0.4	0.4	0.2	0.4	0.5	0.4	0.4
Max AoF (L/min)	15.2	15.2	7.6	8.2	9.2	7.2	7.4	7.4	7.1	7.2	7.2	7.1	6.4	7.0	7.2	7.1	7.1
Min AoF (L/min)	-8.2	-8.2	-9.2	-9.5	-10.1	-9.6	-9.4	-9.1	-9.1	-9.2	-9.0	-9.4	-9.5	-9.1	-9.0	-9.2	-9.3
Mean VAD P (mmHg)	66	66	93	91	97	94	92	92	94	94	94	94	96	93	93	93	93
VAD P Systolic (mmHg)	66	66	106	103	126	107	105	105	106	107	106	106	108	105	104	106	105
VAD P Diastolic (mmHg)	66	66	87	85	67	87	87	88	93	92	93	94	94	93	93	95	94
Mean VAD F (L/min)	0.0	0.0	4.2	4.2	4.0	4.2	4.2	4.2	4.4	4.3	4.3	4.3	4.3	4.3	4.2	4.3	4.3
Max VAD F (L/min)	0.0	0.0	7.0	6.9	6.9	7.0	7.6	7.4	7.5	7.7	7.7	7.8	7.8	8.1	7.8	7.9	7.9
Min VAD F (L/min)	0.0	0.0	0.8	0.8	0.8	0.6	0.3	0.4	0.3	0.3	0.2	0.1	0.1	0.0	0.1	0.1	0.0
Mean TotalFlow (L/min)	3.2	3.2	4.1	4.0	4.3	4.1	4.0	4.0	4.1	4.0	4.1	4.0	4.2	4.0	4.0	4.0	4.0
TotalFlow peak (+) (L/min)	4.4	4.4	4.8	4.6	4.9	4.8	4.7	4.7	4.8	4.7	4.8	4.7	4.8	4.7	4.7	4.8	4.7
TotalFlow peak (-) (L/min)	2.1	2.1	3.5	3.2	3.5	3.6	3.4	3.4	3.6	3.5	3.5	3.6	3.6	3.5	3.5	3.5	3.4
ZART (dynes-sec/cm^5)	65	65	79	77	84	80	78	78	79	79	79	79	80	78	78	78	78
SHE (ergs/cm^3)	2646	2649	640	638	1086	703	735	751	587	647	641	692	714	730	656	697	713
EEP (mmHg)	1567	1568	1544	1550	1559	1544	1540	1539	1540	1551	1541	1546	1539	1546	1544	1544	1546

35% systolic duration co-pulsation:

	Recording																	
Parameter	Baseline-Pre	Baseline-Post	CO - Pulse 1500 - 2500									CO - Pulse 1500 - 3000						
Heart Rate (BPM)	78	78	78	78	78	78	78	78	78	78	78	78	78	78	78	78	78	78
Cardiac Output (L/min)	2.9	2.9	1.9	1.9	1.9	1.9	1.9	1.8	1.8	1.9	1.9	1.8	1.8	1.8	1.9	1.8	1.8	1.8
Ejection Fraction (%)	23	23	15	15	15	15	15	15	15	15	15	15	15	15	15	15	15	15
Mean LAP (mmHg)	23	23	22	22	22	22	22	22	22	22	22	22	22	22	22	22	22	22
LAP Systolic (mmHg)	21	21	19	19	19	19	19	19	19	19	19	18	18	18	18	18	18	18
LAP Diastolic (mmHg)	23	23	22	22	22	22	22	22	22	22	22	22	22	22	22	22	22	22
Mean LVP (mmHg)	38	38	36	36	36	36	36	36	36	36	36	35	35	35	35	36	36	35
LVP Peak Systolic (mmHg)	110	110	108	109	109	109	109	109	109	109	109	110	110	110	110	111	110	110
LVP End Systolic (mmHg)	90	90	90	90	90	90	90	90	90	90	90	91	91	90	91	91	91	91
LVP End Diastolic (mmHg)	15	14	10	10	10	10	10	10	10	10	10	9	9	10	9	9	9	9
LVP +dP/dt (mmHg/sec)	3499	3499	3558	3537	3555	3557	3566	3544	3539	3556	3542	3546	3568	3533	3571	3543	3571	3518
LVP -dP/dt (mmHg/sec)	-3434	-3434	-3341	-3351	-3349	-3363	-3337	-3360	-3343	-3350	-3344	-3360	-3364	-3346	-3365	-3346	-3345	-3349
LVV End Systole (mL)	128	128	135	135	135	135	135	135	135	135	135	135	135	135	135	136	135	135
LVV End Diastole (mL)	166	166	159	159	159	159	159	159	159	159	159	159	159	159	159	159	158	159
LVV Stroke Volume (mL)	38	38	25	24	24	24	24	24	24	24	24	23	24	24	24	23	23	24
LV External Work (mmHg*mL)	4317	4318	2840	2850	2857	2865	2884	2872	2861	2855	2860	2689	2698	2647	2668	2675	2699	2669
Mean AoP (mmHg)	63	63	76	76	76	76	76	76	76	76	76	80	80	80	80	80	80	80
AoP Systolic (mmHg)	84	84	92	92	92	92	93	93	93	92	92	95	95	95	95	96	95	96
AoP Diastolic (mmHg)	46	46	59	59	59	59	60	60	60	59	60	64	64	64	63	64	64	64
DeltaP_AoP (mmHg)	38	38	33	33	33	33	33	33	33	33	33	31	31	31	32	32	31	32
Mean AoF (L/min)	3.0	3.0	1.3	1.3	1.3	1.3	1.3	1.3	1.3	1.3	1.3	1.0	1.0	1.0	1.0	1.0	1.0	1.0
Max AoF (L/min)	15.2	15.2	10.5	10.5	10.5	10.6	10.6	10.5	10.5	10.5	10.5	9.8	9.8	9.7	9.8	9.7	9.7	9.8
Min AoF (L/min)	-8.2	-8.2	-9.3	-9.5	-9.5	-10.0	-10.0	-9.4	-9.3	-9.4	-9.6	-9.3	-9.7	-9.6	-9.4	-9.3	-9.8	-9.9
Mean VAD P (mmHg)	66	66	85	85	85	85	85	85	85	85	85	92	91	91	91	92	92	92
VAD P Systolic (mmHg)	66	66	114	114	114	113	114	113	113	113	113	121	120	121	121	121	121	123
VAD P Diastolic (mmHg)	66	66	61	61	61	60	59	60	60	60	60	64	64	65	65	64	63	64
Mean VAD F (L/min)	0.0	0.0	3.0	3.0	3.0	3.0	3.0	3.0	3.0	3.0	3.0	3.6	3.5	3.5	3.5	3.6	3.6	3.6
Max VAD F (L/min)	0.0	0.0	5.7	5.7	5.7	5.7	5.5	5.6	5.6	5.7	5.7	6.2	6.3	6.5	6.4	6.3	6.2	6.4
Min VAD F (L/min)	0.0	0.0	0.7	0.7	0.7	0.7	0.9	0.8	0.9	0.7	0.8	1.0	0.8	0.7	0.7	1.0	1.0	0.8
Mean TotalFlow (L/min)	3.2	3.2	3.9	3.9	3.9	3.9	3.9	3.9	4.0	3.9	3.9	4.2	4.1	4.1	4.1	4.1	4.1	4.1
TotalFlow peak (+) (L/min)	4.4	4.4	4.7	4.7	4.7	4.7	4.7	4.7	4.7	4.7	4.7	4.8	4.8	4.8	4.8	4.8	4.8	4.9
TotalFlow peak (-) (L/min)	2.1	2.1	3.0	3.0	3.1	3.1	3.0	3.1	3.1	3.0	3.1	3.3	3.3	3.3	3.3	3.3	3.4	3.3
ZART (dynes-sec/cm^5)	65	65	77	77	77	77	77	77	77	77	77	81	81	80	81	81	81	81
SHE (ergs/cm^3)	2646	2649	1522	1522	1468	1520	1452	1434	1446	1468	1468	1182	1254	1296	1314	1155	1194	1297
EEP (mmHg)	1567	1568	1545	1545	1539	1539	1545	1549	1541	1541	1541	1546	1545	1547	1549	1551	1547	1548

35% systolic duration co-pulsation:

	Recording																	
Parameter	Baseline-Pre	Baseline-Post	CO - Pulse 1500 - 3500							CO - Pulse 1500 - 4000								
Heart Rate (BPM)	78	78	78	78	78	78	78	78	78	78	78	77	78	78	78	78	78	78
Cardiac Output (L/min)	2.9	2.9	1.8	1.8	1.8	1.8	1.9	1.8	1.8	1.8	1.9	1.8	1.8	1.8	1.9	1.8	1.9	1.9
Ejection Fraction (%)	23	23	15	15	15	15	15	15	15	15	15	15	15	15	15	15	15	15
Mean LAP (mmHg)	23	23	21	21	21	21	21	21	21	21	21	21	21	21	21	21	21	21
LAP Systolic (mmHg)	21	21	17	17	17	17	18	17	17	16	16	16	17	16	17	16	16	16
LAP Diastolic (mmHg)	23	23	21	21	21	21	21	21	21	21	21	21	21	21	21	21	21	21
Mean LVP (mmHg)	38	38	35	35	35	35	35	35	35	35	35	35	35	35	35	35	35	35
LVP Peak Systolic (mmHg)	110	110	111	111	112	112	111	112	112	113	113	113	113	113	113	113	113	113
LVP End Systolic (mmHg)	90	90	91	91	92	92	91	92	92	92	92	92	92	92	92	92	92	92
LVP End Diastolic (mmHg)	15	14	9	8	8	8	9	8	8	7	8	8	8	7	8	7	8	7
LVP +dP/dt (mmHg/sec)	3499	3499	3600	3535	3564	3549	3609	3559	3566	3559	3588	3580	3587	3577	3562	3573	3554	3570
LVP -dP/dt (mmHg/sec)	-3434	-3434	-3381	-3353	-3385	-3376	-3351	-3372	-3369	-3375	-3352	-3396	-3364	-3377	-3359	-3407	-3375	-3382
LVV End Systole (mL)	128	128	135	135	135	135	134	135	135	134	134	134	135	134	134	134	134	134
LVV End Diastole (mL)	166	166	158	159	159	159	159	158	158	158	158	158	158	157	158	157	158	158
LVV Stroke Volume (mL)	38	38	24	24	24	24	24	24	23	24	24	24	24	23	24	23	24	24
LV External Work (mmHg*mL)	4317	4318	2509	2531	2530	2537	2480	2534	2553	2425	2437	2434	2416	2411	2366	2457	2439	2442
Mean AoP (mmHg)	63	63	83	83	83	84	83	83	84	86	86	87	86	86	86	87	86	87
AoP Systolic (mmHg)	84	84	97	97	97	97	97	98	98	100	100	100	100	100	99	99	100	100
AoP Diastolic (mmHg)	46	46	67	67	67	68	67	67	68	70	71	71	70	70	70	71	71	71
DeltaP_AoP (mmHg)	38	38	30	30	30	30	31	30	30	30	29	29	30	30	29	28	29	29
Mean AoF (L/min)	3.0	3.0	0.7	0.7	0.7	0.8	0.7	0.7	0.7	0.6	0.6	0.5	0.6	0.5	0.5	0.6	0.5	0.6
Max AoF (L/min)	15.2	15.2	9.3	9.2	9.2	9.2	9.2	9.3	9.2	8.9	8.9	8.8	8.9	8.8	8.7	8.9	8.9	8.8
Min AoF (L/min)	-8.2	-8.2	-10.2	-10.0	-10.1	-9.3	-10.1	-9.7	-9.9	-9.8	-10.3	-10.5	-9.8	-9.9	-9.8	-9.7	-10.7	-10.3
Mean VAD P (mmHg)	66	66	97	97	97	97	97	97	97	102	102	102	101	102	102	102	102	102
VAD P Systolic (mmHg)	66	66	128	128	126	127	127	130	128	135	134	135	134	134	134	134	132	134
VAD P Diastolic (mmHg)	66	66	68	67	67	67	69	67	67	69	69	69	69	69	70	68	69	69
Mean VAD F (L/min)	0.0	0.0	4.0	4.0	4.0	4.0	3.9	4.0	4.0	4.3	4.3	4.4	4.3	4.3	4.3	4.4	4.4	4.4
Max VAD F (L/min)	0.0	0.0	7.0	7.0	6.9	6.9	7.1	7.0	6.8	7.4	7.3	7.3	7.5	7.5	7.6	7.2	7.3	7.2
Min VAD F (L/min)	0.0	0.0	0.7	0.7	0.8	0.8	0.6	0.8	0.9	0.6	0.7	0.8	0.6	0.6	0.6	0.7	0.8	0.8
Mean TotalFlow (L/min)	3.2	3.2	4.3	4.3	4.3	4.3	4.3	4.3	4.3	4.4	4.4	4.4	4.4	4.4	4.4	4.4	4.4	4.5
TotalFlow peak (+) (L/min)	4.4	4.4	4.9	4.9	4.9	4.9	4.9	4.9	4.9	5.0	5.0	5.0	5.1	5.0	5.0	5.0	5.0	5.0
TotalFlow peak (-) (L/min)	2.1	2.1	3.5	3.5	3.5	3.5	3.5	3.5	3.5	3.7	3.7	3.7	3.6	3.7	3.7	3.7	3.7	3.7
ZART (dynes-sec/cm^5)	65	65	84	84	84	84	84	84	84	87	87	87	87	87	87	87	87	87
SHE (ergs/cm^3)	2646	2649	1121	1076	1086	1079	1178	1056	1051	974	957	903	1046	989	973	906	928	911
EEP (mmHg)	1567	1568	1552	1550	1559	1558	1552	1551	1555	1561	1560	1560	1559	1559	1560	1557	1562	1555

40% systolic duration counter-pulsation:

	Recording															
Parameter	Baseline-Pre	Baseline-Post	Counter Pulse - 1500 - 2500							Counter Pulse - 1500 - 3000						
Heart Rate (BPM)	78	78	78	78	78	78	78	78	78	78	78	78	78	78	78	78
Cardiac Output (L/min)	2.9	2.9	3.8	3.8	3.8	3.8	3.8	3.8	3.8	3.9	3.9	3.9	3.8	4.0	4.0	4.0
Ejection Fraction (%)	23	23	16	16	16	16	16	15	15	15	15	15	16	16	15	15
Mean LAP (mmHg)	23	23	22	22	22	22	23	22	22	22	22	22	22	21	21	22
LAP Systolic (mmHg)	21	21	19	19	18	19	19	19	19	18	18	18	18	18	17	18
LAP Diastolic (mmHg)	23	23	23	23	23	22	23	23	22	22	22	22	22	23	22	22
Mean LVP (mmHg)	38	38	35	35	35	35	35	35	35	35	35	35	34	35	36	35
LVP Peak Systolic (mmHg)	110	110	102	102	102	102	102	102	102	102	102	102	101	103	103	103
LVP End Systolic (mmHg)	90	90	91	92	92	91	92	92	92	93	94	93	91	94	94	94
LVP End Diastolic (mmHg)	15	15	7	7	7	7	7	7	7	5	5	5	5	5	5	5
LVP +dP/dt (mmHg/sec)	3500	3506	3461	3398	3458	3460	3429	3454	3435	3406	3419	3415	3426	3410	3440	3439
LVP -dP/dt (mmHg/sec)	-3434	-3441	-3354	-3357	-3368	-3355	-3363	-3354	-3360	-3372	-3401	-3384	-3349	-3394	-3389	-3403
LVV End Systole (mL)	128	128	135	134	134	134	134	135	134	134	135	135	134	134	134	134
LVV End Diastole (mL)	166	166	159	159	159	159	159	159	159	158	158	158	159	159	158	158
LVV Stroke Volume (mL)	38	38	25	25	25	25	25	24	24	24	24	24	25	25	24	24
LV External Work (mmHg*mL)	4320	4316	2618	2605	2639	2627	2653	2644	2627	2402	2418	2409	2604	2282	2321	2433
Mean AoP (mmHg)	63	63	73	73	73	73	73	73	73	76	76	76	74	77	77	76
AoP Systolic (mmHg)	84	84	90	90	91	90	90	91	90	92	92	92	90	93	93	92
AoP Diastolic (mmHg)	46	46	61	61	61	61	61	61	61	65	65	65	64	65	66	65
DeltaP_AoP (mmHg)	38	38	30	30	30	30	30	30	29	27	27	27	25	27	27	27
Mean AoF (L/min)	3.0	3.0	1.2	1.2	1.2	1.2	1.2	1.2	1.2	0.9	0.9	0.9	1.1	0.8	0.8	0.9
Max AoF (L/min)	15.2	15.2	9.6	9.5	9.6	9.5	9.6	9.6	9.5	8.6	8.6	8.6	9.3	8.2	8.3	8.7
Min AoF (L/min)	-8.3	-8.5	-9.2	-9.0	-9.1	-9.0	-9.2	-9.5	-9.1	-9.2	-9.1	-9.0	-9.3	-9.1	-9.5	-9.3
Mean VAD P (mmHg)	63	83	82	82	83	82	83	83	83	87	88	87	86	88	89	88
VAD P Systolic (mmHg)	63	83	102	101	102	102	102	102	101	103	105	104	102	105	106	105
VAD P Diastolic (mmHg)	63	83	69	70	68	69	67	68	69	76	75	75	74	78	76	74
Mean VAD F (L/min)	0.0	0.0	3.0	3.0	3.1	3.1	3.1	3.1	3.0	3.6	3.7	3.6	3.6	3.6	3.6	3.7
Max VAD F (L/min)	0.0	0.0	5.7	5.8	5.6	5.6	5.5	5.5	5.6	6.1	6.0	6.1	5.9	6.2	6.0	5.9
Min VAD F (L/min)	0.0	0.0	0.2	0.1	0.3	0.2	0.4	0.3	0.3	0.4	0.6	0.5	0.5	0.3	0.4	0.7
Mean TotalFlow (L/min)	3.2	3.2	3.8	3.8	3.8	3.8	3.8	3.8	3.8	3.9	3.9	3.9	3.8	4.0	4.0	4.0
TotalFlow peak (+) (L/min)	4.4	4.4	4.6	4.6	4.6	4.6	4.6	4.6	4.6	4.7	4.7	4.6	4.6	4.7	4.7	4.7
TotalFlow peak (-) (L/min)	2.1	2.1	3.0	3.0	3.1	3.0	3.1	3.1	3.1	3.3	3.3	3.3	3.0	3.3	3.4	3.3
ZART (dynes-sec/cm^5)	65	65	74	74	74	74	74	74	74	76	77	77	75	77	78	77
SHE (ergs/cm^3)	2649	2651	1186	1190	1146	1177	1169	1184	1162	927	824	892	894	905	886	850
EEP (mmHg)	1568	1566	1543	1536	1543	1544	1541	1540	1542	1546	1545	1543	1550	1536	1541	1540

40% systolic duration counter-pulsation:

	Recording																			
Parameter	Baseline-Pre	Baseline-Post	Counter Pulse 1500 - 3500									Counter Pulse 1500 - 4000								
Heart Rate (BPM)	78	78	78	78	78	78	78	78	78	78	78	78	78	78	78	78	78	78	78	78
Cardiac Output (L/min)	2.9	2.9	4.0	4.0	4.0	4.0	4.0	4.0	4.1	4.0	4.0	4.0	4.2	4.0	4.2	4.0	4.0	4.0	3.9	4.0
Ejection Fraction (%)	23	23	15	15	15	16	15	15	15	15	15	16	16	16	15	16	16	16	16	16
Mean LAP (mmHg)	23	23	22	22	22	22	21	22	21	22	22	22	21	22	21	22	22	21	22	21
LAP Systolic (mmHg)	21	21	18	18	18	18	17	18	16	18	18	18	15	18	15	18	18	17	18	18
LAP Diastolic (mmHg)	23	23	22	22	22	22	22	22	22	22	22	22	22	22	22	22	22	22	22	22
Mean LVP (mmHg)	38	38	35	35	35	35	35	35	36	35	35	35	36	35	36	35	35	35	35	35
LVP Peak Systolic (mmHg)	110	110	102	101	101	101	101	101	104	101	101	100	104	101	105	99	99	101	99	100
LVP End Systolic (mmHg)	90	90	95	95	95	94	94	95	96	94	94	95	98	95	98	94	94	95	94	95
LVP End Diastolic (mmHg)	15	15	3	4	4	4	3	3	4	4	4	3	3	3	3	3	3	3	3	3
LVP +dP/dt (mmHg/sec)	3500	3506	3403	3356	3411	3349	3412	3380	3406	3374	3392	3377	3348	3384	3371	3360	3350	3393	3329	3379
LVP -dP/dt (mmHg/sec)	-3434	-3441	-3416	-3400	-3392	-3379	-3390	-3398	-3407	-3395	-3397	-3405	-3421	-3421	-3429	-3388	-3374	-3404	-3369	-3396
LVV End Systole (mL)	128	128	134	134	134	134	134	134	133	134	134	133	133	134	133	133	133	133	133	133
LVV End Diastole (mL)	166	166	158	158	158	158	157	158	157	158	158	158	158	158	157	159	158	158	159	158
LVV Stroke Volume (mL)	38	38	24	24	24	25	24	24	24	24	24	25	25	25	24	25	25	25	26	25
LV External Work (mmHg*mL)	4320	4316	2240	2222	2199	2210	2272	2245	2082	2214	2207	2126	1876	2165	1927	2122	2143	2199	2113	2153
Mean AoP (mmHg)	63	63	78	78	77	77	77	78	80	77	77	77	80	77	80	76	77	78	76	77
AoP Systolic (mmHg)	84	84	93	93	93	93	93	93	95	93	93	93	96	93	97	93	93	93	92	93
AoP Diastolic (mmHg)	46	46	68	68	68	68	68	68	69	68	68	68	70	68	69	68	68	69	67	68
DeltaP_AoP (mmHg)	38	38	25	25	25	25	25	25	27	25	25	25	27	25	27	25	25	25	25	25
Mean AoF (L/min)	3.0	3.0	0.7	0.7	0.7	0.7	0.7	0.7	0.5	0.7	0.7	0.6	0.3	0.6	0.3	0.6	0.6	0.7	0.6	0.6
Max AoF (L/min)	15.2	15.2	8.0	8.0	7.9	7.9	8.1	8.0	7.5	7.9	7.9	7.7	6.8	7.8	7.0	7.7	7.7	7.8	7.7	7.7
Min AoF (L/min)	-8.3	-8.5	-9.1	-9.0	-9.1	-9.0	-9.2	-9.3	-9.6	-9.4	-9.1	-8.8	-9.4	-9.1	-9.0	-9.2	-9.0	-9.0	-9.4	-9.0
Mean VAD P (mmHg)	63	83	91	91	91	90	90	91	93	90	90	91	94	91	94	90	91	92	90	91
VAD P Systolic (mmHg)	63	83	105	105	104	104	104	106	108	105	104	105	108	106	109	103	105	106	103	106
VAD P Diastolic (mmHg)	63	83	81	81	82	83	78	81	80	83	83	84	87	83	81	86	86	80	89	84
Mean VAD F (L/min)	0.0	0.0	4.0	4.0	4.0	4.0	4.0	4.0	3.9	3.9	4.0	4.0	4.0	4.0	4.0	4.0	4.0	4.1	4.0	4.0
Max VAD F (L/min)	0.0	0.0	6.5	6.6	6.7	6.8	6.5	6.6	6.2	6.7	6.8	7.1	6.7	6.8	6.4	7.3	7.2	6.8	7.4	7.0
Min VAD F (L/min)	0.0	0.0	0.5	0.4	0.4	0.2	0.6	0.4	0.4	0.3	0.2	-0.1	0.0	0.1	0.1	-0.1	0.0	0.3	-0.2	0.1
Mean TotalFlow (L/min)	3.2	3.2	4.0	4.0	4.0	4.0	4.0	4.0	4.1	4.0	4.0	4.0	4.2	4.0	4.2	4.0	4.0	4.0	3.9	4.0
TotalFlow peak (+) (L/min)	4.4	4.4	4.7	4.7	4.7	4.7	4.7	4.7	4.8	4.7	4.7	4.7	4.8	4.7	4.8	4.7	4.7	4.7	4.7	4.7
TotalFlow peak (-) (L/min)	2.1	2.1	3.5	3.4	3.5	3.4	3.5	3.4	3.6	3.5	3.4	3.5	3.7	3.5	3.7	3.4	3.5	3.5	3.4	3.5
ZART (dynes-sec/cm^5)	65	65	78	78	78	78	78	78	80	78	77	77	81	78	81	77	77	78	76	78
SHE (ergs/cm^3)	2649	2651	705	697	700	757	694	709	714	716	728	715	745	730	725	718	721	643	751	696
EEP (mmHg)	1568	1566	1543	1544	1547	1546	1542	1544	1538	1543	1543	1546	1542	1541	1541	1541	1541	1544	1540	1550

40% systolic duration co-pulsation:

	Recording																			
Parameter	Baseline-Pre	Baseline-Post	CO-Pulse 1500 - 2500									CO-Pulse 1500 - 3000								
Heart Rate (BPM)	78	78	78	78	78	78	78	78	78	78	78	78	78	78	78	78	78	78	78	78
Cardiac Output (L/min)	2.9	2.9	3.9	3.9	3.9	3.9	3.9	3.9	3.9	3.9	3.9	4.1	4.1	4.1	4.1	4.1	3.9	4.1	4.1	4.0
Ejection Fraction (%)	23	23	15	15	15	15	15	15	15	15	15	15	15	15	15	15	16	15	15	15
Mean LAP (mmHg)	23	23	22	22	22	22	22	22	22	22	22	21	21	21	21	21	22	21	21	22
LAP Systolic (mmHg)	21	21	19	19	19	19	19	19	19	19	19	18	18	18	18	18	19	18	18	18
LAP Diastolic (mmHg)	23	23	22	22	22	22	22	22	22	22	22	21	21	21	21	21	21	21	21	22
Mean LVP (mmHg)	38	38	36	36	36	36	36	36	36	36	36	35	35	36	36	36	34	35	36	35
LVP Peak Systolic (mmHg)	110	110	109	109	109	109	109	109	109	109	109	110	110	110	110	111	107	110	110	104
LVP End Systolic (mmHg)	90	90	89	89	90	89	89	89	89	89	89	90	90	90	90	90	88	90	90	94
LVP End Diastolic (mmHg)	15	15	11	11	11	11	11	10	11	11	11	9	10	9	9	9	9	10	10	5
LVP +dP/dt (mmHg/sec)	3500	3506	3529	3560	3551	3544	3541	3557	3540	3539	3560	3559	3583	3548	3566	3539	3547	3536	3602	3446
LVP -dP/dt (mmHg/sec)	-3434	-3441	-3329	-3334	-3350	-3317	-3340	-3343	-3342	-3321	-3332	-3333	-3361	-3342	-3347	-3335	-3319	-3334	-3352	-3407
LVV End Systole (mL)	128	128	136	136	135	135	135	135	135	135	135	135	136	136	135	136	135	136	135	134
LVV End Diastole (mL)	166	166	159	159	159	159	160	159	160	160	159	159	160	159	159	159	160	159	159	158
LVV Stroke Volume (mL)	38	38	24	24	24	24	24	24	24	25	24	24	24	24	24	23	25	24	24	24
LV External Work (mmHg*mL)	4320	4316	2916	2916	2925	2914	2913	2927	2917	2921	2923	2767	2765	2765	2783	2782	2845	2773	2769	2488
Mean AoP (mmHg)	63	63	75	75	75	75	75	75	75	75	75	79	79	79	79	79	76	79	79	77
AoP Systolic (mmHg)	84	84	92	92	92	92	92	92	92	92	93	94	94	95	95	95	92	94	95	93
AoP Diastolic (mmHg)	46	46	58	58	58	58	58	59	58	59	59	62	62	62	62	63	61	62	63	65
DeltaP_AoP (mmHg)	38	38	34	34	34	34	34	34	34	34	34	32	32	32	32	32	31	32	32	27
Mean AoF (L/min)	3.0	3.0	1.4	1.4	1.4	1.3	1.4	1.4	1.4	1.4	1.4	1.1	1.1	1.1	1.1	1.1	1.2	1.1	1.1	0.9
Max AoF (L/min)	15.2	15.2	10.7	10.8	10.7	10.7	10.8	10.7	10.8	10.8	10.7	10.2	10.1	10.2	10.2	10.2	10.6	10.2	10.1	8.8
Min AoF (L/min)	-8.3	-8.5	-9.5	-9.5	-9.4	-10.3	-9.4	-9.6	-9.5	-9.3	-9.3	-9.5	-9.4	-9.6	-10.2	-10.0	-10.1	-9.5	-9.6	-9.0
Mean VAD P (mmHg)	63	83	84	84	84	84	84	84	84	84	84	90	90	90	90	90	87	90	90	89
VAD P Systolic (mmHg)	63	83	113	114	114	113	113	113	113	114	114	121	121	121	119	120	119	121	122	107
VAD P Diastolic (mmHg)	63	83	60	60	60	59	60	59	59	59	60	62	63	62	62	62	62	62	63	70
Mean VAD F (L/min)	0.0	0.0	2.8	2.8	2.8	2.8	2.8	2.9	2.8	2.8	2.8	3.4	3.3	3.4	3.4	3.4	3.4	3.3	3.3	3.7
Max VAD F (L/min)	0.0	0.0	5.7	5.7	5.6	5.7	5.8	5.6	5.7	5.6	5.7	6.3	6.3	6.4	6.2	6.2	6.5	6.3	6.3	5.6
Min VAD F (L/min)	0.0	0.0	0.4	0.5	0.5	0.4	0.4	0.6	0.5	0.5	0.5	0.5	0.5	0.6	0.6	0.7	0.5	0.5	0.5	1.0
Mean TotalFlow (L/min)	3.2	3.2	3.9	3.9	3.9	3.9	3.9	3.9	3.9	3.9	3.9	4.1	4.1	4.1	4.1	4.1	3.9	4.1	4.1	4.0
TotalFlow peak (+) (L/min)	4.4	4.4	4.7	4.7	4.7	4.7	4.7	4.7	4.7	4.7	4.7	4.8	4.8	4.8	4.8	4.8	4.7	4.8	4.8	4.7
TotalFlow peak (-) (L/min)	2.1	2.1	3.0	3.0	3.0	3.0	3.0	3.0	3.0	3.0	3.0	3.2	3.2	3.2	3.2	3.2	2.9	3.2	3.2	3.4
ZART (dynes-sec/cm^5)	65	65	76	76	76	76	76	76	76	76	77	80	80	80	80	80	78	80	80	78
SHE (ergs/cm^3)	2649	2651	1595	1618	1588	1586	1601	1482	1584	1576	1552	1349	1367	1310	1337	1333	1489	1363	1335	811
EEP (mmHg)	1568	1566	1541	1539	1546	1540	1545	1542	1545	1543	1543	1546	1547	1545	1551	1544	1550	1551	1551	1541

40% systolic duration co-pulsation:

	Recording															
Parameter	Baseline-Pre	Baseline-Post	CO-Pulse 1500 - 3500							CO-Pulse 1500 - 4000						
Heart Rate (BPM)	78	78	78	78	78	78	78	78	77	78	78	78	77	77	78	78
Cardiac Output (L/min)	2.9	2.9	4.3	4.2	4.2	4.2	4.2	4.2	4.2	4.4	4.4	4.4	4.4	4.3	4.4	4.4
Ejection Fraction (%)	23	23	15	15	15	15	15	15	15	15	15	15	16	15	15	15
Mean LAP (mmHg)	23	23	21	21	21	21	21	21	21	21	21	21	21	21	21	21
LAP Systolic (mmHg)	21	21	17	17	17	17	17	17	18	17	16	17	17	17	17	17
LAP Diastolic (mmHg)	23	23	21	21	21	21	21	21	21	20	20	20	20	20	20	20
Mean LVP (mmHg)	38	38	35	35	35	35	35	35	35	35	35	35	35	35	35	35
LVP Peak Systolic (mmHg)	110	110	112	111	112	111	111	111	112	113	113	113	113	113	113	113
LVP End Systolic (mmHg)	90	90	91	90	91	90	90	91	90	91	92	91	91	91	91	91
LVP End Diastolic (mmHg)	15	15	9	8	9	9	9	9	10	8	8	8	9	9	8	9
LVP +dP/dt (mmHg/sec)	3500	3506	3583	3535	3589	3550	3595	3566	3579	3588	3584	3577	3581	3579	3584	3630
LVP -dP/dt (mmHg/sec)	-3434	-3441	-3354	-3356	-3341	-3339	-3341	-3361	-3331	-3353	-3366	-3360	-3371	-3364	-3379	-3340
LVV End Systole (mL)	128	128	135	134	135	135	135	135	135	134	135	135	134	134	134	134
LVV End Diastole (mL)	166	166	159	158	158	159	158	159	159	158	158	159	159	158	158	159
LVV Stroke Volume (mL)	38	38	24	24	23	24	24	24	24	24	23	24	25	24	24	24
LV External Work (mmHg*mL)	4320	4316	2634	2661	2639	2632	2636	2630	2610	2576	2548	2558	2514	2564	2567	2535
Mean AoP (mmHg)	63	63	82	81	82	82	82	82	82	85	85	85	85	85	85	85
AoP Systolic (mmHg)	84	84	97	96	97	97	97	97	96	99	99	99	99	99	99	99
AoP Diastolic (mmHg)	46	46	65	65	66	65	65	65	65	68	69	68	67	69	68	67
DeltaP_AoP (mmHg)	38	38	32	31	31	31	32	31	32	30	31	31	31	30	30	32
Mean AoF (L/min)	3.0	3.0	0.9	0.9	0.9	0.9	0.9	0.8	0.9	0.7	0.7	0.7	0.7	0.7	0.7	0.7
Max AoF (L/min)	15.2	15.2	9.6	9.7	9.7	9.7	9.7	9.6	9.6	9.3	9.2	9.4	9.2	9.3	9.3	9.3
Min AoF (L/min)	-8.3	-8.5	-10.2	-9.8	-9.7	-9.8	-10.1	-10.1	-9.8	-10.0	-9.7	-10.3	-9.9	-9.9	-10.6	-9.9
Mean VAD P (mmHg)	63	83	95	94	95	95	95	95	95	99	100	99	99	99	99	99
VAD P Systolic (mmHg)	63	83	128	126	126	128	127	128	128	133	132	134	134	133	132	134
VAD P Diastolic (mmHg)	63	83	65	64	65	65	64	65	66	67	67	67	68	67	67	67
Mean VAD F (L/min)	0.0	0.0	3.8	3.8	3.8	3.7	3.7	3.8	3.7	4.1	4.1	4.0	4.0	4.1	4.1	4.0
Max VAD F (L/min)	0.0	0.0	6.9	6.8	6.9	6.9	6.9	6.9	7.1	7.2	7.2	7.4	7.6	7.2	7.2	7.5
Min VAD F (L/min)	0.0	0.0	0.4	0.5	0.5	0.4	0.4	0.5	0.3	0.4	0.4	0.4	0.2	0.4	0.4	0.2
Mean TotalFlow (L/min)	3.2	3.2	4.3	4.2	4.2	4.2	4.2	4.2	4.2	4.4	4.4	4.4	4.4	4.3	4.4	4.4
TotalFlow peak (+) (L/min)	4.4	4.4	4.9	4.9	4.9	4.9	4.9	4.9	4.9	5.0	5.0	5.0	5.0	5.0	5.0	5.0
TotalFlow peak (-) (L/min)	2.1	2.1	3.4	3.4	3.4	3.4	3.4	3.4	3.4	3.5	3.7	3.5	3.5	3.6	3.6	3.6
ZART (dynes-sec/cm^5)	65	65	83	82	83	83	83	83	83	86	86	85	86	86	86	86
SHE (ergs/cm^3)	2649	2651	1199	1196	1170	1278	1220	1209	1281	1083	1046	1191	1175	1103	1063	1168
EEP (mmHg)	1568	1566	1546	1550	1554	1552	1553	1551	1550	1556	1552	1554	1557	1563	1556	1552